

NUREG 0612
CONTROL OF HEAVY LOADS

R. E. GINNA NUCLEAR POWER PLANT
ROCHESTER GAS AND ELECTRIC CORP.

DOCKET NO. 50-244

FINAL REPORT

DATED: 3/19/84

MF3J

8404020065 840326
PDR ADCK 05000244
PDR



1950
1951
1952
1953
1954
1955
1956
1957
1958
1959
1960

TABLE OF CONTENTS

<u>SECTION</u>	<u>TITLE</u>	<u>PAGE</u>
1.0	INTRODUCTION	1
2.0	IDENTIFIED OVERHEAD HANDLING SYSTEMS	1
3.0	RESPONSES TO REQUEST FOR INFORMATION IN SECTIONS 2.2, 2.3, AND 2.4 of ENCLOSURE 3 OF NRC DECEMBER 22, 1980 LETTER	2
4.0	CONCLUSIONS	14
5.0	REFERENCES	15
	ATTACHMENT 1	16
	ATTACHMENT 2	17
	ATTACHMENT 3	18
	ATTACHMENT 4	19

1.0

INTRODUCTION

In response to the NRC Letter of December 22, 1980, "Control of Heavy Loads" this report provides the results of Rochester Gas and Electric's review of the handling of heavy loads at our R. E. Ginna Nuclear Power Plant.

Two reports, dated February 1, 1982 and March 2, 1983, have previously been submitted in response to Section 2.1 of Enclosure 3 of the December 22, 1980 letter. In addition, the NRC issued a Safety Evaluation on this subject dated January 18, 1984.

This report contains the additional requested information responding to Sections 2.2, 2.3 and 2.4 of Enclosure 3 of the December 22, 1980 letter. It identifies the extent to which the controls for heavy loads at Ginna Station comply with NUREG-0612 and the recommendations proposed in order to satisfy the guidelines of NUREG-0612.

2.0

IDENTIFIED OVERHEAD HANDLING SYSTEMS

The heavy load overhead handling systems within the scope of NUREG-0612 were identified in our March 2, 1983 submittal and are listed below:

Outside Containment

1. Upper Intermediate Building Monorail
2. 7 1/2 Ton Screenhouse Crane (East)
3. 2 Ton Spent Fuel Handling Crane in Auxiliary Building
4. Monorail in Basement of Auxiliary Building
5. Auxiliary Building Overhead Crane with Main and Auxiliary Hooks

Inside Containment

1. 1 1/2 Ton Fuel Manipulator Bridge
2. 2 Ton Jib at Personnel Hatch
3. 3 Ton Jib at Equipment Hatch
4. 10 Ton Jib Over Pressurizer Access Hatch
5. Containment Building Overhead Crane With Main and Auxiliary Hooks

3.0

RESPONSES TO REQUESTS FOR INFORMATION IN SECTIONS 2.2,
2.3, AND 2.4 OF ENCLOSURE 3 OF NRC DECEMBER 22, 1980 LETTER

RESPONSE: The following pages list the questions and provide the required information to Sections 2.2, 2.3, and 2.4.

2.2

SPECIFIC REQUIREMENTS FOR OVERHEAD HANDLING SYSTEMS
OPERATING IN THE VICINITY OF FUEL STORAGE POOLS

NUREG 0612, Section 5.1.2, provides guidelines concerning the design and operation of load-handling systems in the vicinity of stored, spent fuel. Information provided in response to this section should demonstrate that adequate measures have been taken to ensure that in this area, either the likelihood of a load drop which might damage spent fuel is extremely small, or that the estimated consequences of such a drop will not exceed the limits set by the evaluation criteria of NUREG 0612, Section 5.1, Criteria I through III.

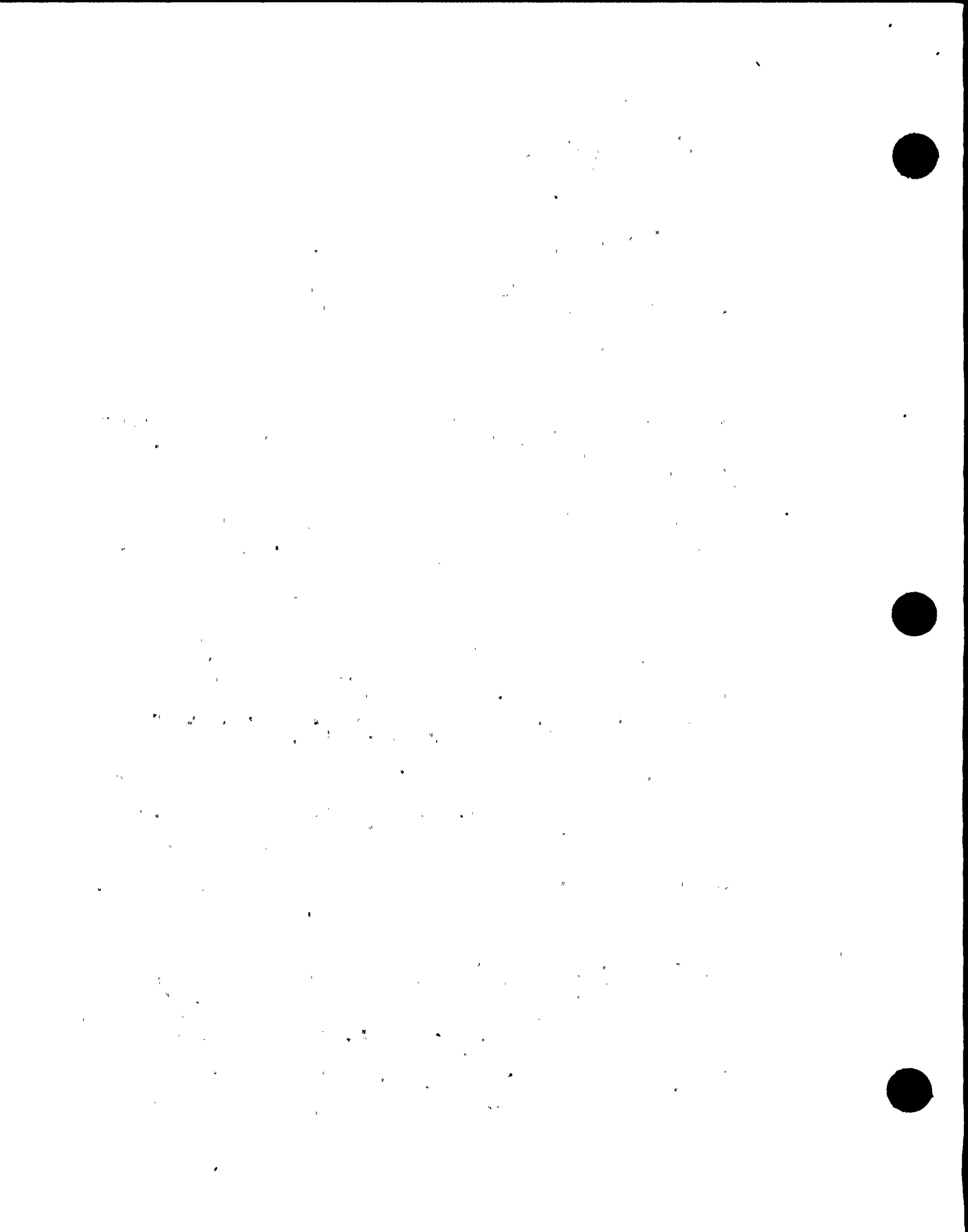
- 2.2-1 Identify by name, type, capacity, and equipment designator, any cranes physically capable (i.e., ignoring interlocks, moveable mechanical stops, or operating procedures) of carrying loads which could, if dropped, land or fall into the spent fuel pool.

RESPONSE: There are two overhead handling systems in the Auxiliary Building which are capable of carrying heavy loads over the spent fuel pool. These cranes are a 40 ton Shaw Box overhead crane with a 5 ton auxiliary hoist and a 2 ton spent fuel bridge crane.

- 2.2-2 Justify the exclusion of any cranes in this area from the above category by verifying that they are incapable of carrying heavy loads or are permanently prevented from movement of the hook centerline closer than 15 feet to the pool boundary, or by providing a suitable analysis demonstrating that for any failure mode, no heavy load can fall into the fuel-storage pool.

RESPONSE: There are no other overhead handling systems in the vicinity of spent fuel pool. The 40 ton crane main and auxiliary hooks can move over the spent fuel pool after a series of electrical interlocks have been defeated. The 2 ton spent fuel pool crane is located over the pool. This crane is restricted to loads equal to or less than 1500 lbs. by Ginna Station administrative procedures. For further discussion see response to Section 2.2-4.

- 2.2-3 Identify any cranes listed in 2.2-1, above, which you have evaluated as having sufficient design features to make the likelihood of a load drop extremely small for all loads to be carried and the basis for this evaluation (i.e., complete compliance with NUREG 0612, Section 5.1.6 or partial compliance supplemented by suitable alternative or additional design features). For each crane so evaluated, provide the load-handling-system (i.e., crane-load-combination) information required.



RESPONSE: For the two overhead handling systems in the vicinity of the fuel storage racks neither has been eliminated from further evaluation based on Section 5.1.6 of NUREG-0612.

2.2-4

For cranes identified in 2.2-1, above, not categorized according to 2.2-3, demonstrate that the criteria of NUREG 0612, Section 5.1, are satisfied. Compliance with Criterion IV will be demonstrated in response to Section 2.4 of this request. With respect to Criteria I through III, provide a discussion of your evaluation of crane operation in the spent fuel area and your determination of compliance. This response should include the following information for each crane:

- a. Which alternatives (e.g., 2, 3, or 4) from those identified in NUREG 0612, Section 5.1.2, have been selected.
- b. If Alternative 2 or 3 is selected, discuss the crane motion limitation imposed by electrical interlocks or mechanical stops and indicate the circumstances, if any, under which these protective devices may be bypassed or removed. Discuss any administrative procedures invoked to ensure proper authorization of bypass or removal, and provide any related or proposed technical specification (operational and surveillance) provided to ensure the operability of such electrical interlocks or mechanical stops.
- c. Where reliance is placed on crane operational limitations with respect to the time of the storage of certain quantities of spent fuel at specific post-irradiation decay times, provide present and/or proposed technical specifications and discuss administrative or physical controls provided to ensure that these assumptions remain valid.
- d. Where reliance is placed on the physical location of specific fuel modules at certain post-irradiation decay times, provide present and/or proposed technical specifications and discuss administrative or physical controls provided to ensure that these assumptions remain valid.
- e. Analyses performed to demonstrate compliance with Criteria I through III should conform to the guidelines of NUREG 0612, Appendix A. Justify any exception taken to these guidelines, and provide the specific information requested in Attachment 2, 3, or 4, as appropriate, for each analysis performed.



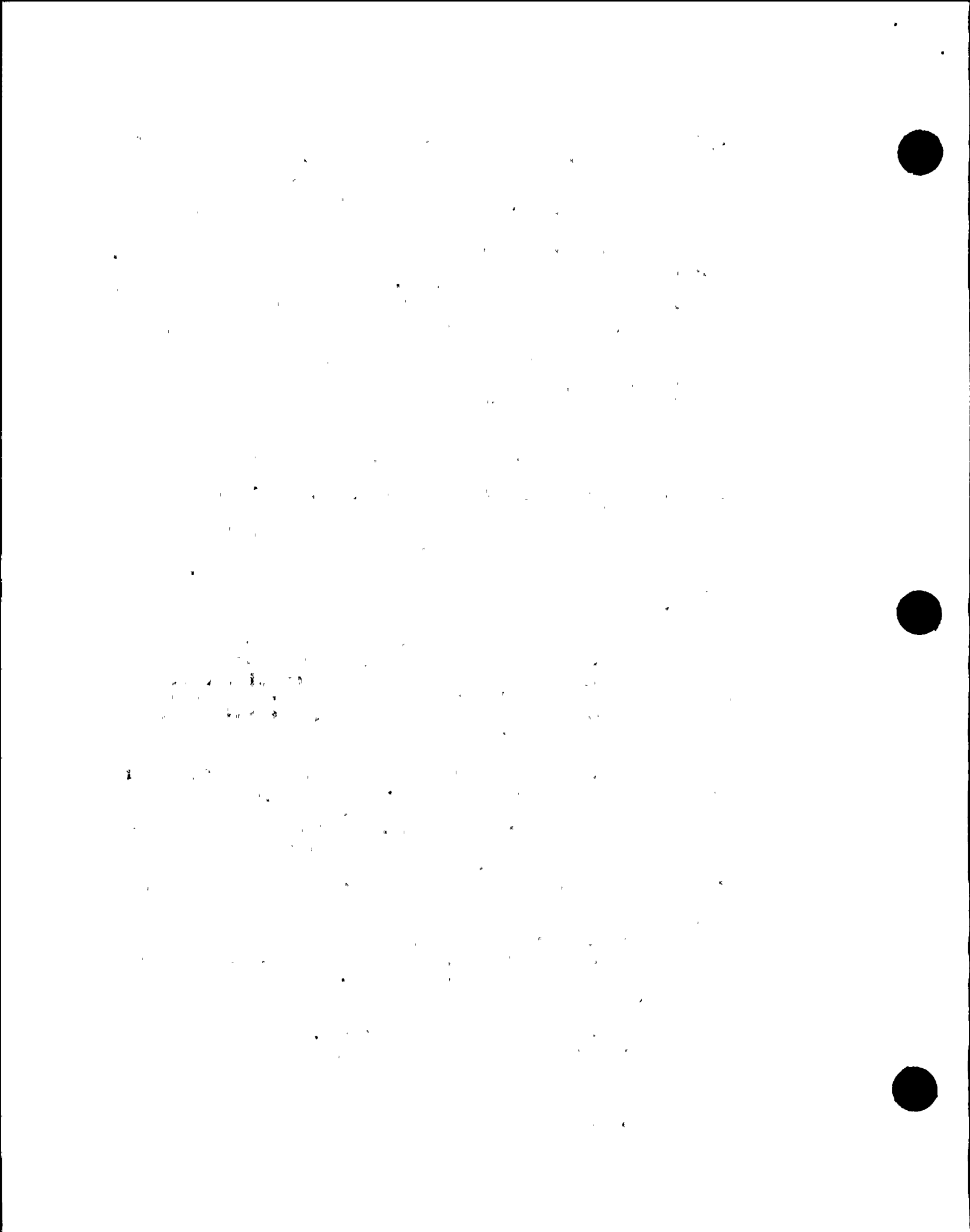
RESPONSE: (*2 Ton Spent Fuel Bridge Crane) The 2 ton spent fuel pool crane is restricted to lifting fuel assemblies, fuel components such as flow mixers, control rods and sources, and their associated handling tools. Since this crane only handles spent fuel, and related items the crane has been eliminated from further evaluation based on previous analysis [which satisfies NUREG 0612, Section 5.1.2(4)]. Previous analysis, done in response to SEP Topic XV-20, (Ref. 8) "Radiological Consequences of Fuel Damaging Accidents", has shown that the releases of radioactive material that could result from a fuel handling accident in this area are well within 10 CFR part 100 limits. This crane is also prohibited from lifting loads greater than 1500 lbs. Thus, this crane satisfies the criteria of NUREG-0612 and need not be considered further.

RESPONSE: (40 Ton Auxiliary Bldg. Crane Main Hook) As a result of the potential need to handle spent fuel casks RG&E has decided to modify the main hook of the 40 ton auxiliary building crane. This modification will allow the main hook to comply with section 5.1.2(1) of NUREG 0612 (single-failure-proof). A description of the modification has been submitted to the NRC with a license amendment request dated January 18, 1984.

The auxiliary 5 ton hook on this crane along with the main hook is restricted from moving over the spent fuel pool by a set of electrical interlocks. The normal hook travel is allowed right to the edge of the pool on the east end and restricted to 3'-6" from the south edge of the pool. The safe load paths of this crane are shown on Attachment 1.

In addition to the existing electrical interlocks Ginna administrative procedures and technical specifications restrict the auxiliary building overhead crane from movement over the spent fuel pool. The safe load paths shown on Attachment 1 allow for the movement of miscellaneous equipment and material into and out of the decontamination area. These loads are generally less than 1500 lbs. In addition, there are no specific heavy loads which require movement in the area immediately adjacent to the fuel pool. The area just east of the pool is the transfer canal and the crane is used here for inspection of the canal and removing miscellaneous equipment.

* The 2 ton spent fuel bridge crane consists of a 2 ton capacity bridge with (2) 1 ton hoists attached.



2.3

SPECIFIC REQUIREMENTS OF OVERHEAD HANDLING SYSTEMS OPERATING
IN THE CONTAINMENT

NUREG 0612, Section 5.1.3, provides guidelines concerning the design and operation of load-handling systems in the vicinity of the reactor core. Information provided in response to this section should be sufficient to demonstrate that adequate measures have been taken to ensure that in this area, either the likelihood of a load drop which might damage spent fuel is extremely small, or that the estimated consequences of such a drop will not exceed the limits set by the evaluation criteria of NUREG 0612, Section 5.1, Criteria I through III.

2.3-1

Identify by name, type, capacity, and equipment designator any cranes physically capable (i.e., taking no credit for any interlocks or operating procedures) of carrying heavy loads over the reactor vessel.

RESPONSE: There are two overhead handling systems inside the containment building which are physically capable of carrying loads over the reactor vessel. These cranes are a 1 1/2 ton fuel manipulator bridge crane manufactured by Stearns-Roger Corporation and a 100 ton overhead rectangular service crane manufactured by Whiting Corporation. The rectangular service crane also has a 20 ton auxiliary hoist.

2.3-2

Justify the exclusion of any cranes in this area from the above category by verifying that they are incapable of carrying heavy loads, or are permanently prevented from the movement of any load either directly over the reactor vessel or to such a location where, in the event of any load-handling-system failure, the load may land in or on the reactor vessel.

RESPONSE: The remaining overhead handling systems located in the containment building which are within the scope of NUREG-0612 are incapable of carrying a heavy load over or near the reactor vessel. These overhead handling systems are listed below:

- o 10 Ton Jib Over Pressurizer Access Hatch
- o 2 Ton Jib at Personnel Hatch
- o 3 Ton Jib at Equipment Hatch

2.3-3

Identify any cranes listed in 2.3-1, above, which you have evaluated as having sufficient design features to make the likelihood of a load drop extremely small for all loads to be carried and the basis for this evaluation (i.e., complete compliance with NUREG 0612, Section 5.1.6, or partial compliance supplemented by suitable



alternative or additional design features). For each crane so evaluated, provide the load-handling-system (i.e., crane-load-combination) information required.

RESPONSE: One crane/heavy load combination has been eliminated from further consideration. This is the 100 ton crane load block in the unloaded condition. This crane load block is used for handling numerous heavy loads including those approaching the crane load rating of 100 tons. In the unloaded condition, as opposed to the loaded condition, the stresses in the mechanical and structural components are negligible. Based on this plus the presence of 2 electrical brakes and one mechanical load brake, the random mechanical failure of a major load bearing component when moving the crane in the unloaded condition is not considered credible.

2.3-4

For cranes identified in 2.3-1, above, not categorized according to 2.3-3, demonstrate that the evaluation criteria of NUREG 0612, Section 5.1, are satisfied. Compliance with Criterion IV will be demonstrated in your response to Section 2.4 of this request. With respect to Criteria I through III, provide a discussion of your evaluation of crane operation in the containment and your determination of compliance. This response should include the following information for each crane:

- a. Where reliance is placed on the installation and use of electrical interlocks or mechanical stops indicate the circumstances under which these protective devices can be removed or bypassed and the administrative procedures invoked to ensure proper authorization of such action. Discuss any related or proposed technical specification concerning the bypassing of such interlocks.
- b. Where reliance is placed on other, site-specific considerations (e.g., refueling sequencing), provide present or proposed technical specifications and discuss administrative or physical controls provided to ensure the continued validity of such considerations.
- c. Analyses performed to demonstrate compliance with Criteria I through III should conform with the guidelines of NUREG 0612, Appendix A. Justify any exception taken to these guidelines, and provide the specific information requested in Attachment 2, 3, or 4, as appropriate, for each analysis performed.

11-11-68

11-11-68

11-11-68

11-11-68

11-11-68

11-11-68

11-11-68

11-11-68

11-11-68

11-11-68

11-11-68

11-11-68

11-11-68

11-11-68

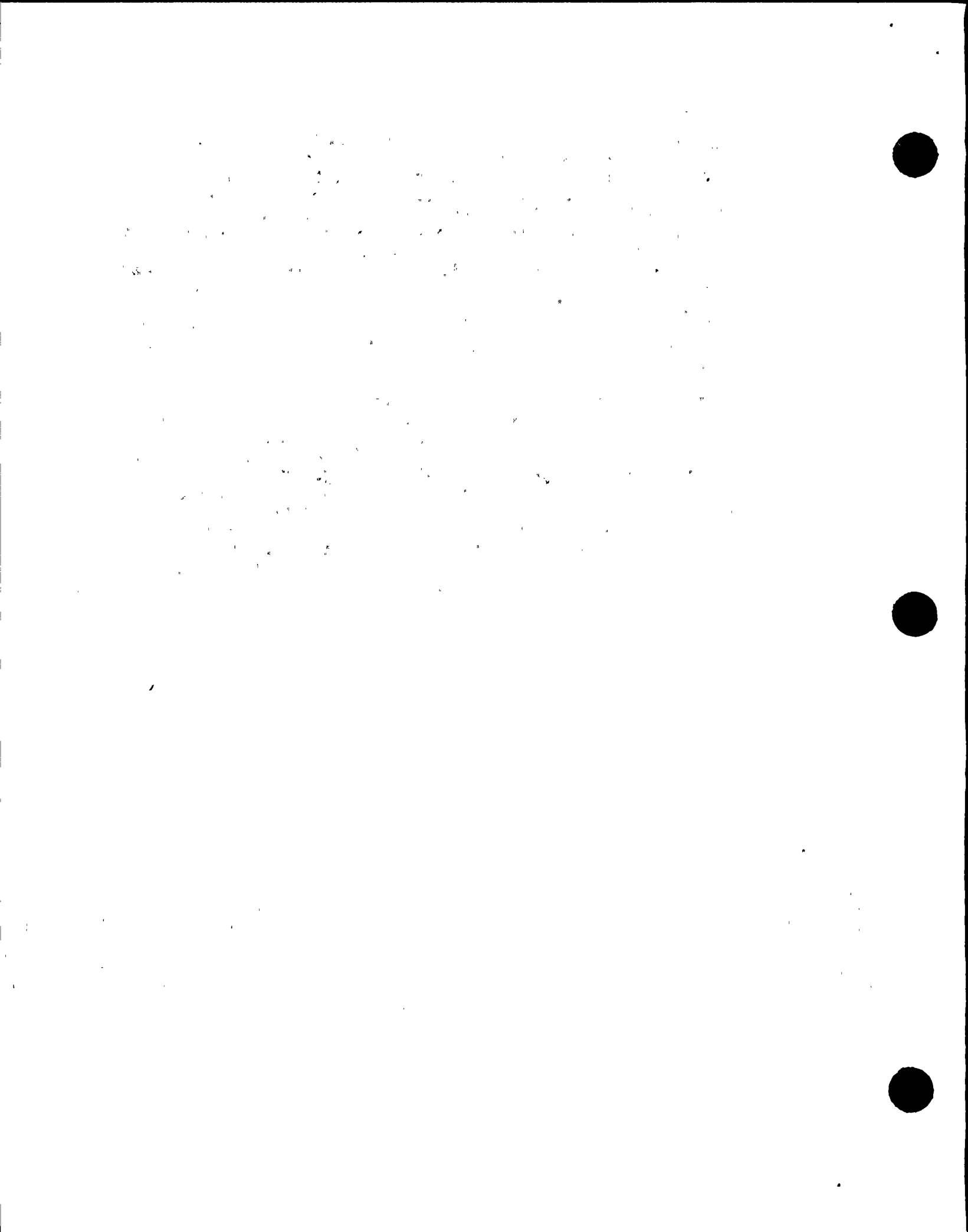
11-11-68

11-11-68

11-11-68

RESPONSE: RG&E's Ginna Plant has only two specific loads which must be carried directly over the reactor vessel, the reactor vessel head and the upper internals package. In response to this section load drop analyses in accordance with Appendix A of the NUREG were performed. Based on the modified safe load paths and procedures in place, the consequences of a drop of the vessel head on the flange from 16' and the drop of the upper internals package from 15' on the core have been determined to be acceptable. (These values represent the maximum lift heights above the vessel allowed by plant procedures.) The Attachments No. 2 and 3 describe the analyses in detail.

Ginna Station Administrative Procedure A-1305.1 diagrams the area of the reactor vessel as a "Restricted Area" when transferring heavy loads. This area is restricted for the movement of all loads with the exception of the reactor head, upper internals package and the reactor coolant pump and motor parts. In some isolated cases RCP parts are allowed to pass over the very edge of the vessel flange. This load path is necessary because of the physical restrictions in the containment building and it is limited to the smallest area possible by plant administrative procedures.



2.4

SPECIFIC REQUIREMENTS FOR OVERHEAD HANDLING SYSTEMS
OPERATING IN PLANT AREAS CONTAINING EQUIPMENT REQUIRED
FOR REACTOR SHUTDOWN, CORE DECAY HEAT REMOVAL, OR SPENT
FUEL POOL COOLING

NUREG 0612, Section 5.1.5, provides guidelines concerning the design and operation of load-handling systems in the vicinity of equipment or components required for safe reactor shutdown and decay heat removal. Information provided in response to this section should be sufficient to demonstrate that adequate measures have been taken to ensure that in these areas, either the likelihood of a load drop which might prevent safe reactor shutdown or prohibit continued decay heat removal is extremely small, or that damage to such equipment from load drops will be limited in order not to result in the loss of these safety-related functions. Cranes which must be evaluated in this section have been previously identified in your response to 2.1-1, and their loads in your response to 2.1-3-c.

2.4-1

Identify any cranes listed in 2.1-1, above, which you have evaluated as having sufficient design features to make the likelihood of a load drop extremely small for all loads to be carried and the basis for this evaluation (i.e., complete compliance with NUREG 0612, Section 5.1.6, or partial compliance supplemented by suitable alternative or additional design features). For each crane so evaluated, provide the load-handling-system (i.e., crane-load-combination) information specified in Attachment 1.

RESPONSE: RG&E has investigated the operation of the upper intermediate building monorail during plant operation and has restricted the use of this monorail to periods of time when the plant is in a cold shutdown mode. The trolley on the monorail will be locked and warnings posted. Systems evaluations below the monorail have shown that a load drop during cold shutdown would not effect any of the required decay heat removal equipment. It is therefore concluded that the use of this overhead handling system cannot effect safe shutdown equipment or equipment used for decay heat removal or spent fuel pool cooling.

2.4-2

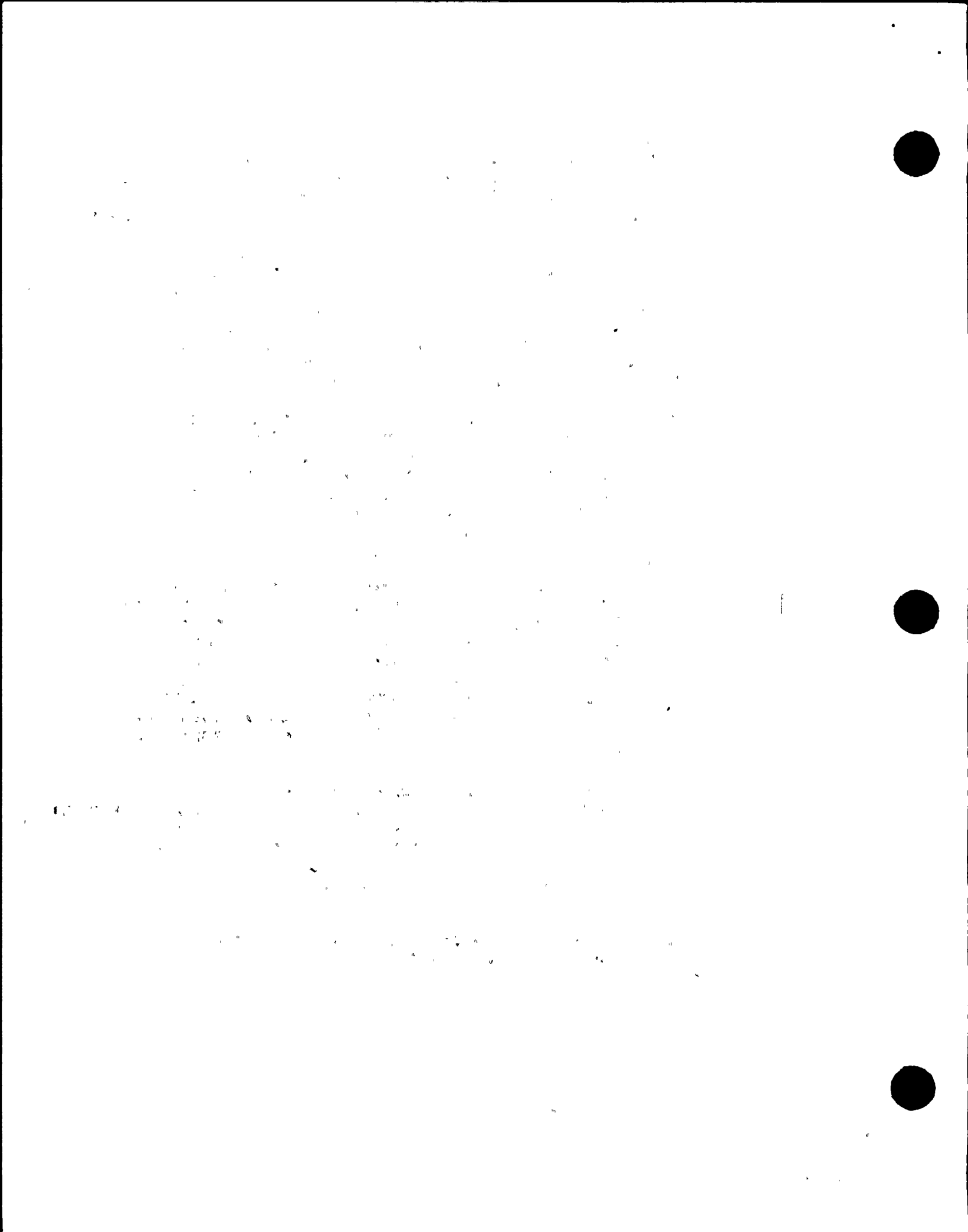
For any cranes identified in 2.1-1 not designated as single-failure-proof in 2.4-1, a comprehensive hazard evaluation should be provided which includes the following information:

- a. The presentation in a matrix format of all heavy loads and potential impact areas where damage might occur to safety-related equipment. Heavy loads identification should include designation

and weight or cross-reference to information provided in 2.1-3-c. Impact areas should be identified by construction zones and elevations or by some other method such that the impact area can be located on the plant general arrangement drawings.

- b. For each interaction identified, indicate which of the load and impact area combinations can be eliminated because of separation and redundancy of safety-related equipment, mechanical stops and/or electrical interlocks, or other site-specific considerations. Elimination on the basis of the aforementioned considerations should be supplemented by the following specific information:
- (1) For load/target combinations eliminated because of separation and redundancy of safety-related equipment, discuss the basis for determining that load drops will not affect continued system operation (i.e., the ability of the system to perform its safety-related function).
 - (2) Where mechanical stops or electrical interlocks are to be provided, present details showing the areas where crane travel will be prohibited. Additionally, provide a discussion concerning the procedures that are to be used for authorizing the bypassing of interlocks or removable stops, for verifying that interlocks are functional prior to crane use, and for verifying that interlocks are restored to operability after operations which require bypassing have been completed.
 - (3) Where load/target combinations are eliminated on the basis of other, site-specific considerations (e.g., maintenance sequencing), provide present and/or proposed technical specifications and discuss administrative procedures or physical constraints invoked to ensure the continued validity of such considerations.

RESPONSE: The load/impact matrix sheets for the cranes which are located above safety related equipment are contained in Attachment 4. A discussion of the analyses and results follows:



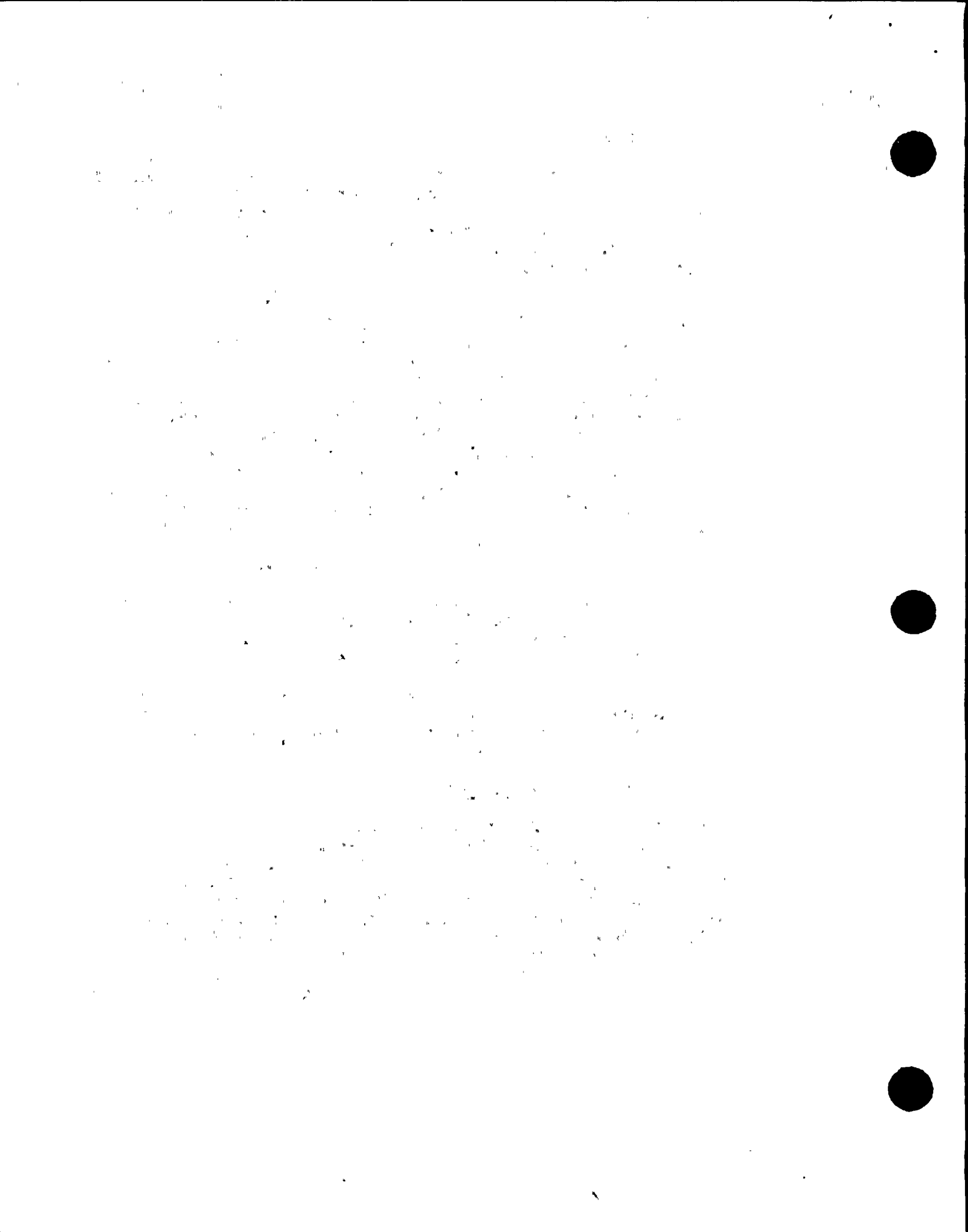
7½ Ton Screenhouse Crane

The 7 1/2 ton overhead handling crane in the screenhouse is limited to travel west of column line 5 by a locked track switch which prohibits moving the hoist east of column line 5. No safety related equipment is located west of column line 5. Use of this crane east of column line 5 is restricted to the lifts provided in Attachment 4 and transfer of the hoist into this area is controlled by the Shift Supervisor. The only safety related equipment in this area are the service water (SW) pumps and their associated electrical buses. During normal maintenance operations in this area, only one pump would be damaged if a motor were being overhauled. Very infrequently, however, an entire pump assembly may be pulled. Damage to all four SW pumps, considered a very low likelihood, could be possible under these circumstances. Even if it did occur, safe shutdown would not be affected. Loss of SW under normal operating conditions would require a plant shutdown. Even if all service water were lost, previous evaluations have shown that safe shutdown can still be achieved and decay heat can still be removed. [References: NUREG-0821, August 1983, and Appendix R Submittal, dated 1/16/84].

Margin is available in terms of alternative sources of water. RG&E has installed the capability to provide cooling water to the Diesel Generator and Auxiliary Feedwater System from the yard fire hydrant systems. Procedures are also already in place to cope with a loss of all SW. Thus, although damage to the SW system is considered a very low probability event, RG&E can cope with this loss through systems and procedures already in place at Ginna.

10 Ton Jib Over Pressurizer

This jib is normally used when the plant is at cold or refueling shutdown. However, periodic in-service inspection requirements have required the use of this jib during operation to lift and remove one pressurizer cavity concrete hatch cover. In order to prohibit a potential load drop into the cavity during operation, a modification to the hatch cover will be installed by July 85. The modification will structurally prohibit the block from falling into the pressurizer cavity. No other heavy loads are lifted by this jib during operation.



1½ Ton Fuel Manipulator Bridge

This crane handles only fuel assemblies and their associated handling tools. The analyses done under SEP Topic XV-20 (Reference 8), as in the 2 ton spent fuel pool crane, has shown that the postulated drop of a fuel assembly from this crane satisfies section 5.1.2(4) of NUREG 0612.

2 Ton Jib Crane at Personnel Hatch

Systems analyses have been performed on the piping & equipment below this jib for postulated load drops. The following equipment could be impacted by a dropped load if the load fell all the way to the basement.

B Accumulator Line to Loop A
Fan Cooler D and its Service Water Lines

The consequences of a load drop during various modes of shutdown and during plant operation have been determined acceptable with the criteria listed in NUREG-0612 Section 2.4.

Monorail in Basement of Auxiliary Building

The effects of load drops from this monorail are still being evaluated.

3 Ton Jib at Equipment Hatch

The effects of load drops from this jib crane are still being evaluated.

40/5 Ton Auxiliary Building Overhead Crane

The effects of load drops from this crane are still being evaluated.

100/5 Ton Containment Overhead Crane

The load/impact matrix sheets in Attachment 4 detail the analyses performed to date. Some additional evaluations are still being evaluated.

- c. For interactions not eliminated by the analysis of 2.4-2-b, above, identify any handling systems for specific loads which you have evaluated as having sufficient design features to make the likelihood of a load drop extremely small and the basis for this evaluation (i.e., complete compliance with NUREG 0612, Section 5.1.6, or partial compliance supplemented by suitable alternative or additional design features). For each crane so evaluated, provide the load-handling-system (i.e., crane-load-combination) information required.

RESPONSE: As described in response to NRC Section 2.3-3, the crane load block for the 100 ton containment overhead crane in the unloaded condition, has been eliminated based on sufficient design factors of safety.

- d. For interactions not eliminated in 2.4-2(b) or 2.4-2(c), above, demonstrate using appropriate analysis that damage would not preclude operation of sufficient equipment to allow the system to perform its safety function following a load drop (NUREG 0612, Section 5.1, Criterion IV). For each analysis so conducted, the following information should be provided:
- (1) An indication of whether or not, for the specific load being investigated, the overhead crane-handling system is designed and constructed such that the hoisting system will retain its load in the event of seismic accelerations equivalent to those of a safe shutdown earthquake (SSE).
 - (2) The basis for any exceptions taken to the analytical guidelines of NUREG 0612, Appendix A.
 - (3) The information requested in Attachment 4 of Reference No. 1.

RESPONSE: Systems evaluations and justification for the operation of equipment has been addressed in response to Section 2.4-2(b).



4.0

CONCLUSIONS

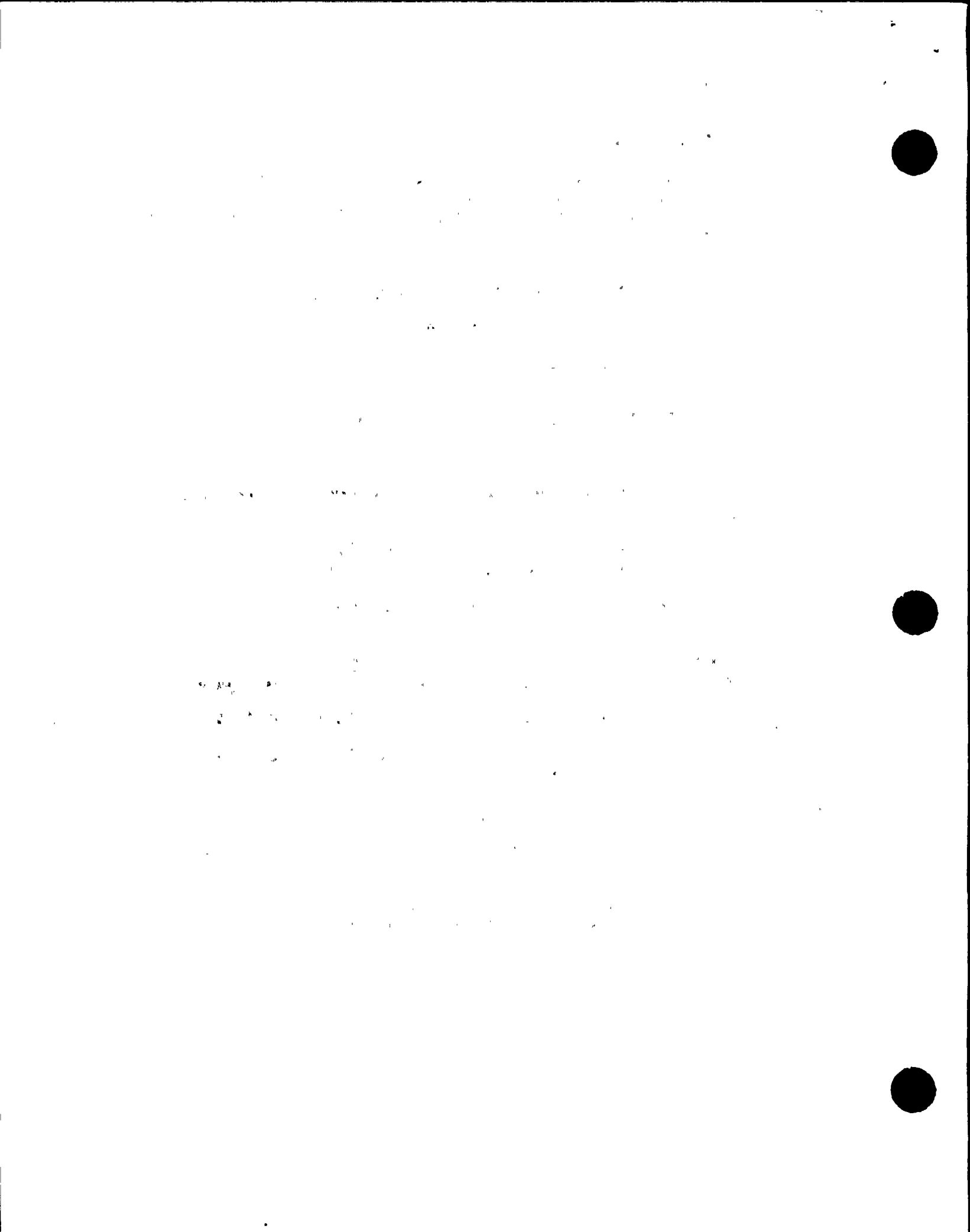
Structural analyses and systems evaluations have shown that the following cranes at Ginna Station operate safely and that the consequences of a load drop have been determined to be acceptable using the criteria set forth in NUREG 0612:

1. Upper Intermediate Building Monorail
2. 7½ Ton Screenhouse Crane (East)
3. 2 Ton Spent Fuel Handling Crane in Auxiliary Building
4. 1½ Ton Fuel Manipulator Bridge
5. 2 Ton Jib at Equipment Hatch
6. 10 Ton Jib Over Pressurizer Access Hatch (with modification installed)
7. Containment Overhead Crane Lifting the Reactor Vessel Head and Upper Internals
8. Containment Overhead Crane Load Block in the Unloaded Condition

Additional evaluations are being performed on the following cranes and their potential load drops:

1. Monorail in Basement of Auxiliary Building
2. Auxiliary Building Overhead Crane with Main and Auxiliary Hooks
3. 3 Ton Jib at Equipment Hatch
4. Additional Load Paths for Containment Building Overhead Crane

The results of these evaluations will be sent in as an addition to this submittal by June 29, 1984.

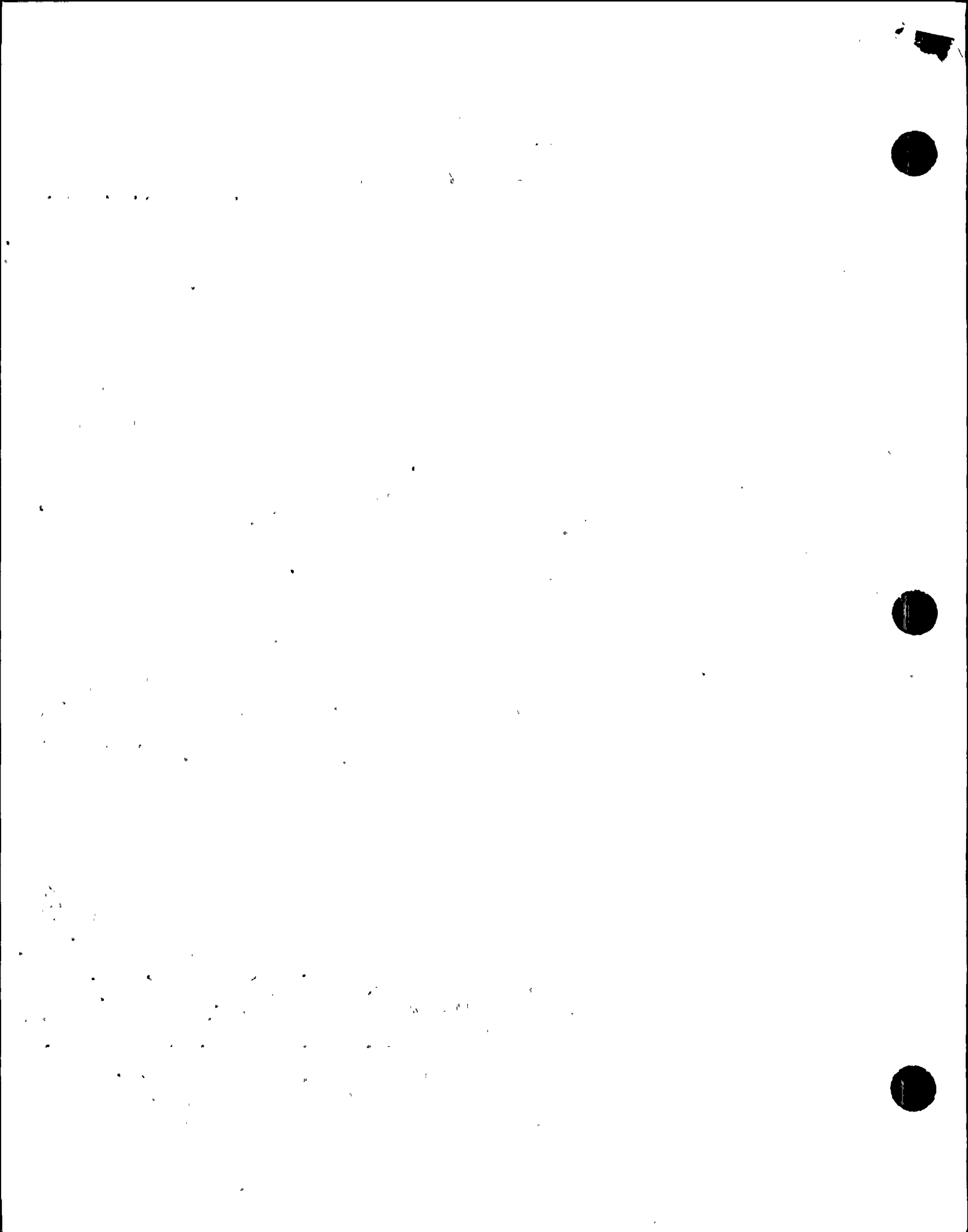


REFERENCES

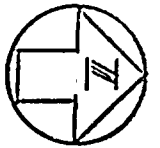
1. NRC Generic Letter "To all Licensees of Operating Plants and Applicants for Operating Licenses and Holders of Construction Permits" on the Control of Heavy Loads, December 22, 1980.
2. NUREG-0612, Control of Heavy Loads at Nuclear Power Plants, USNRC, July 1980.
3. RG&E Submittal in Response to Reference No. 1, dated February 1, 1982.
4. RG&E Submittal in Response to Reference No. 1, dated March 2, 1983.
5. RG&E Submittal in Response to Reference No. 1, dated October 12, 1983.
6. NRC Draft Technical Evaluation Report, dated August 19, 1982.
7. NRC Safety Evaluation Report, Phase I, dated January 18, 1984.
8. Letter to John Maier, RG&E, from Dennis M. Crutchfield, NRC, on SEP Topic XV-20, "Fuel Handling Accident Inside Containment", dated October 7, 1981.

ATTACHMENT 1

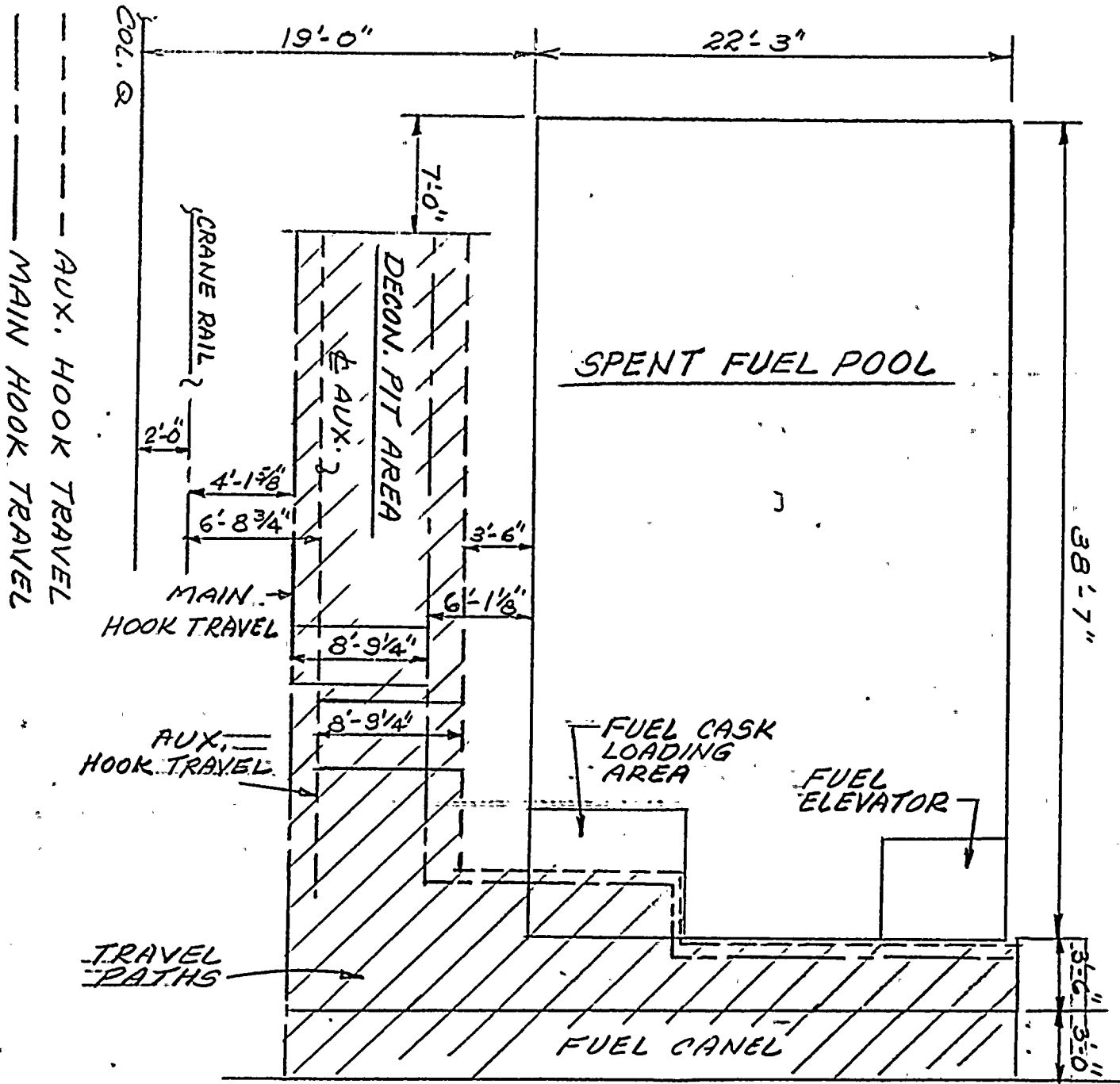
Auxiliary Building Crane Travel



ATTACHMENT NO 1



OF HOOKS CAN TRAVEL TO EDGE OF POOL ON EAST END



AUXILIARY BUILDING OVERHEAD CRANE
TRAVEL RESTRICTIONS UNLESS INTERLOCK
SYSTEM IS BY PASSED

EWR # 3059

0	ORIGINAL	INITIAL DATE	NJA 1-17-84	MBF 3/19/84	MBF 3/19/84	TRM 3-15-84
NUMBER	REVISION		DRAWN BY	CHECKED BY	RESP. ENG.	ENG. MANG'R.
ROCHESTER GAS & ELECTRIC CORP. ROCHESTER, NEW YORK			AUX. BLDG. CRANE TRAVEL			SCALE ~ NO. 03021-562



ATTACHMENT 2

Reactor Head Drop Analysis



FINAL REPORT
FOR THE
REACTOR HEAD DROP ANALYSIS FOR GINNA STATION
JOB NO. 83084

R. E. GINNA NUCLEAR POWER STATION

ROCHESTER GAS AND ELECTRIC CORPORATION
ROCHESTER, NEW YORK

COPY NO. 2

Prepared

Robert L. Bishman 3/9/84
Lead Engineer

Approved

John D. McWilliam 3/9/84
Project Manager

Approved

Mark B. Fitzsimmons 3/16/84
Rochester Gas & Electric

TABLE OF CONTENTS

<u>Section</u>	<u>Page</u>
1.0 Introduction	1
2.0 Reactor Vessel Description	1
3.0 Problem Description	3
4.0 Acceptance Criteria	4
5.0 Analysis Methodology and Results	
5.1 Basic Finite Element Model	6
5.2 Uniform Drop Analysis	9
5.3 Concentrated Drop Analysis	11
6.0 Conclusions and Recommendations	16

Appendices

- A References
- B Figures 1 through 51



FINAL REPORT

Reactor Head Drop Analysis

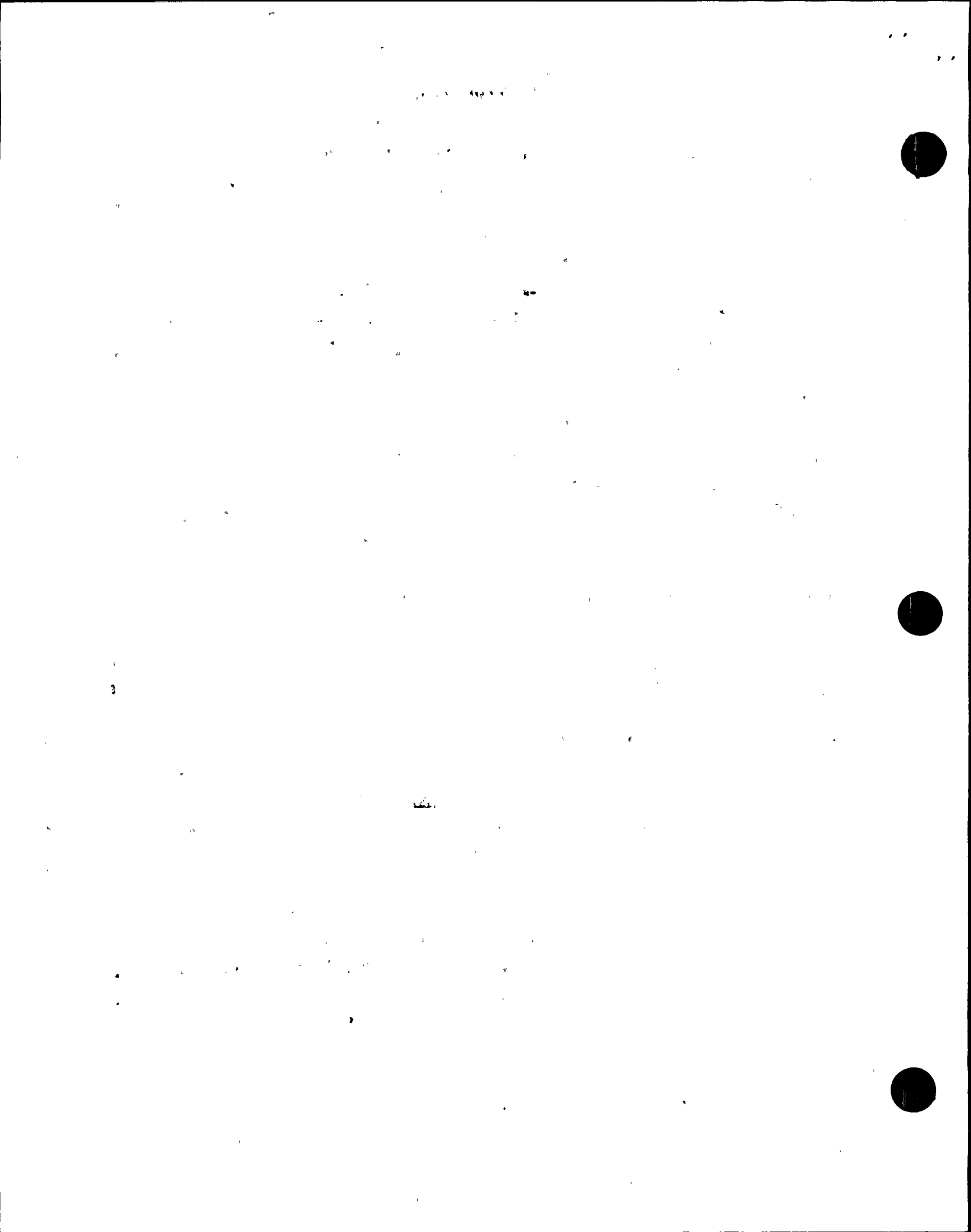
1.0 INTRODUCTION

This report documents the results of Cygna's pilot study analysis of the reactor vessel head dropping onto the reactor vessel at Ginna. The study is intended to form the basis for a response to issues raised in NUREG-0612.

Two basic analyses were conducted. The first was an elastic time-history analysis of the reactor head dropping uniformly onto the vessel flange. The second was a plastic time-history analysis of the reactor head dropping on edge (concentrated drop) onto the vessel flange directly over a primary coolant nozzle. The study concludes that core cooling can be maintained in the unlikely event of either a uniform drop from fifteen feet or a concentrated drop from sixteen feet.

2.0 REACTOR VESSEL DESCRIPTION

The Reactor Pressure Vessel (RPV) at Ginna consists of five basic components. These components include (1) a hemispherical closure assembly (RPV head), (2) a flange forging to receive the closure head assembly, (3) an upper shell region containing the low head safety injection and primary coolant inlet and outlet nozzles, (4) an intermediate shell region, and (5) a bottom hemispherical shell containing instrumentation nozzles (Figure 1). The vessel



is approximately 13 feet in diameter and is supported at six points by the four reactor coolant loop nozzles plus two lugs which all rest on support pads. The six supports are located approximately 8'-6" below the vessel flange and are spaced circumferentially at 60° intervals (Figures 2 & 3).

The reactor vessel flange is a machined forging welded to the upper shell. The 14.5" thick flange is fabricated from SA-336 manganese-molybdenum steel conforming to ASME Code Case 1332-1 and is clad internally with weld deposited austenitic stainless steel.

The upper shell of the vessel is a machined forging welded to the reactor vessel flange and to the intermediate shell. The 9.0" thick upper shell is also fabricated from SA-336 manganese-molybdenum steel conforming to ASME Code Case 1332-1 and is clad internally with weld deposited stainless steel. The upper shell contains the four primary coolant nozzles, the vessel supports, and the two safety injection nozzles. The two 27.5" I.D. inlet nozzles and the two 29.0" I.D. outlet nozzles are approximately 10" thick. These nozzle forgings are fabricated from the same material as the upper shell and are also clad internally with weld deposited austenitic stainless steel. The two safety injection nozzles are welded into the upper shell. These nozzles inject water into the vessel in the event of a primary coolant failure. The centerline of both the safety injection nozzles and the primary coolant nozzles are located approximately 6'-2" below the top surface of the vessel flange.

The upper shell is welded to the intermediate shell which is fabricated from A-508 Class 2 manganese-molybdenum steel. The intermediate shell is 6.5" thick and is internally clad with weld deposited austenitic stainless steel.

The bottom hemispherical head is welded to the intermediate shell of the vessel. The 4.1" thick hemispherical head is forged from a single plate of SA-302 Grade B manganese-molybdenum steel and is clad internally with weld deposited austenitic stainless steel.

3.0 PROBLEM DESCRIPTION

During refueling operations the RPV head, which weighs 134,550 pounds, is lifted vertically from the vessel flange by the 100 ton containment overhead crane. Vertical alignment is maintained during part of this lift by three guide studs approximately 15 feet high which are engaged in the vessel flange (Figures 4 & 5). After clearing the guide studs, the head is lifted for some additional height (Figure 6) before being moved laterally to the south (over the refueling cavity floor), and eventually to the head storage stand on the operating floor.

While the RPV head is over the vessel, two types of drops can occur. One is a uniform drop onto the RPV flange which is most likely to occur while the RPV head is on the guide studs. The other is a concentrated drop onto the RPV flange which can only occur when the RPV head has been lifted above the top of the guide studs.

In the analyses performed by Cygna, the uniform drop was based upon the head falling 15 feet through air. This is the maximum drop height for which the head would still be aligned on the guide studs, thus insuring a uniform drop (Figure 7). After clearing the guide studs, a uniform drop can no longer be guaranteed. However, at this point, the head is now free to move laterally to the south from its position directly over the core.



10

11

12

13

14

15

For this reason, the concentrated drop was based upon the head falling 16 feet, since this was the minimum height for which a concentrated drop scenario could be postulated (Figures 8 & 9).

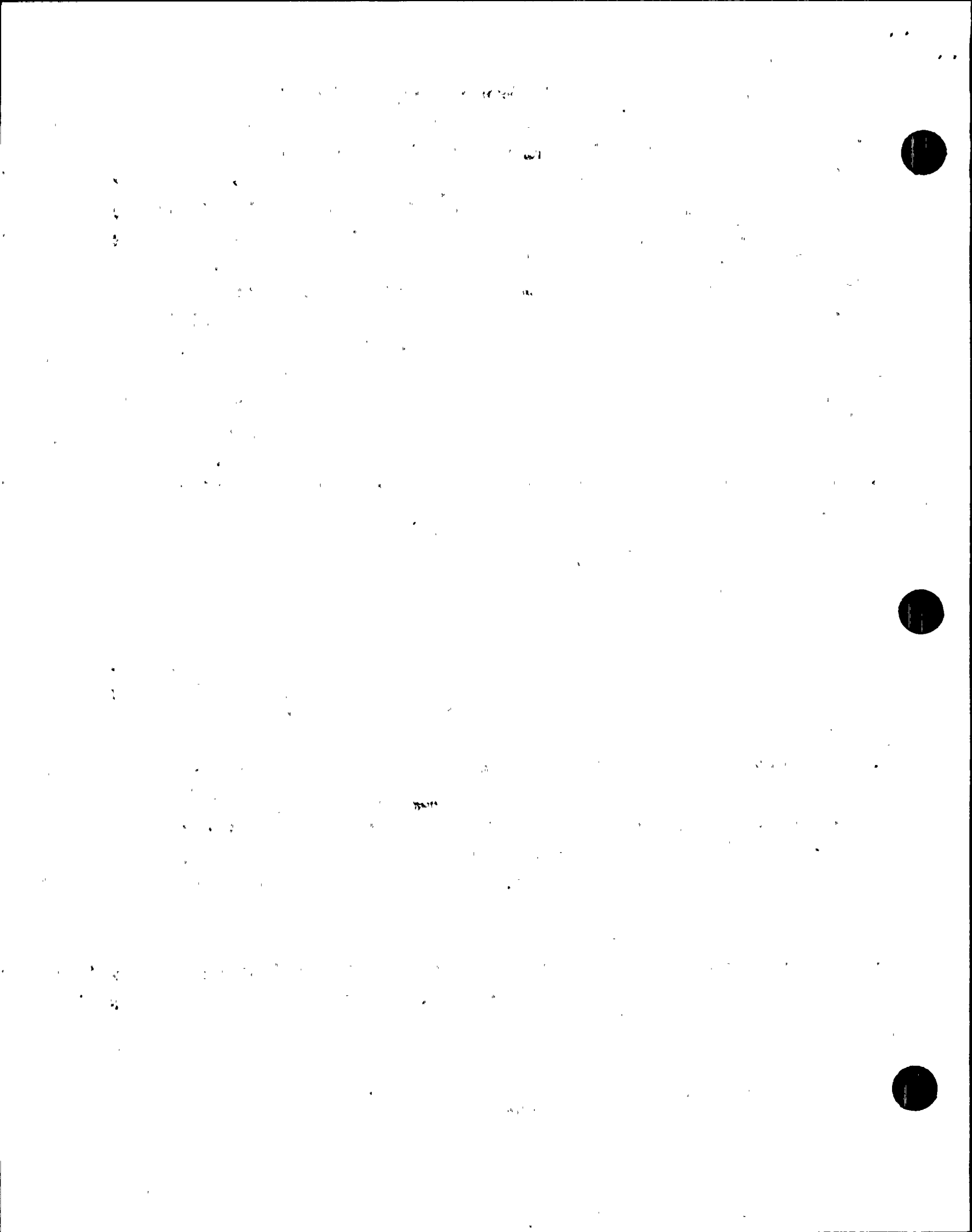
For both the uniform drop and the concentrated drop it was conservatively assumed that, in addition to the weight of the RPV head, the total load dropped onto the RPV flange included the weight of the lifting rig (30,000 pounds) and the crane hook block (8,500 pounds). Thus, the total load dropped was 173,050 pounds.

As required by NUREG-0612, the head was conservatively assumed to be rigid in all analyses; thus it absorbed no energy. Furthermore, it was assumed that during the concentrated drop the entire load struck the RPV flange directly above a primary coolant nozzle, thus imposing the most severe conditions on a single nozzle.

4.0 ACCEPTANCE CRITERIA

During reactor shutdown, it is essential to provide cooling water to the reactor core. As a minimum this requires that the safety injection nozzles maintain structural integrity after a RPV head drop event. Thus, the consequences of a head drop over the RPV are acceptable if the analysis conservatively demonstrates that the structural integrity of the safety injection nozzles is maintained after a RPV head drop. Therefore, it is essential that during a head drop event the reactor support system be maintained, since this virtually insures the integrity of the safety injection nozzles.

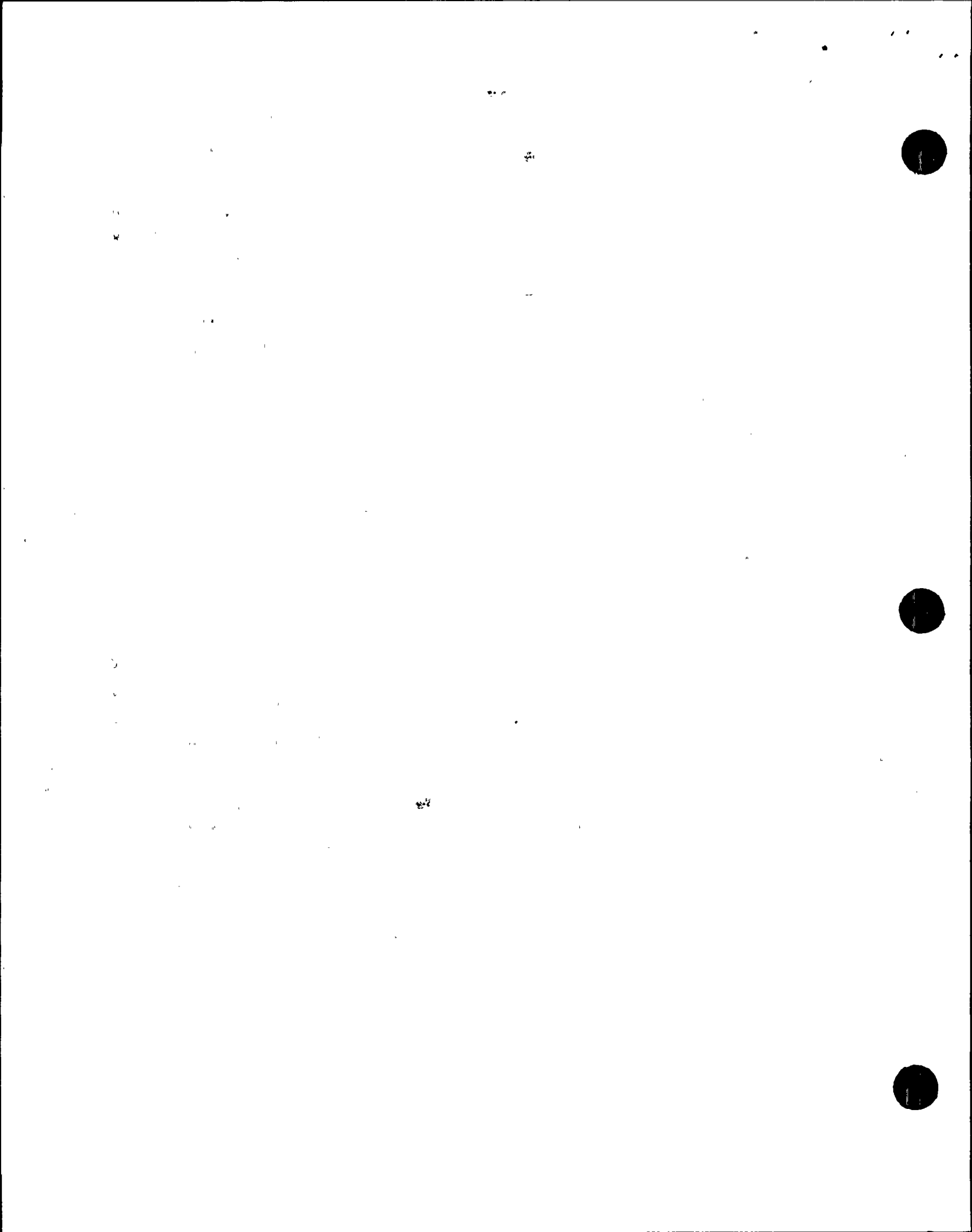
Unlike the safety injection nozzles, the primary coolant loop nozzles are part of the reactor support system and are directly



loaded during the head drop impact. The basis for determining primary coolant nozzle integrity was developed from ultimate strain behavior. The ultimate strain is the point at which a material will rupture in simple tension. A reasonable acceptance criteria for maintaining primary coolant nozzle integrity is one in which the peak equivalent strain (which is proportional to the octahedral shear strain) in the vicinity of the vessel/nozzle intersection does not exceed one half of the minimum ultimate strain of the material. (It should be noted that in uniaxial tension, the uniaxial ultimate strain is equal to the equivalent ultimate strain.) Since the peak equivalent strain at the nozzle/vessel intersection is a highly localized strain resulting from a combination of geometric discontinuity and strain concentration, limiting the peak equivalent strain to one half of the minimum ultimate strain of the material should insure that the actual impact kinetic energy is well below the kinetic energy level that would produce complete plastic instability (collapse) of the nozzle support.

The material from which the reactor vessel upper shell and coolant nozzles at Ginna is fabricated has a minimum ultimate strain capacity equal to 0.17 in/in for material 9.0 inches thick (ASME Code Case 1236-2). Thus, to maintain nozzle integrity, the peak equivalent strain in the vicinity of the nozzle/vessel intersection shall not exceed 0.085 in/in during a RPV head drop event. Should this strain level be exceeded, the nozzle would not be considered functional from an analytical point of view; however, reactor core cooling could still be maintained by the safety injection nozzles, provided the integrity of these nozzles can be demonstrated.

Under dynamic impact, strain criteria alone is not sufficient to demonstrate material integrity since strain rate effects may also



be important. Therefore, as an additional criteria to conservatively demonstrate material integrity, strain rates should be maintained at a level below 100 in/in/sec.

It is assumed that material flaws are small, and that at the time of impact the vessel material is at a temperature which is equal to or greater than the nil ductility temperature plus sixty degrees fahrenheit.

5.0 ANALYSIS METHODOLOGY AND RESULTS

5.1 Basic Finite Element Model

The basic finite element model for both the uniform and concentrated drop analysis consists of a 30° circumferential segment of the RPV cutting directly through the centerline of a primary coolant loop nozzle (Figure 10 & 11). The basic model was developed on the ANSYS computer program (Version 4.1B) and consists of (1) the vessel flange, (2) the upper shell region, (3) a primary coolant loop nozzle, (4) a vessel support, and (5) an extended intermediate shell which incorporates an additional length to compensate for the hemispherical bottom. By properly specifying the shell boundary conditions at the edges of the 30° segment, this finite element model can represent the entire 360 degrees of the vessel, provided that (1) one assumes that the actual vessel has six nozzle supports instead of four (i.e., two nozzle supports replace the two lug supports), and (2) the loads are uniformly applied to the entire vessel. Thus, the 30° segment model gives almost an exact solution for the case of a uniform head drop. For the concentrated drop analysis, where a single impact occurs directly above one nozzle, the 30° segment model is very conser-

vative since the symmetric boundary conditions imply that the same load is applied to all twelve of the 30° segments comprising the full vessel. Thus, in the concentrated drop analysis using a 30° segment finite element model, a single nozzle (60° segment of the vessel) will resist the impact of the entire head drop.

The 30° segment model is the minimum size finite element model which could be used for the studies. It was intended that this model would produce results which would form the basis for making a decision as to whether to pursue a more refined analytical resolution to the problem using a more elaborate finite element model, or to attempt a different approach, such as a probabilistic (PRA) resolution to the head drop problem.

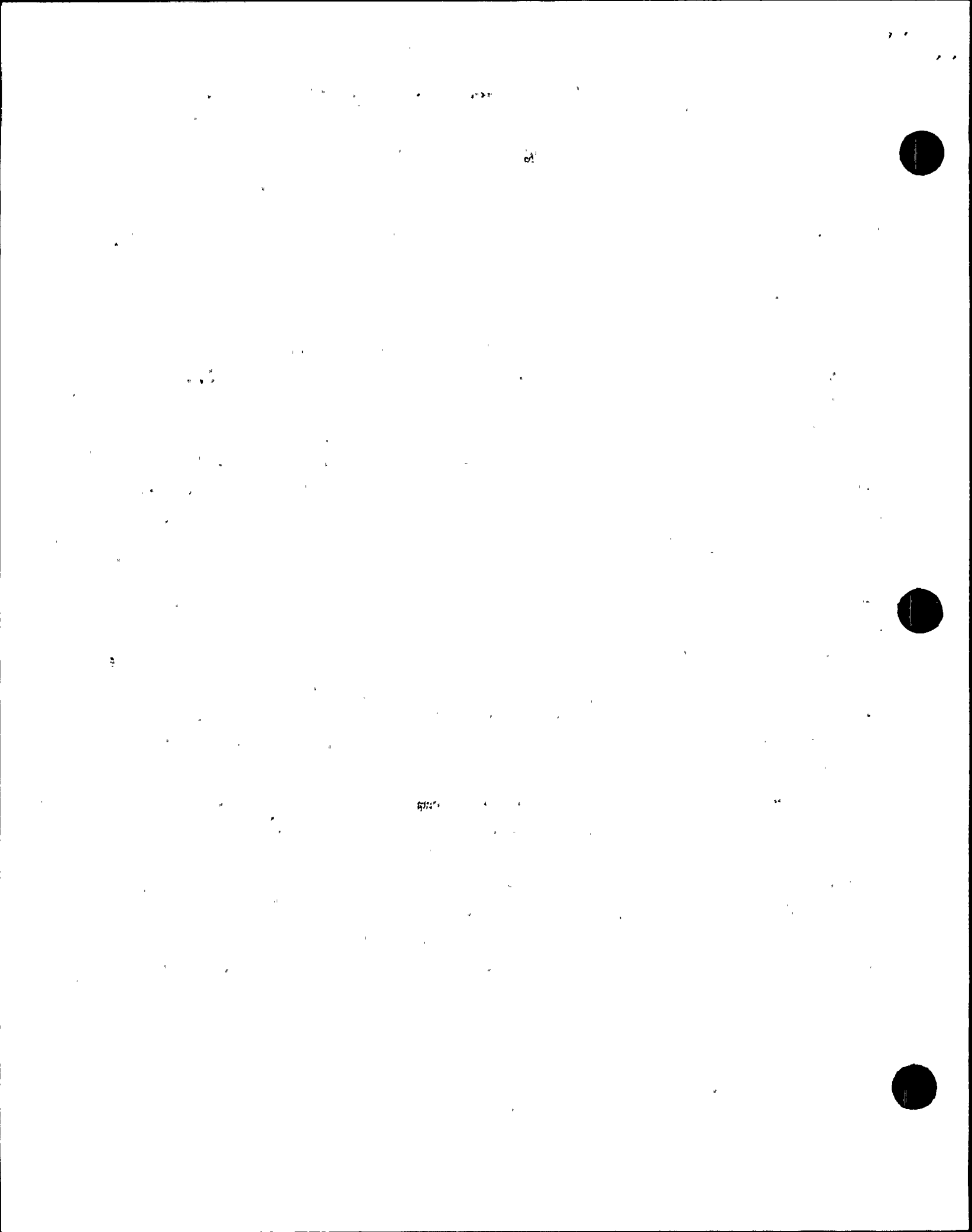
The basic geometry of the finite element mesh for the 30° segment model was determined from the fundamental cylindrical shell parameter \sqrt{Rt} , where R is the mean shell radius and t is the shell thickness. This parameter determines the magnitude of the bending boundary length and is a measure of the rate at which a uniformly applied circumferential disturbance "damps out" along the meridional direction of the shell. For the reactor vessel, this shell parameter is equal to 25 inches, and for the primary coolant nozzle it is equal to 14 inches. From Cygna's experience, when using simple shell elements, elements no larger than approximately $0.4 \sqrt{Rt}$ should be used within the regions where the highest bendings stress gradients are expected. Consequently, for the reactor vessel shell, the minimum element size selected was 8 inches, while for the nozzle a 6 inch minimum size was used.

In the circumferential direction of the vessel, the element length encompasses approximately 10° of arc, while in the nozzle

22.5° of arc was used. The 22.5° of arc was a compromise between efficiency and accuracy but was considered adequate for the accuracy required by the studies, since a model with 15° of arc (the "accepted" maximum) would have increased the model size by 50%. (As will be discussed in Section 5.3 of this report, this arc size was eventually reduced to 11.75° in the most highly stressed regions of the nozzle.)

Thin shell finite elements were used for both elastic and plastic analysis. Overall, more detailed behavior could have been achieved using thick shell elements, however, this would have required using three elements through the shell thickness which would have tripled the size of the basic model and would have made model development, analysis, and post-processing far too time consuming and expensive for pilot studies. Thus, from a cost, efficiency, and schedule point of view, the purpose of the pilot studies dictated that thin shell elements be used. From the standpoint of accuracy, the thin shell elements will error on the conservative side since through-thickness shear deformations are neglected in thin shell elements. This means that impact energy which would have been absorbed in shear deformation must now be expended in bending deformation, resulting in far higher surface normal stresses and strains than would have existed in the thick shell elements.

Initially, three thin shell quadrilateral finite element mesh configurations were developed and tested statically to determine the influence of certain mesh configurations on cost and accuracy. All three meshes gave comparable results which indicated that the model was stable and essentially independent of these configuration changes.



The nozzle supports were modeled with two quadrilateral elements which had an equivalent thickness calculated to duplicate the equivalent axial stiffness of the support from the nozzle to the concrete support structure.

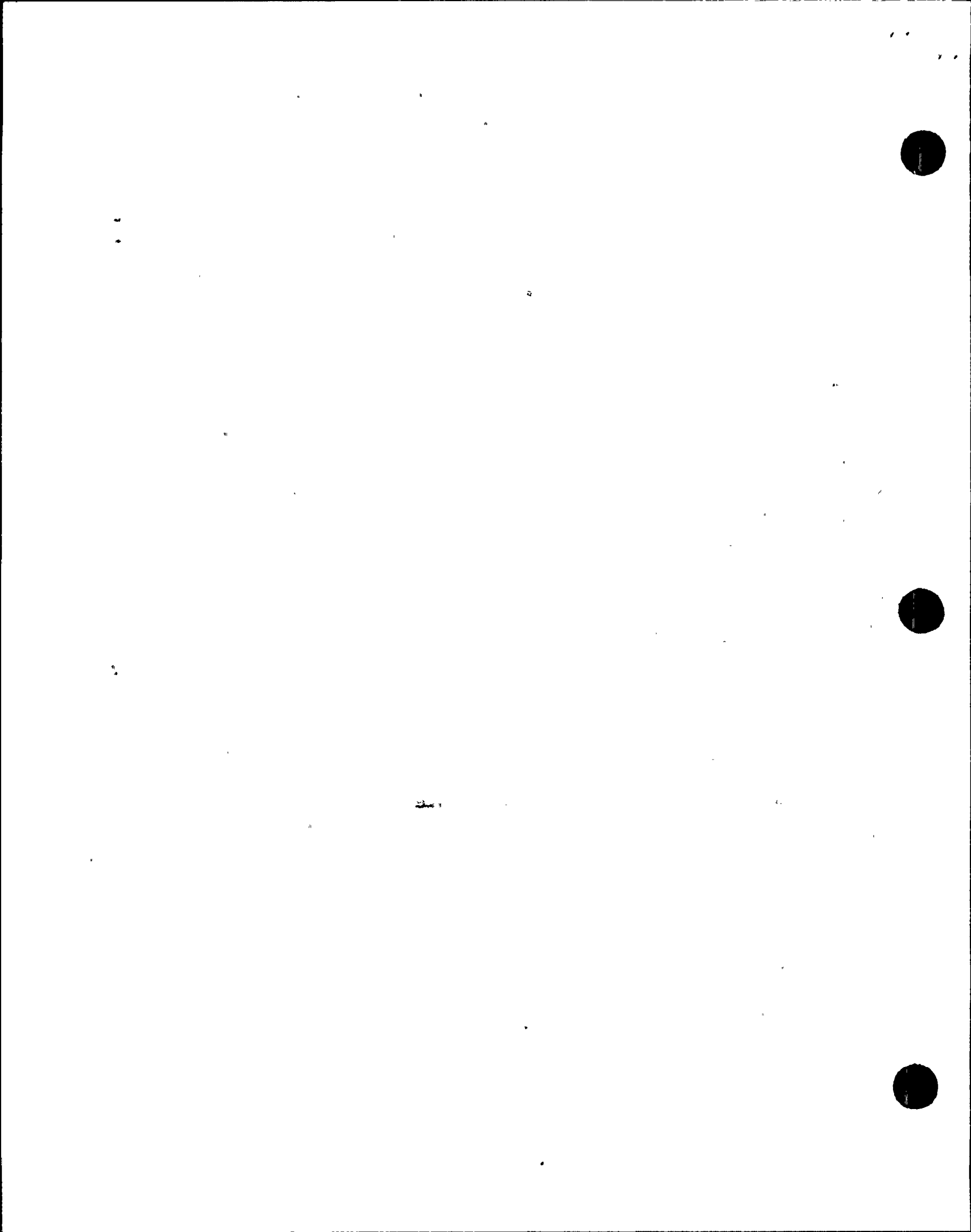
5.2 Uniform Drop Analysis

Description

The uniform drop analysis was performed on the basic finite element model described in Section 5.1. This model (30° circumferential segment) included one nozzle and its supporting pad, and was made from quadrilateral shell elements. The element and node numbers of this model for the upper shell, intermediate shell and primary coolant nozzle are shown in Figures 12 thru 19. To insure that the model was behaving properly, a static analysis was performed.

To simulate the uniform impact of the RPV head with the vessel flange four gap finite elements were used. These gap elements connect nodes 6 through 9 to nodes 10 through 13, respectively (Figure 13). A proportioned mass of the RPV head was placed at nodes 6 through 9, and the finite gap between the RPV head (nodes 6, 7, 8 & 9) and the RPV flange (nodes 10, 11, 12 & 13) was made to close within a prescribed time step so that the head would impact the flange at precisely 373 inches/second (i.e., the calculated velocity dropping through air from 15 feet).

An elastic dynamic impact analysis was then performed for a total duration of 5.0 milliseconds using a time step 0.010 milliseconds. This small time step was required to resolve the response of the vessel at the point of impact of the reactor head

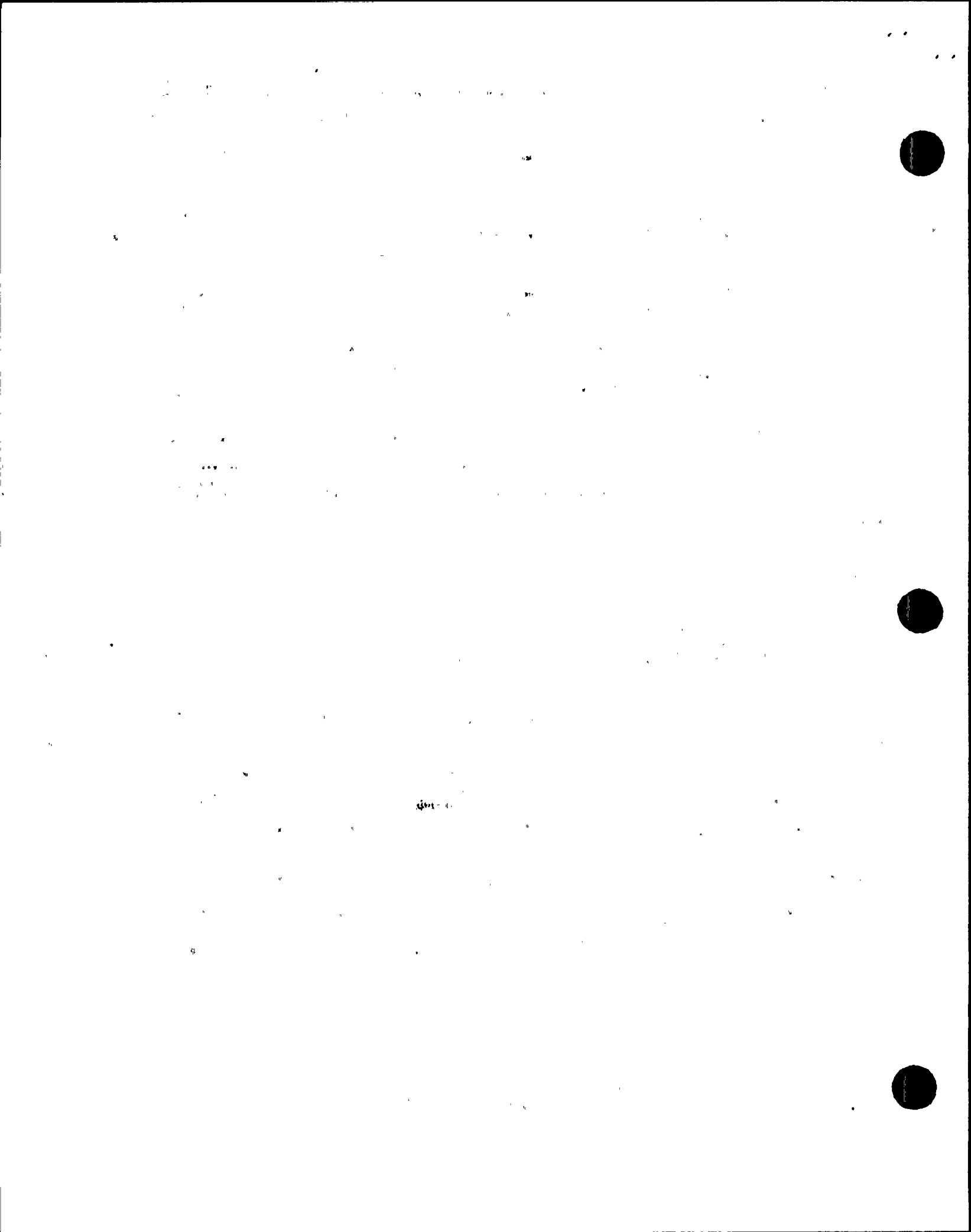


and to insure an accurate representation of the propagation of the compression wave through the smallest element of the vessel shell.

As required by NUREG-0612, the head was conservatively assumed to be rigid during impact; thus it absorbed no energy. In addition, the head mass also included the mass of the lifting device and hook block. All elements were assumed to remain elastic for the uniform drop.

Discussion of Results

When the RPV head is dropped from 15 feet above the vessel, the uniform impact of the head with the flange initially produces very high contact forces of extremely short duration (Figure 20). As the flange begins to displace downward (Figure 21) the compression stress wave propagates through the vessel shell, eventually reaching and displacing the bottom of the vessel as it is reflected from the bottom edge (Figure 22). During this time, high reaction forces develop at the nozzle support (Figure 23). These high reaction forces rotate and deform the nozzle to produce high stresses in the bottom of the nozzle at the nozzle/vessel intersection. The maximum equivalent stress anywhere in the vessel model occurs at this location (element 60, node 35) (Figures 13, 16, 17). The magnitude of this maximum equivalent stress is approximately 200,000 psi, which is well above the material yield point of 50,000 psi, and occurs at 2.36 milliseconds after impact (Figure 24). (The equivalent stress, or Von Mises stress, is used to identify the onset of yielding in a material subjected to a general state of stress. When the equivalent stress for a general state of stress exceeds the yield point in simple tension, the material yields in the general state



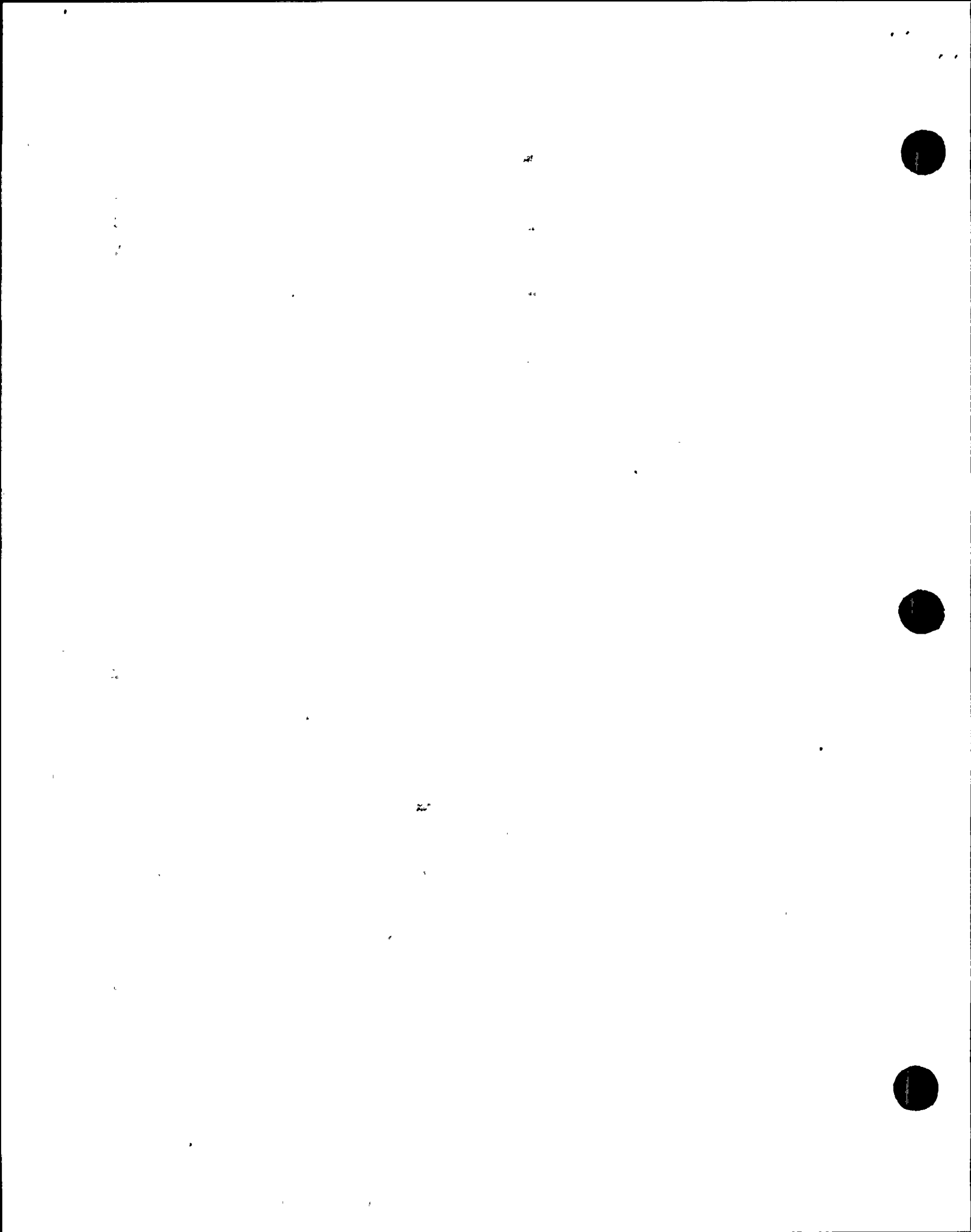
of stress.) The RPV flange does not yield during impact and, as might be expected, general yielding is confined to the nozzle and upper shell within the vicinity of the nozzle/vessel intersection.

It is not possible from this elastic analysis to determine the magnitude of the maximum plastic strains which will occur in the vessel during a uniform drop of the RPV head because the vessel is highly indeterminate. As a consequence, the initiation of plasticity within the vessel will lead to a complex redistribution of internal forces and an overall softening of the dynamic response. However, the maximum plastic response of the vessel during a uniform drop is bounded by the results of the concentrated drop analysis since the total impact kinetic energy of the reactor head in the concentrated drop analysis is six times the energy input to the uniform drop analysis.

5.3 Concentrated Drop Analysis

Description

The initial concentrated drop analyses were performed on the model developed for the uniform drop. Using this model, a dynamic analysis was performed to determine the extent to which the elastic quadrilateral elements exceeded the minimum elastic limit when subjected to a heavy concentrated drop. Those elements identified as potentially capable of developing plastic strains were modified to triangular plasticity elements as required by the element library of the ANSYS program. On the basis of additional analyses, this model was further refined, eventually evolving into the final model shown in Figures 25 thru 38.



To simulate the concentrated impact of the RPV head with the vessel flange, a single gap finite element connecting nodes 6 and 10, was used (Figure 31). Since the 30° segment finite element model constitutes half of a single nozzle segment of the reactor, only one half of the total mass of the RPV head was placed at node 6. The finite gap between the RPV head (node 6) and the RPV flange (node 10) was made to close within a prescribed time step so that the head would impact the flange at precisely 385 inches/second (Figure 51), thus simulating a drop in air of the center of mass of the RPV head through 16 feet.

Using a time step of 0.010 milliseconds, the nonlinear dynamic analysis was then performed for a total duration of 13.0 milliseconds. Lower bound material properties were conservatively assumed with no increase in strength taken for dynamic effects. To insure that maximum energy was absorbed by the nozzle and vessel, the support pad beneath the nozzle was required to remain elastic during all plasticity analyses. As before, the head was conservatively assumed to be rigid during impact; thus it absorbed no energy. In addition, the head mass also included the mass of lifting device and hook block.

Based on the results of this nonlinear dynamic analysis, it became evident that the likelihood was high that the reactor could maintain core cooling after a concentrated head drop from 16 feet, and that a PRA approach would be unnecessary. However, the results from the pilot study models were not refined enough in the most highly stressed regions of the vessel to effectively determine the magnitude of the highest strains. Therefore, Cygna initiated a number of model changes to further refine the finite element mesh in the highly strained tensile region of the vessel/nozzle intersection to insure that the high strain gradients in



this region were not missed in the analysis. This refinement resulted in the ratio of the smallest element dimension in the direction of the strain gradient to the \sqrt{Rt} being equal to 0.2. A nonlinear dynamic analysis was then performed with the refined model using the same time step and duration. The intent of this analysis was to demonstrate that the vessel could inherently absorb sufficient strain energy through plastic deformation without jeopardizing the structural integrity of a single nozzle under the most adverse conditions and with the most conservative assumptions possible.

Discussion of Results

When the RPV head is dropped from 16 feet above the vessel, the concentrated impact of the head with the flange at a point directly above the nozzle (node 10) (Figure 31) produces a nearly a constant contact force of 10 million pounds for a duration of approximately 11 milliseconds (Figure 39). As the flange begins to displace downward (Figure 40), the compressive stress wave propagates through the vessel shell, eventually reaching and displacing the bottom of the vessel (Figure 41). In a local region directly under the point of contact, large amounts of plastic deformation occur, and a considerable amount of strain energy is absorbed. In fact, 52 percent of the initial kinetic energy of the RPV head (Figure 42) is absorbed as strain energy within elements 4 and 5 (Figures 43 & 44). The average strain energy density within these two elements is 2500 in-lbs/cubic inch. The local nature of this plastic deformation is obvious from Figure 40 which shows the displacement of the nodes at the top of the flange. The local nature of this high plasticity is further illustrated by the fact that the total strain energy absorbed by all of the adjacent elements (elements 6, 7, 8, 9,



10 & 24) (Figure 29) amounts to only 10 percent of the initial kinetic energy.

The maximum reaction within the nozzle support pad is slightly greater than 16 million pounds and occurs at 5.5 milliseconds after impact (Figure 45). This reaction is quite high; nevertheless, the support stresses remain within the elastic range, which is consistent with the assumption made in the nonlinear dynamic model.

The most highly stressed tensile region of the reactor vessel is in the bottom of the nozzle at the intersection of the nozzle and vessel shell. The maximum equivalent strain at the intersection is 0.044 in/in and occurs within element 106 at 7.0 milliseconds after impact (Figure 46). This maximum strain is well below the acceptance strain level for nozzle integrity by a factor of 1.9. However, due to the presence of the geometric discontinuity at the intersection of the nozzle and vessel shell, a strain concentration will occur. This in turn will increase the maximum equivalent strain at the intersection. Based on the ratio of nozzle fillet radius to shell thickness, the strain concentration factor is approximately 1.4. An estimate of the peak equivalent strain can be made by multiplying the maximum equivalent strain by the strain concentration factor. This results in an estimated peak equivalent strain of 0.062 in/in which is well below the acceptance strain for nozzle integrity by a factor of 1.37. The peak strain rate of 22 in/in/second (15.5×1.4) occurs at 2.3 milliseconds after impact (Figure 47) and is well below the acceptance value for nozzle integrity. Therefore, the nozzle remains intact.

The two safety injection nozzles are each located adjacent to a primary coolant inlet nozzle. Their location corresponds closely



The page contains extremely faint and illegible text, likely bleed-through from the reverse side of the document. The text is scattered across the page and cannot be transcribed.

with node 34 (Figure 31) on the finite element model. The vertical and radial displacements and rotation of this node are shown in Figures 48, 49 and 50. Based upon the magnitude of these displacements and the layout of the safety injection piping, the stresses in the safety injection piping should remain within the elastic range during a concentrated head drop event, thereby insuring the integrity of the safety injection system.

It has already been noted that the energy absorbed in plastic deformation at the point of impact of the reactor head with the flange is approximately 52% of the total kinetic energy of the reactor head at the moment of impact. In the unlikely event of an actual head drop, much of the remaining kinetic energy, which has been assumed in the analysis to be totally absorbed by a single nozzle and support, would be absorbed by the adjacent nozzle on one side and lug support on the other. (A simple static calculation shows that for a concentrated force applied directly to the flange above a nozzle, 56% of this force is reacted by the nozzle support directly beneath the applied force and 22% is reacted by each of the adjacent nozzle/lug supports.) In the actual situation, when the nozzle directly under the point of impact begins to absorb energy in plastic deformation, the adjacent nozzle and lug support would be absorbing energy elastically. The plastic "softening" of the nozzle would result in a significant redistribution of forces from the plastically deforming nozzle to the adjacent nozzle and lug support. As this redistribution continues, the adjacent nozzle and lug support would begin to deform plastically and absorb large amounts of energy. In addition, it is important to note that the mass of the resisting structure (30° segment model) grossly underestimates the effective mass of the actual vessel that would be mobilized during the impact. By underestimating the active mass of the



vessel, the inertial resistance of the vessel is reduced and vessel response (stresses, strains and displacements) is increased. Therefore, since all of the energy which could be absorbed by the adjacent supports has been neglected, and since the resisting mass of the adjacent portions of the reactor has been neglected, and in view of the numerous other conservative assumptions already mentioned, the calculated peak equivalent strain of 0.062 in/in is considered a very conservative upper bound.

6.0 CONCLUSION AND RECOMMENDATIONS

Cygna's analyses have conservatively demonstrated that the RPV head can be dropped through air from a clear height of 16 feet above the vessel flange while still maintaining the integrity of the vessel support system. With the vessel support system intact, core cooling is maintained, since, as an absolute minimum, the integrity of the safety injection nozzles is assured.

Based on the results of these analyses, the reactor pressure vessel can withstand the consequences of a postulated head drop from a height of 16 feet. However, the present operating procedures call for the head to be lifted to an elevation above the operating floor level (i.e., a lifted height greater than 23 feet) before moving to the south over the refueling cavity floor area.

Cygna recommends that the RPV head lifting procedures be modified slightly to allow the head to move laterally to the south as soon as the head safely clears the guide studs. The head should be moved sufficiently to the south to completely clear the area over the vessel before proceeding vertically again. This recommendation is made for the following reasons:



1. The vessel can withstand a postulated head drop under this revised procedure.
2. Moving the head away from the area directly over the core is most consistent with the NRC's "defense in depth" philosophy with regards to NUREG-0612.
3. The horizontal load path traversed by this revised procedure is the same as for the current procedure. The head would not be lifted over any different area.

APPENDIX A

References

REFERENCES

1. Instruction Manual - Reactor Pressure Vessel, RGE-105, The Babcock and Wilcox Company, Contract No. 610-0110.
2. ANSYS Engineering Analysis System User's Manual, Revision 4.1, Swanson Analysis System, Inc., Houston, PA.
3. ANSYS Engineering Analysis System Theoretical Manual, November 1977, Swanson Analysis Systems, Inc., Houston, PA.
4. Theory and Design of Modern Pressure Vessels, by John F. Harvey, Second Edition, Van Nostrand Reinhold Co., 1974.
5. Roark, Hartenberg and Williams: "Influence of Form and Scale on Strength", Engineering Experiment Station, University of Wisconsin Bulletin, 1938.
6. Gilbert Associates, Inc., Drawing Nos. D-421-018, Rev. 5; D-421-051, Rev. 0; D-421-052, Rev. 0; D-521-044, Rev. 10 and D-521-046, Rev. 5.
7. Babcock and Wilcox Co., Drawing Nos. 117825E, Rev. 5, 117820E, Rev. 5.
8. Letter: M. Fitzsimmons (RG&E) to J. McWilliam (Cygna) 8/10/83.
9. Letter: M. Fitzsimmons (RG&E) to J. McWilliam (Cygna) 8/12/83.
10. Letter: M. Fitzsimmons (RG&E) to J. McWilliam (Cygna) 8/22/82.

APPENDIX B

Figures 1 through 51



LIST OF FIGURES

1. Reactor Pressure Vessel Cross Section
2. Reactor Pressure Vessel - Longitudinal Section Dimensions
3. Reactor Pressure Vessel - Horizontal Section through Nozzles
4. Reactor Vessel with Reactor Head Attached
5. Reactor Head at Top of Guide Studs
6. Reactor Head Decoupled from Guide Studs
7. Reactor Head Uniform Drop
8. Nonuniform Drop of Reactor Head
9. Reactor Head Concentrated Drop - Impact Directly above Nozzle
10. ANSYS Finite Element Model for Uniform Drop Analysis - Side View of Complete Model
11. ANSYS Finite Element Model for Uniform Drop Analysis - 3D Hidden Line Plot of Complete Model
12. Element Numbers for the Flange and Upper Shell Portions of the Uniform Drop Model

13. Node Numbers for the Flange and Upper Shell Portions of the Uniform Drop Model
14. Element Numbers for the Extended Intermediate Shell Portion of the Uniform Drop Model
15. Node Numbers for the Extended Intermediate Shell Portion of the Uniform Drop Model
16. Nozzle Element Numbers for the Uniform Drop Model
17. Nozzle Node Numbers for the Uniform Drop Model
18. Support Saddle Element Numbers for the Uniform Drop Model
19. Support Saddle Node Numbers for the Uniform Drop Model
20. Contact Force (lbs) between the Reactor Head and Vessel Flange for a Uniform Drop versus Time (seconds)
21. Displacement (inches) of Nodes 10, 11, 12 and 13 at the Top of the Reactor Vessel Flange for a Uniform Drop versus Time (seconds)
22. Displacement (inches) of Node 61 at the Bottom of the Vessel for a Uniform Drop versus Time (seconds)
23. Reaction Force (lbs) at the Nozzle Support for a Uniform Drop versus Time (seconds)
24. Equivalent Stress (psi) in Element 60 at Node 35 versus Time (seconds)

25. ANSYS Finite Element Model for Concentrated Drop Analysis -
3D Hidden Line Plot of Complete Model
26. ANSYS Finite Element Model for Concentrated Drop Analysis -
3D Hidden Line Plot of the Vessel Flange and Upper Shell
27. ANSYS Finite Element Model for Concentrated Drop Analysis -
Side View of Complete Model
28. ANSYS Finite Element Model for Concentrated Drop Analysis -
Front View of Complete Model
29. Element Numbers for the Flange and Upper Shell Portions of
the Concentrated Drop Model
30. Element Numbers for the Lower Half of the Upper Shell
Portion of the Concentrated Drop Model
31. Node Numbers for the Flange and Upper Shell Portions of the
Concentrated Drop Model
32. Node Numbers for the Lower Half of the Upper Shell Portion
of the Concentrated Drop Model
33. Element Numbers for the Extended Intermediate Shell Portion
of the Concentrated Drop Model
34. Node Numbers for the Extended Intermediate Shell Portion of
the Concentrated Drop Model
35. Nozzle Element Numbers for the Concentrated Drop Model -
Side View



36. Element Numbers for the Lower Half of the Nozzle - Top View, Concentrated Drop Model
37. Nozzle Node Numbers for the Concentrated Drop Model - Side View
38. Node Numbers for the Lower Half of the Nozzle - Top View, Concentrated Drop Model
39. Contact Force (lbs) between the Reactor Head and Vessel Flange for a Concentrated Drop versus Time (seconds)
40. Displacement (inches) of Nodes 10, 11, 12 and 13 at the Top of the Reactor Vessel Flange for a Concentrated Drop versus Time (seconds)
41. Displacement (inches) of Node 61 at the Bottom of the Vessel for a Concentrated Drop versus Time (seconds)
42. Kinetic Energy (inch-pounds) of the Reactor Head versus Time (seconds)
43. Strain Energy (inch-pounds) Absorbed by Element 4 versus Time (seconds)
44. Strain Energy (inch-pounds) absorbed by Element 5 versus Time (seconds)
45. Reaction Force (lbs) at the Nozzle Support for a Concentrated Drop versus Time (seconds)
46. Equivalent Strain at the Top (Positive Face) and Bottom (Negative Face) of Element 106 for a Concentrated Drop versus Time (seconds)

47. Equivalent Strain Rate (in/in/sec) at the Top (Positive Face) of Element 106 for a Concentrated Drop versus Time (seconds)
48. Vertical Displacement (inches) of Node 34, which is the approximate location of the Safety Injection Nozzle, versus Time (seconds)
49. Radial Displacement (inches) of Node 34, which is the approximate location of the Safety Injection Nozzle, versus Time (seconds).
50. Rotation (radians) about the Circumferential Axis of Node 34, which is the Approximate Location of the Safety Injection Nozzle, versus Time (seconds)
51. Reactor Head Velocity (inches/second, Node 6) versus Time (seconds)

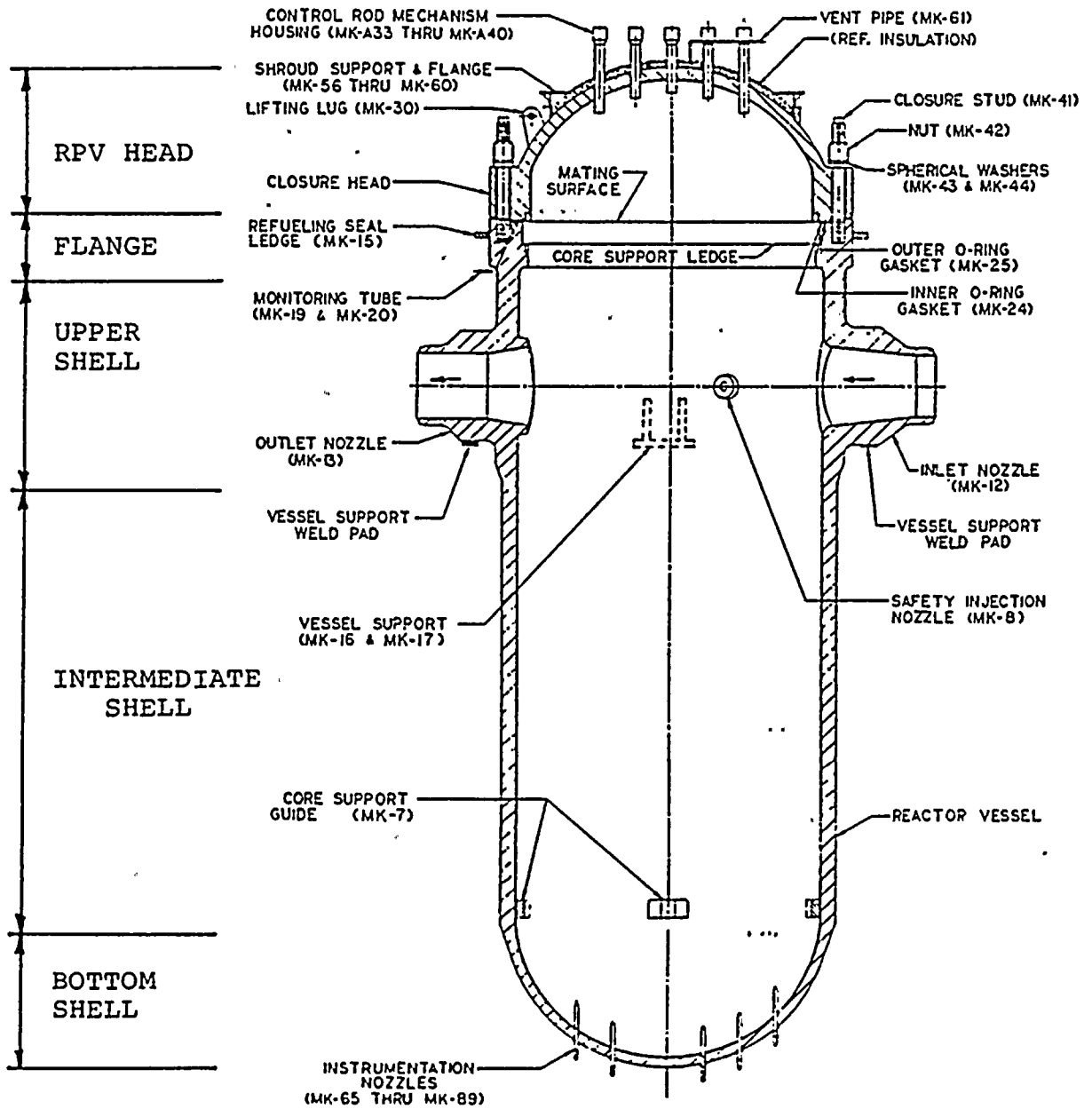


FIGURE 1: Reactor Pressure Vessel Cross Section

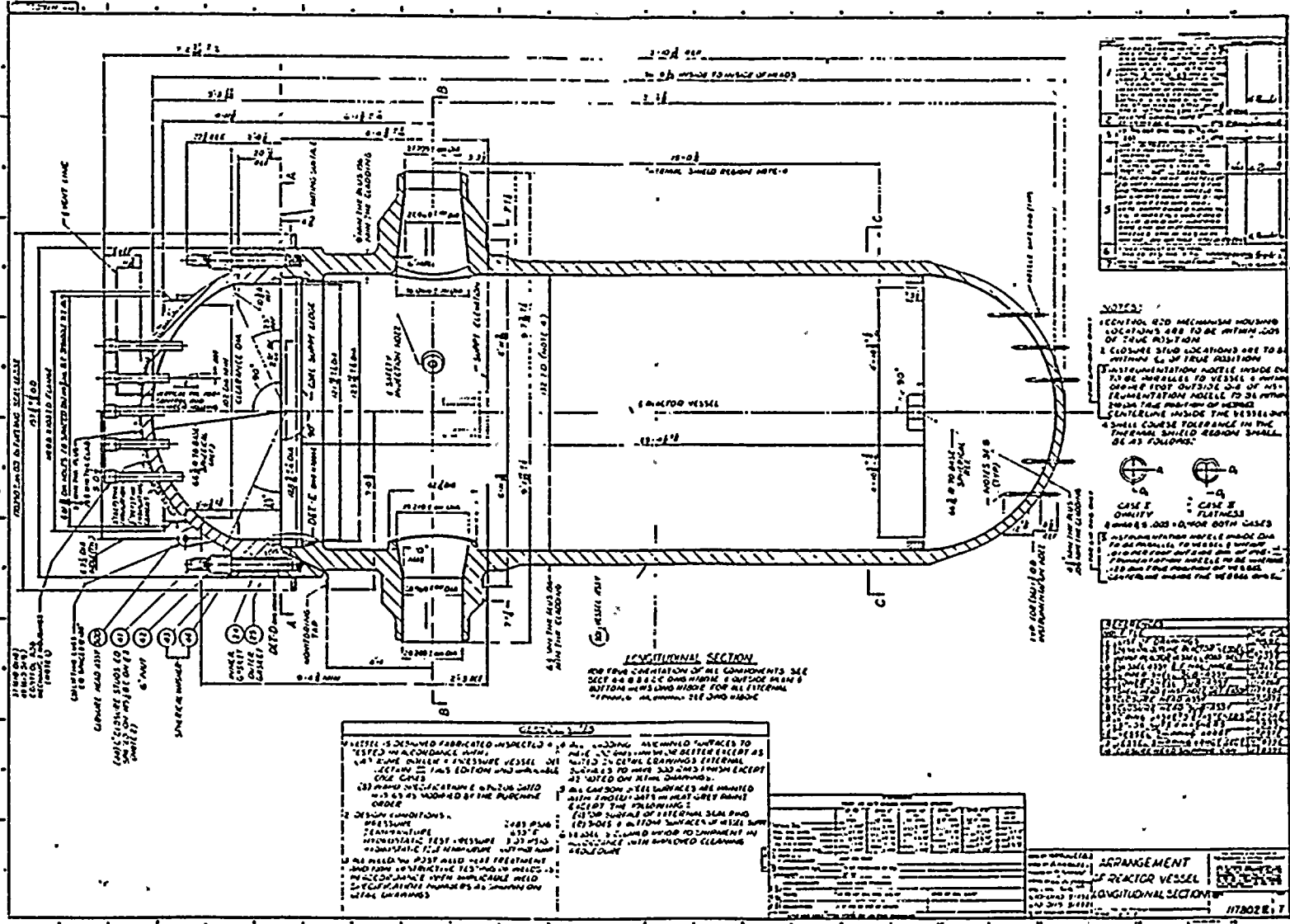


FIGURE 2: Reactor Pressure Vessel - Longitudinal Section Dimensions





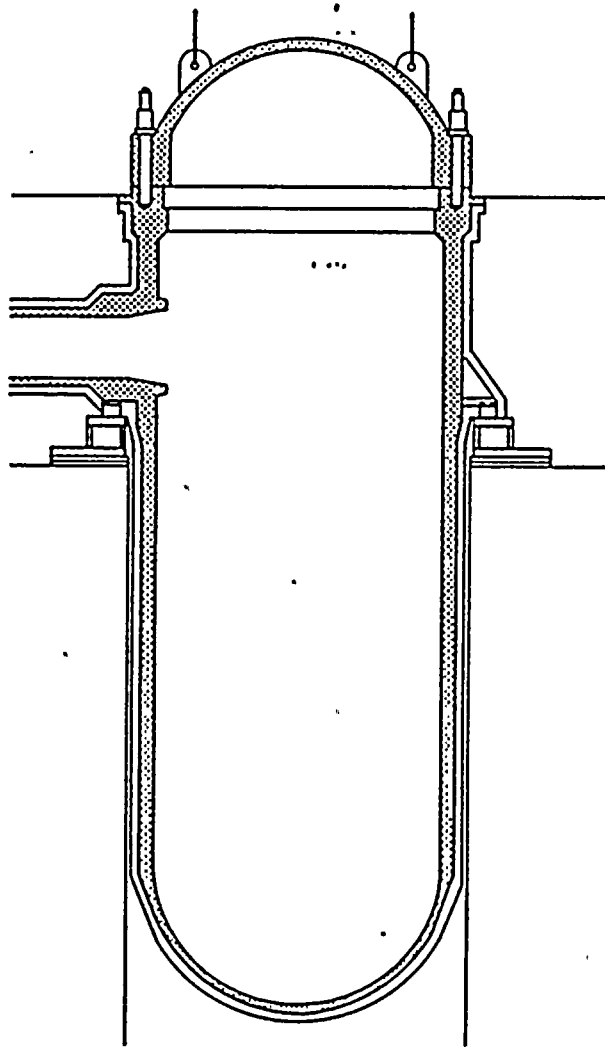


FIGURE 4: Reactor Vessel with Reactor Head Attached

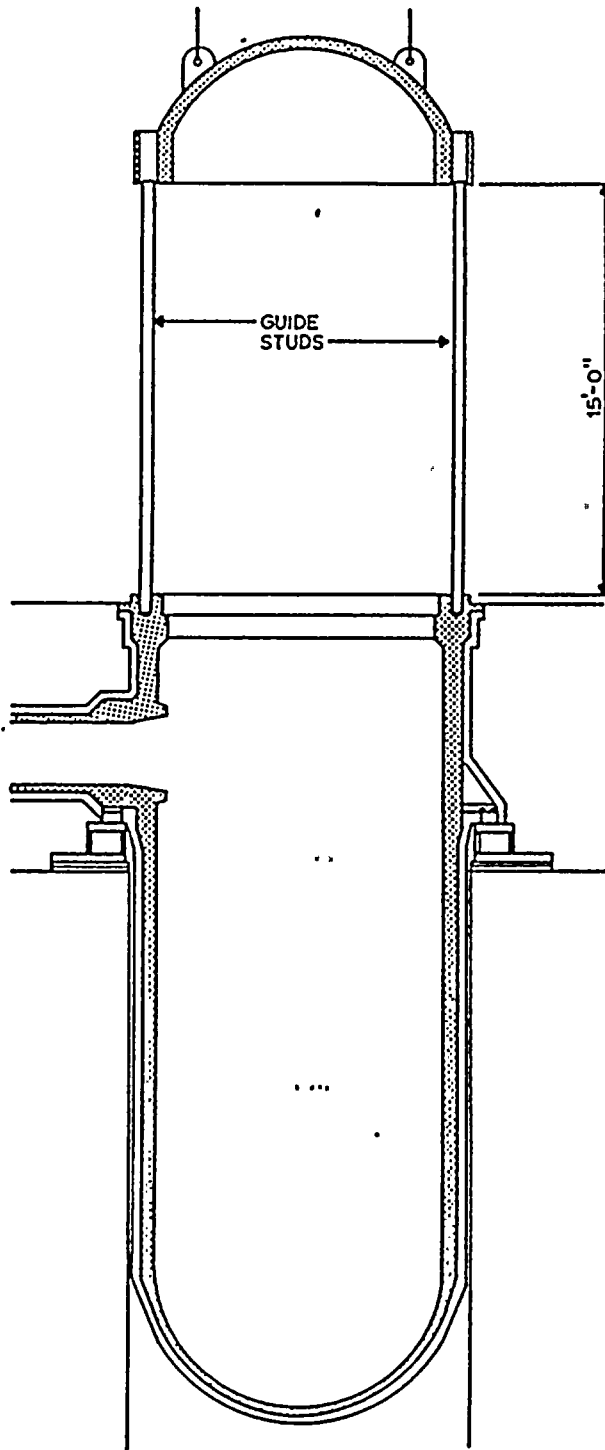


FIGURE 5: Reactor Head at Top of Guide Studs

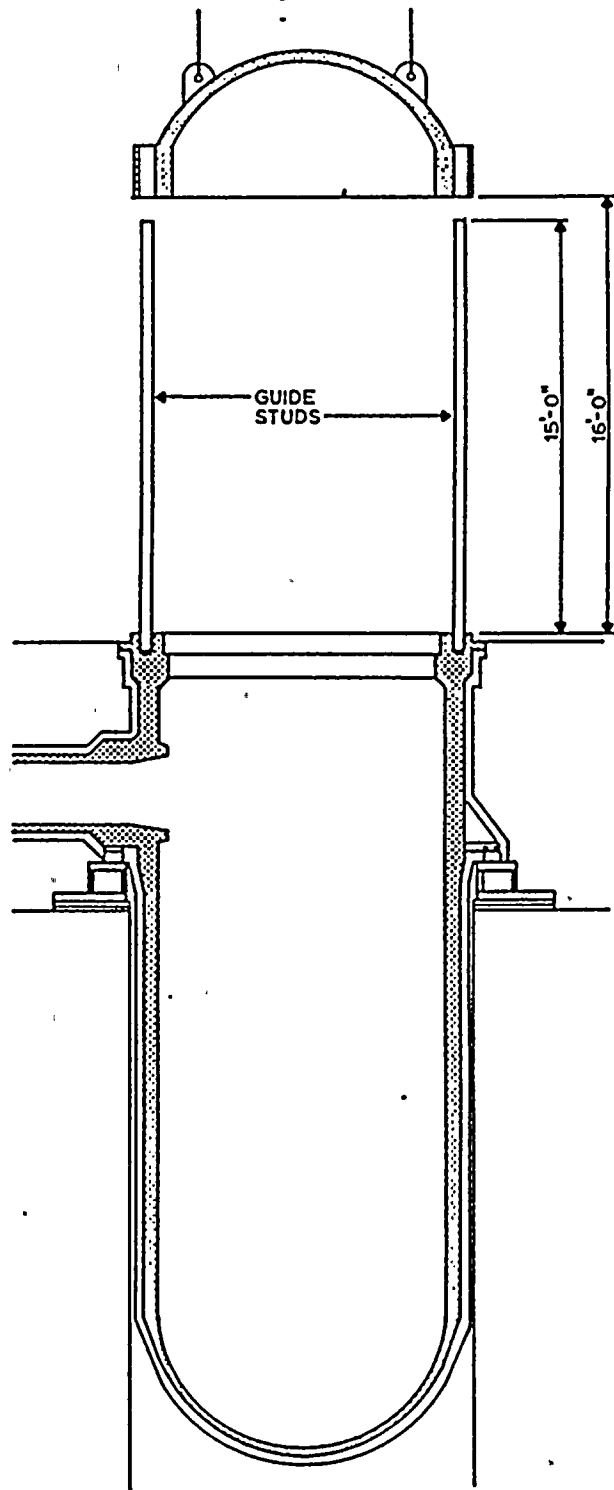


FIGURE 6: Reactor Head Decoupled from Guide Studs



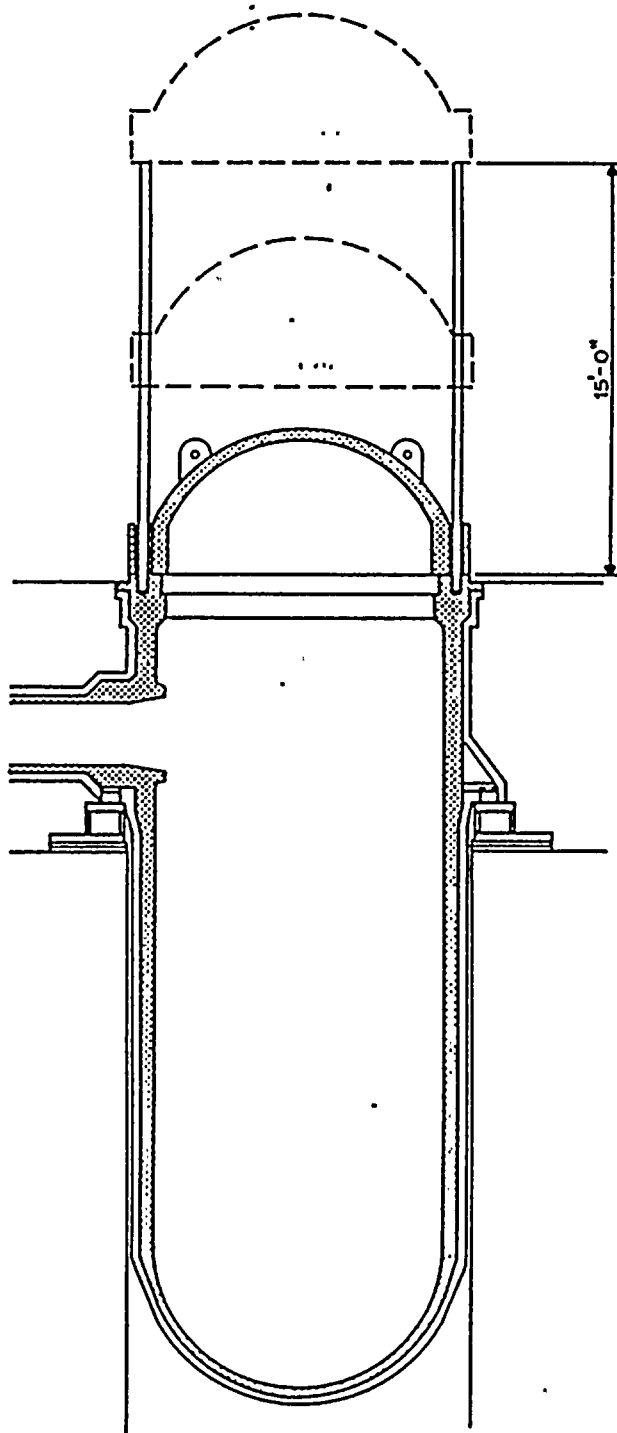


FIGURE 7: Reactor Head Uniform Drop



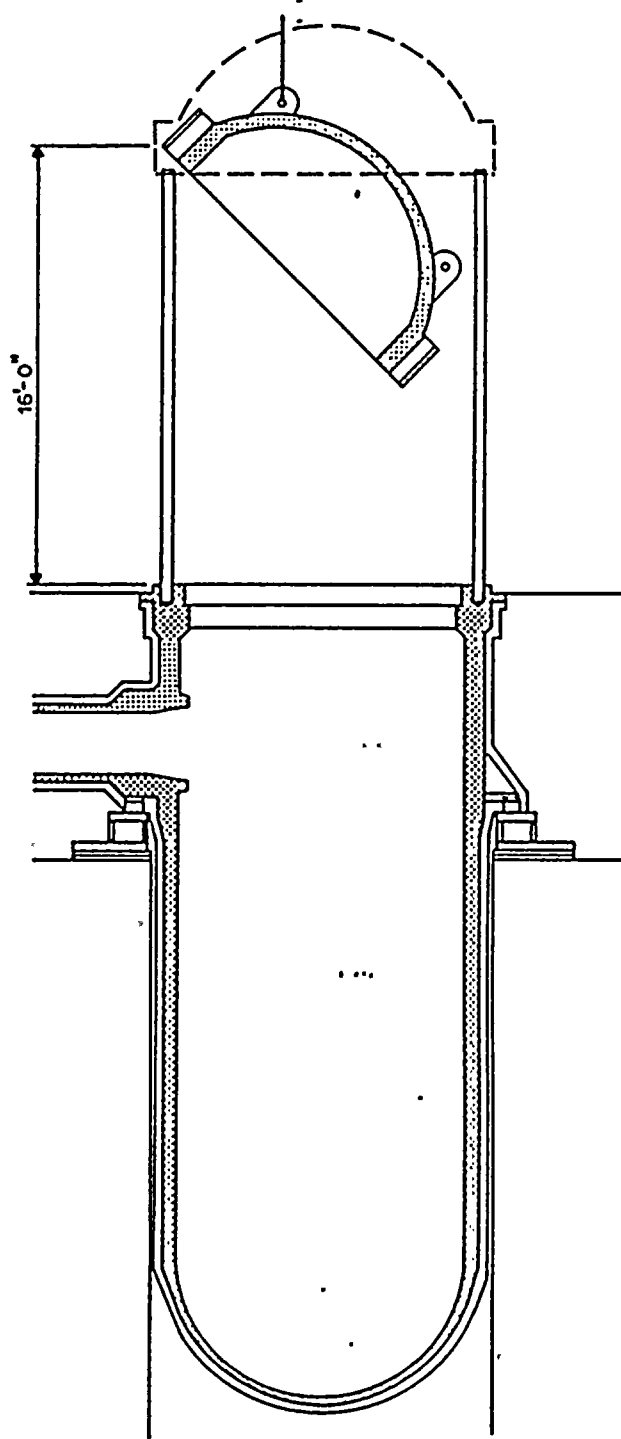


FIGURE 8: Nonuniform Drop of Reactor Head

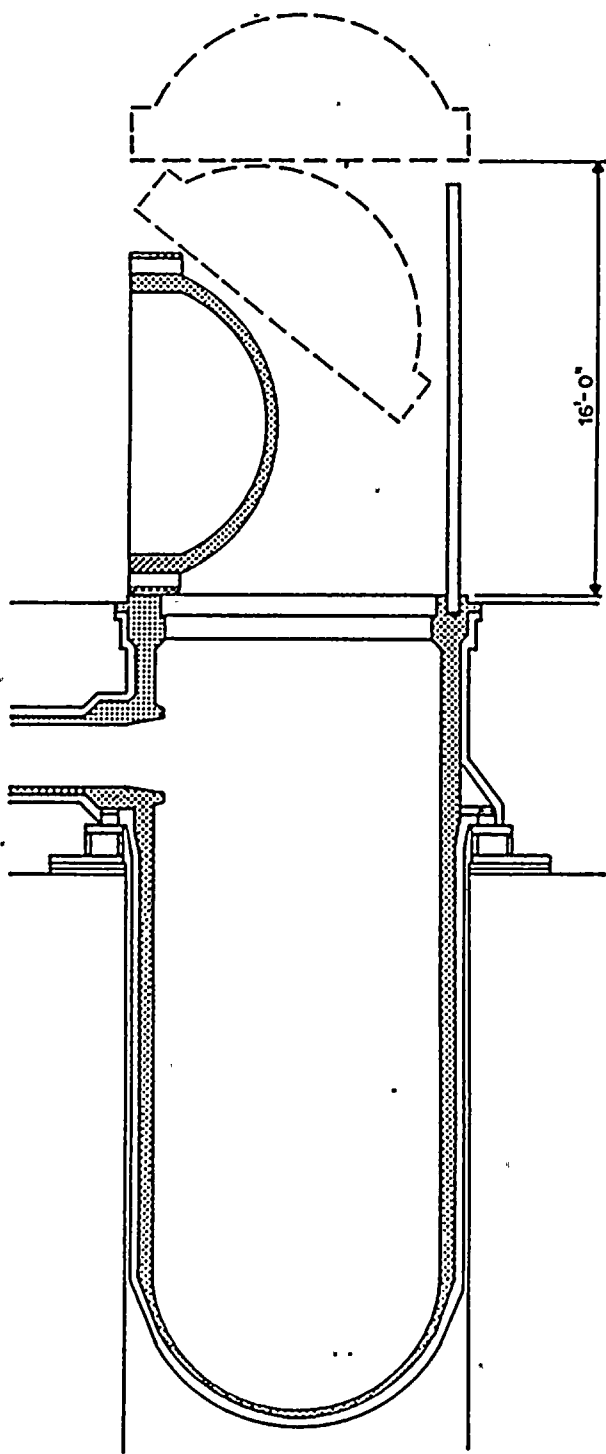


FIGURE 9: Reactor Head Concentrated Drop - Impact Directly above Nozzle

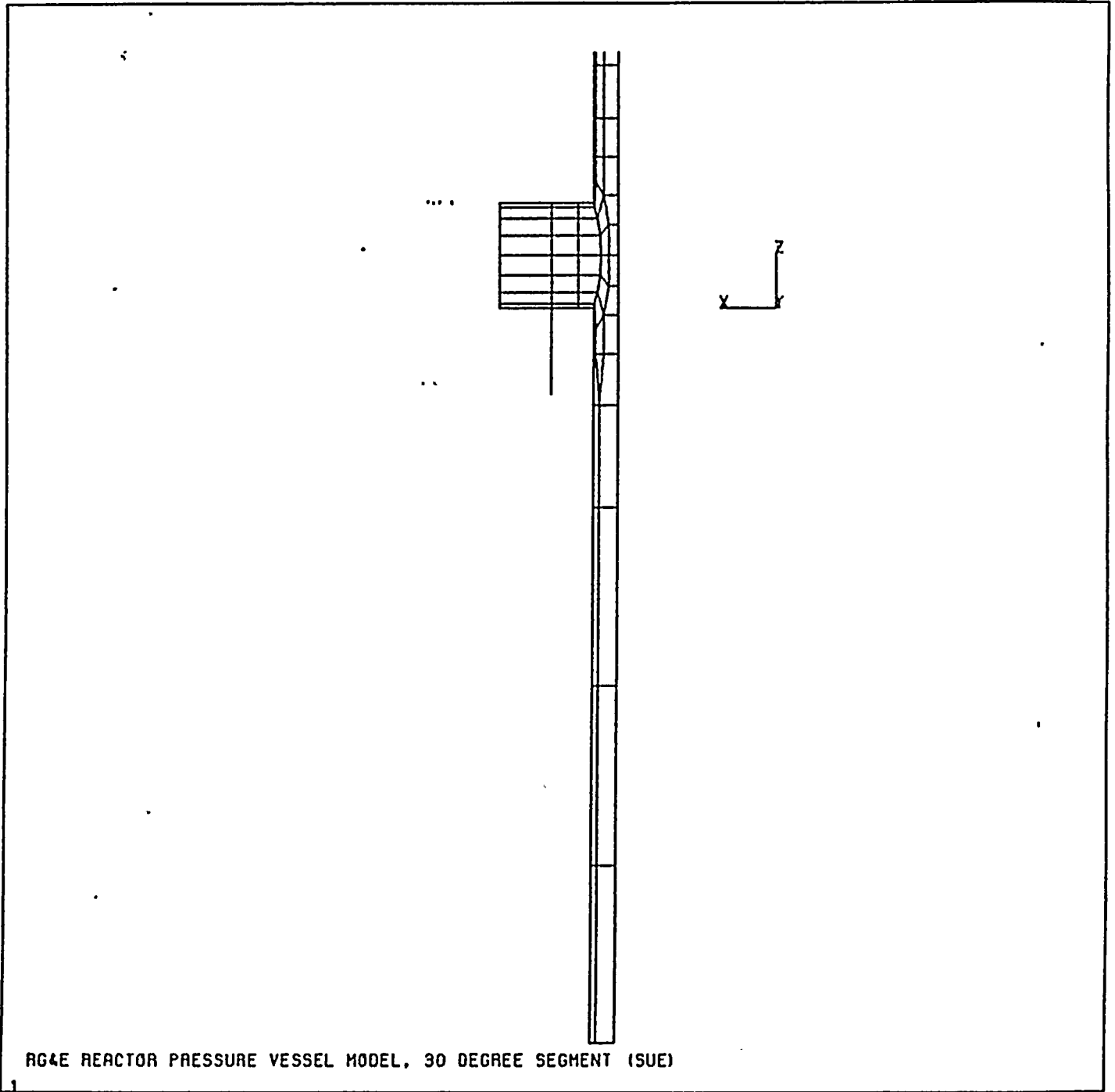


FIGURE 10: ANSYS Finite Element Model for Uniform Drop Analysis - Side View of Complete Model



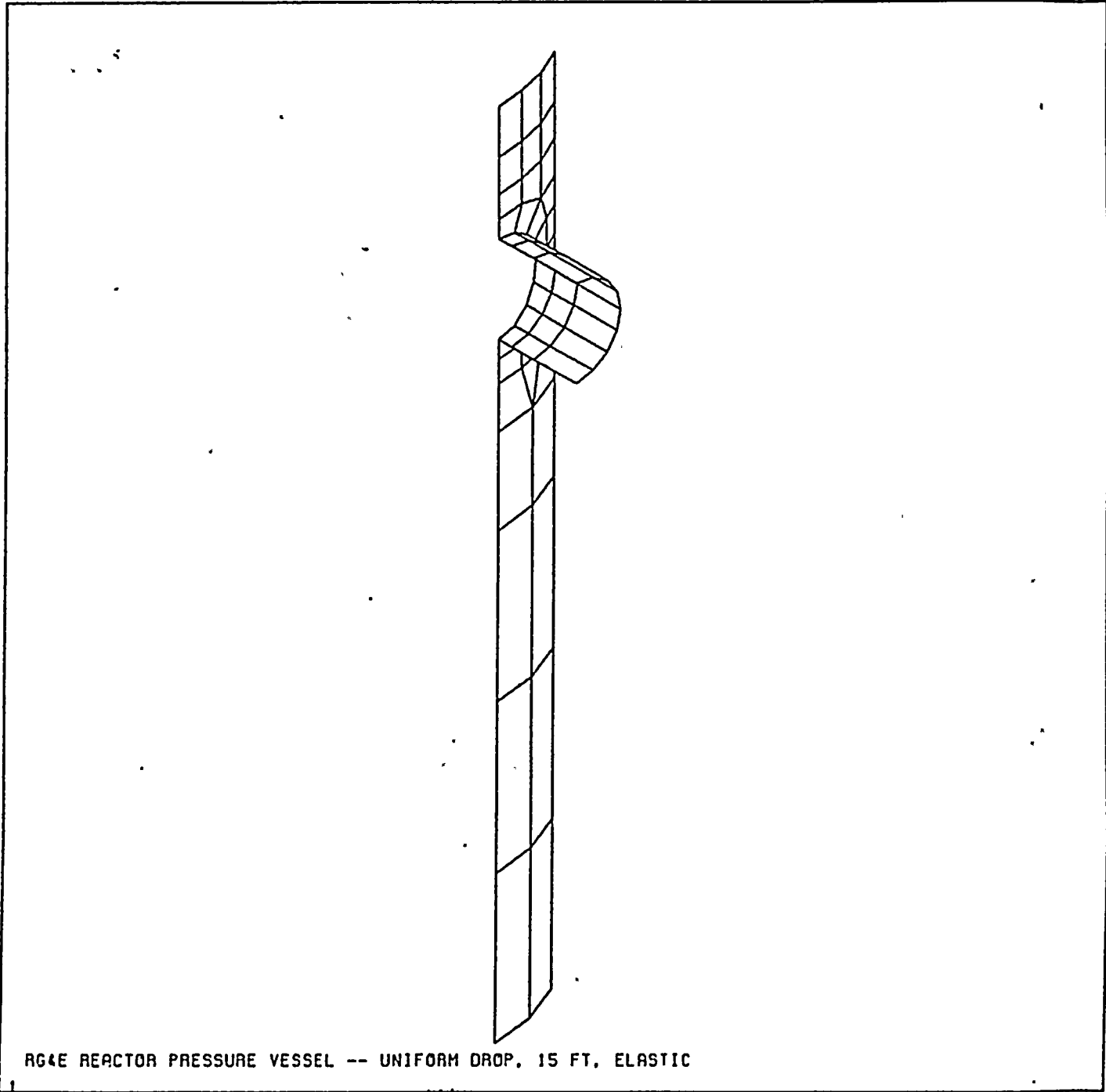
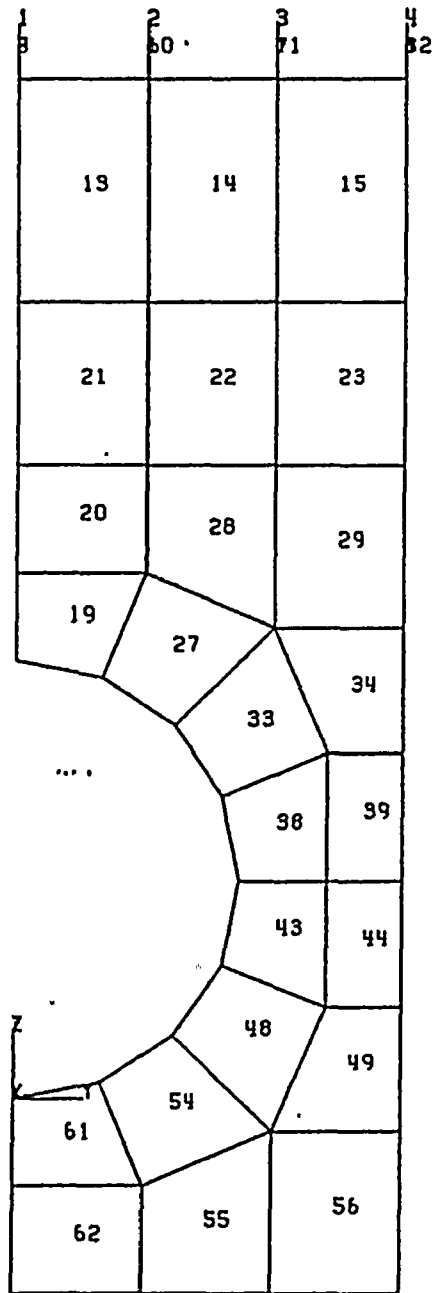


Figure 11: ANSYS Finite Element Model for Uniform Drop Analysis - 3D Hidden Line Plot of Complete Model





RG&E REACTOR PRESSURE VESSEL MODEL, 30 DEGREE SEGMENT (SUE)

FIGURE 12: Element Numbers for the Flange and Upper Shell Portions of the Uniform Drop Model

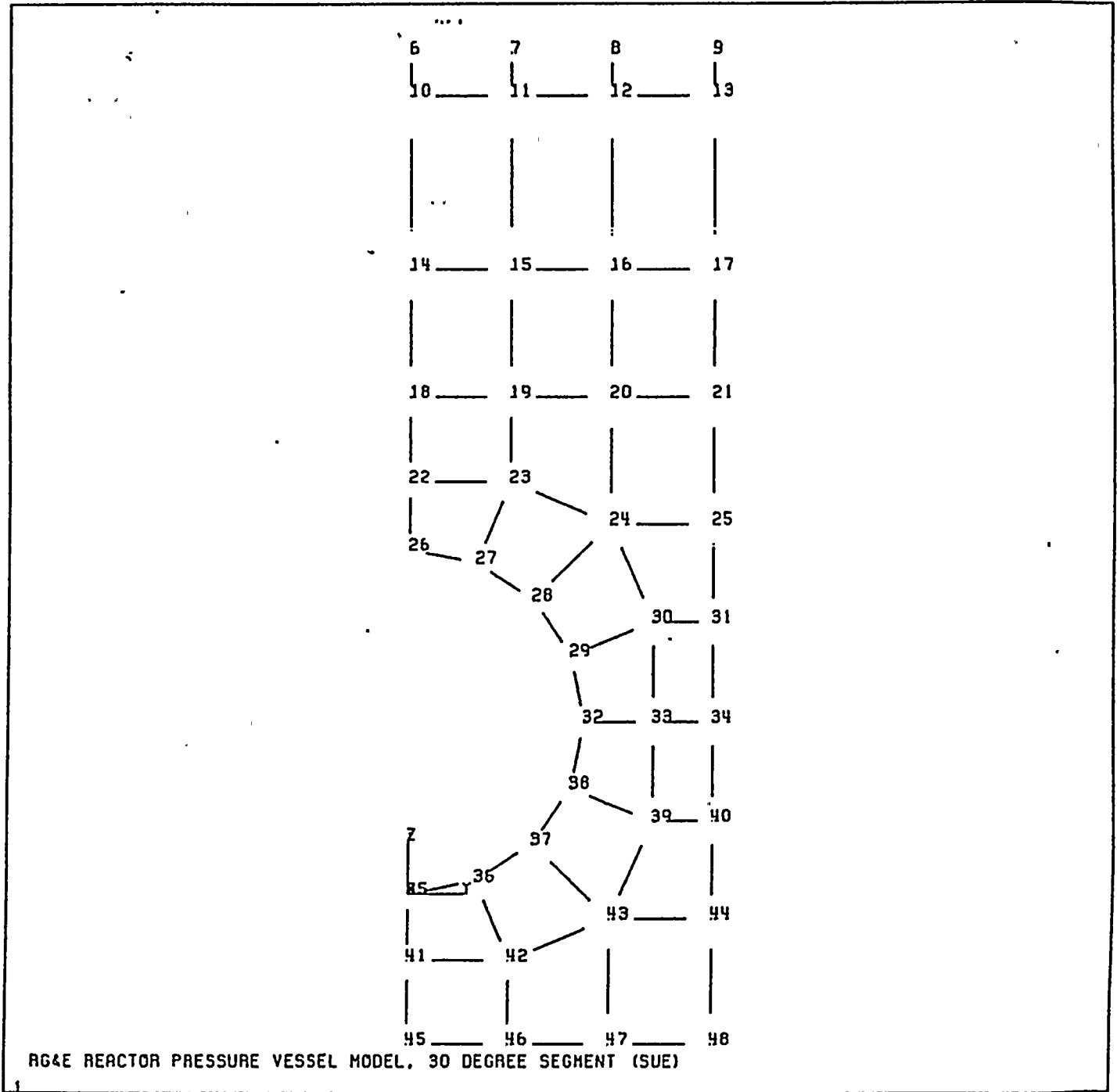


FIGURE 13: Node Numbers for the Flange and Upper Shell Portions of the Uniform Drop Model

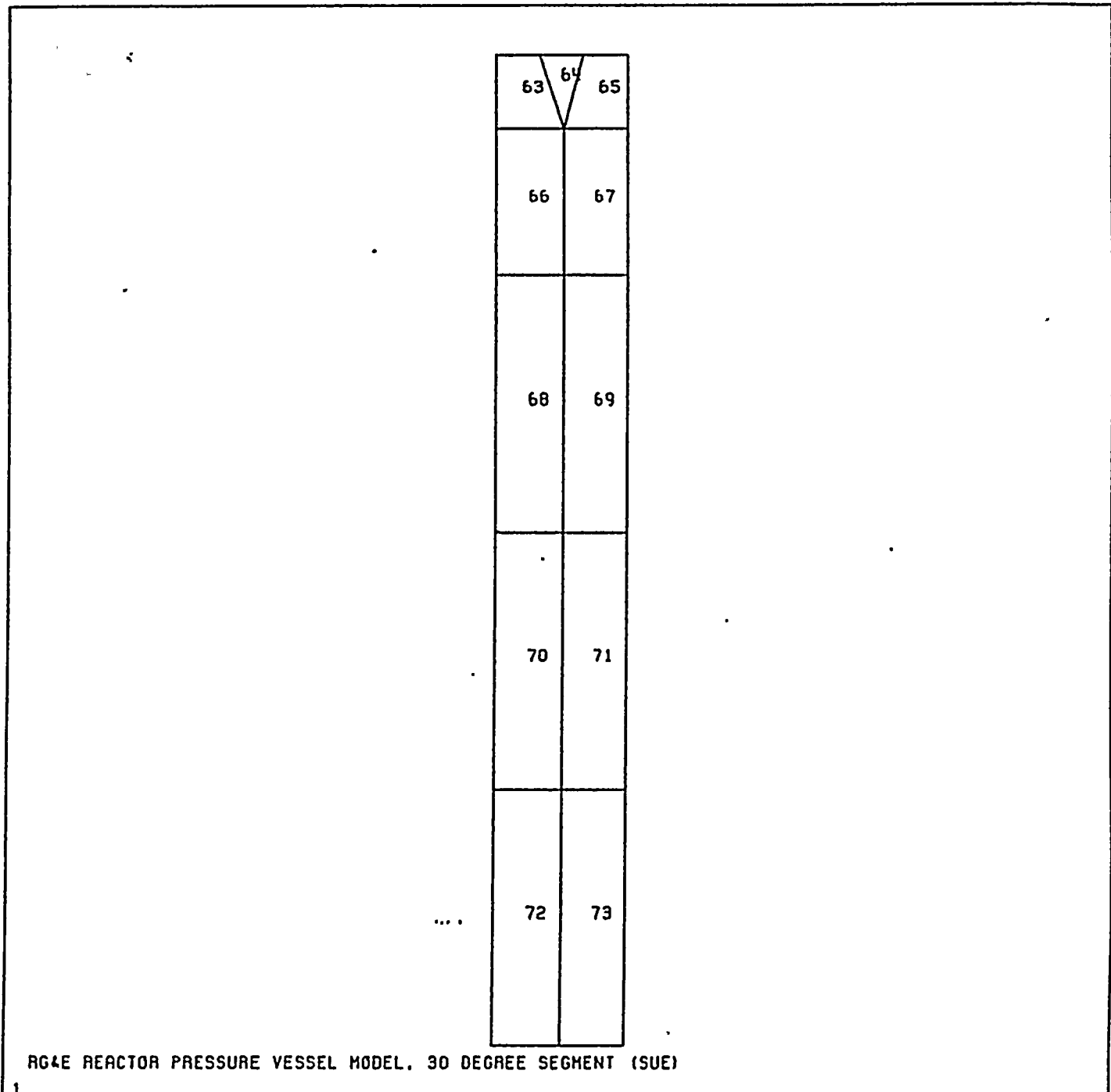


FIGURE 14: Element Numbers for the Extended Intermediate Shell Portion of the Uniform Drop Model

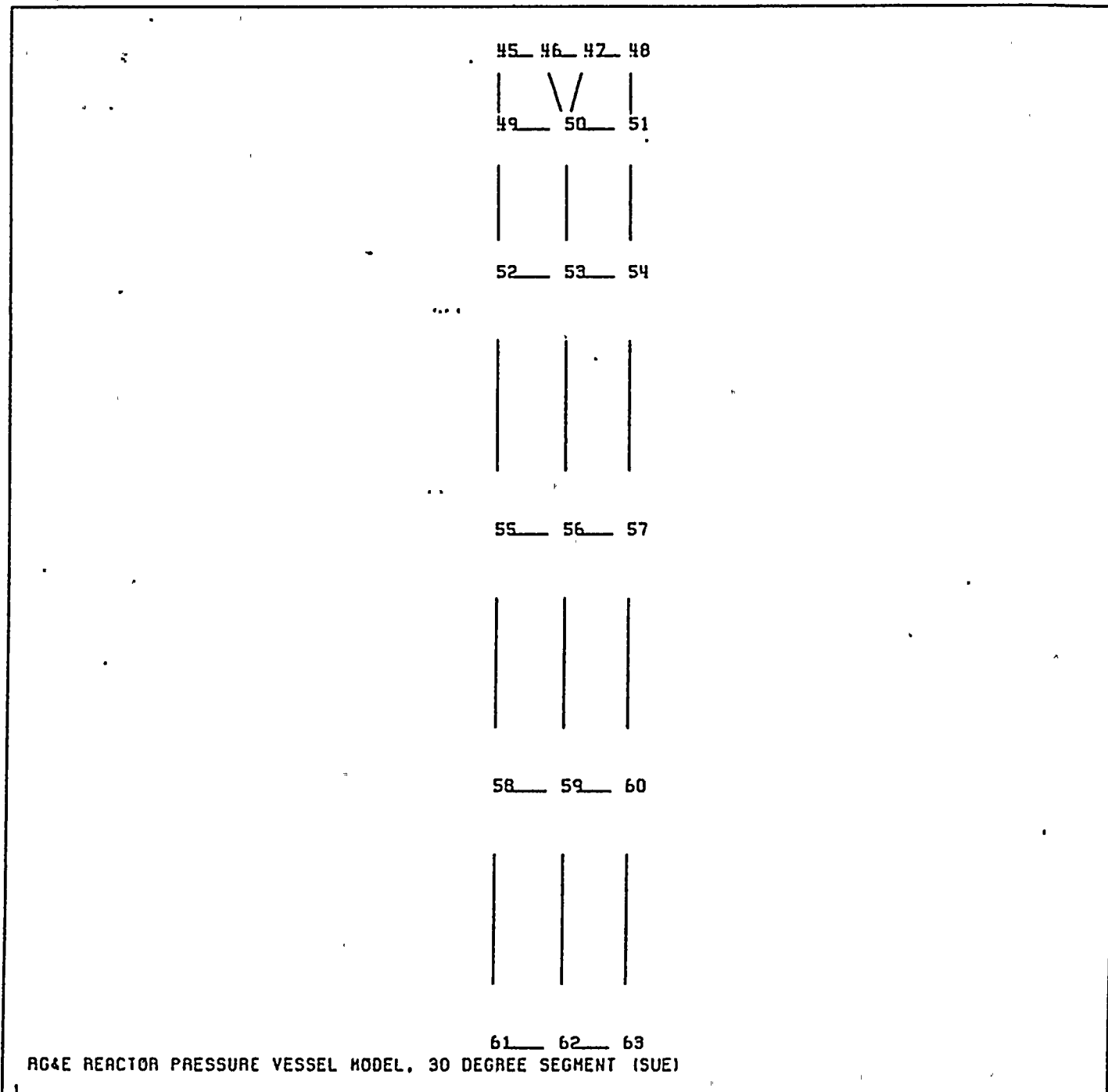


FIGURE 15: Node Numbers for the Extended Intermediate Shell Portion of the Uniform Drop Model



16	17	18
24	25	26
30	31	32
35	36	37
40	41	42
45	46	47
50	52	53
57	59	60

RG&E REACTOR PRESSURE VESSEL MODEL, 30 DEGREE SEGMENT (SUE)

FIGURE 16: Nozzle Element Numbers for the Uniform Drop Model

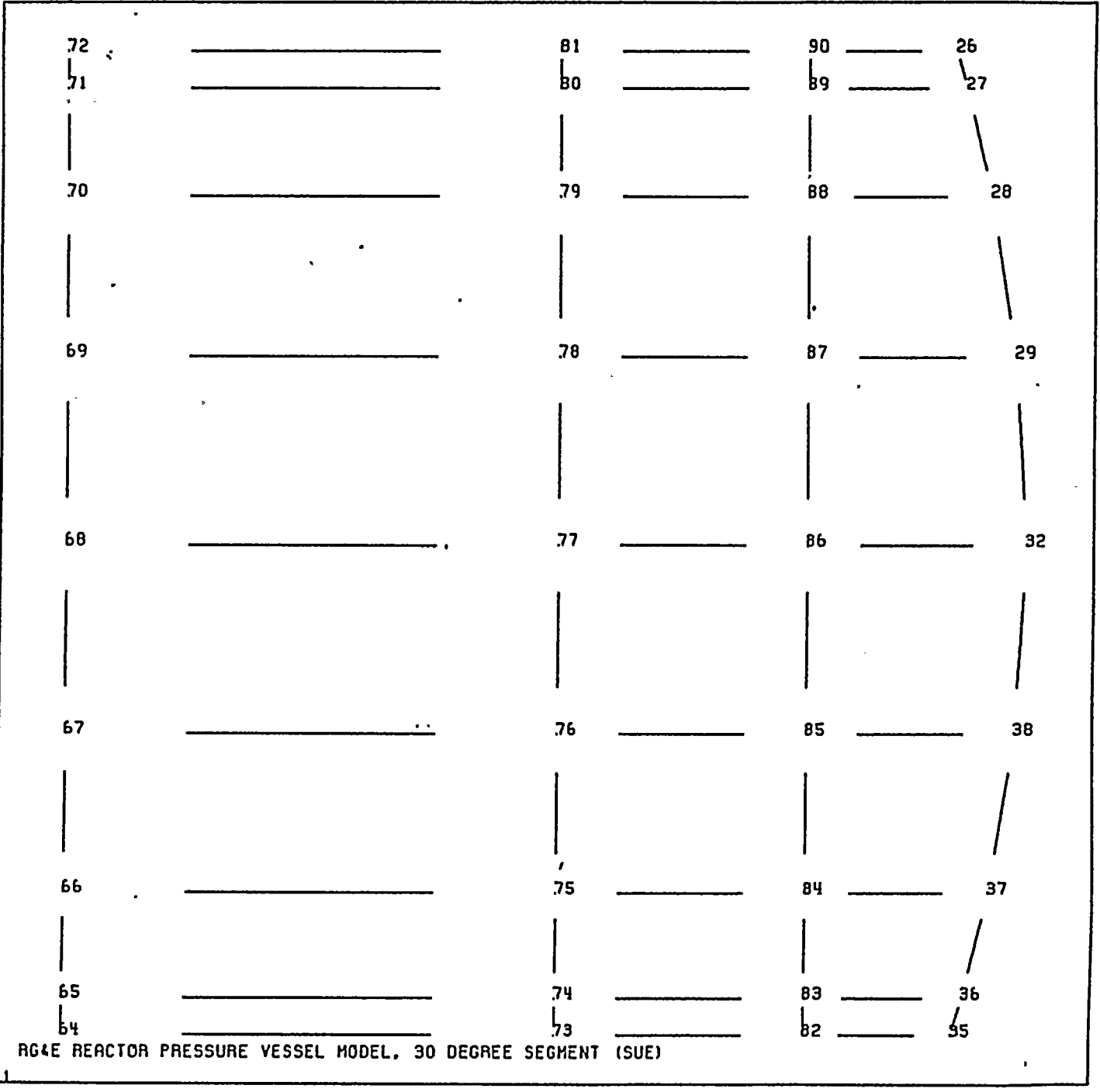


FIGURE 17: Nozzle Node Numbers for the Uniform Drop Model

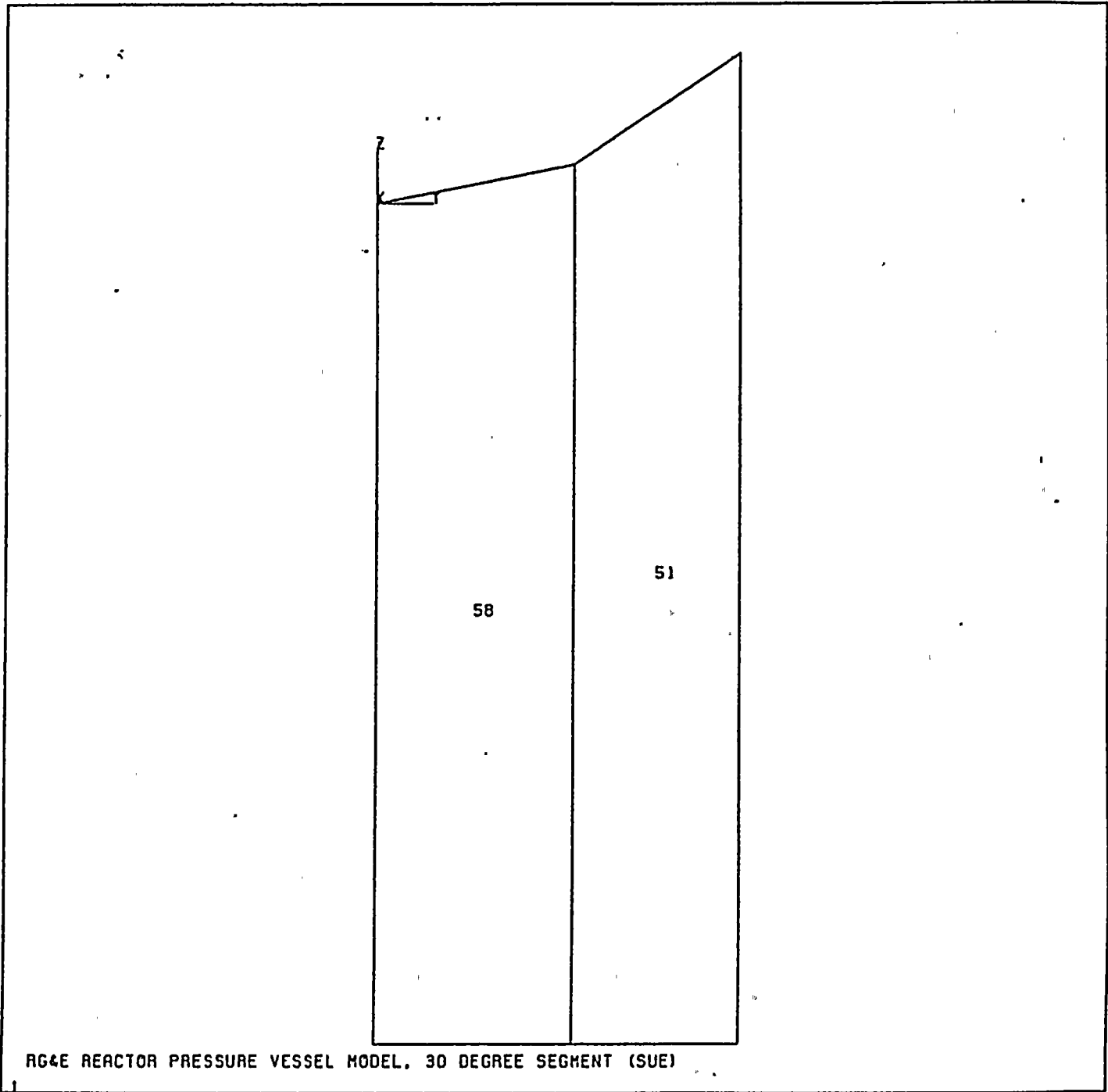


FIGURE 18: Support Saddle Element Numbers for the Uniform Drop Model



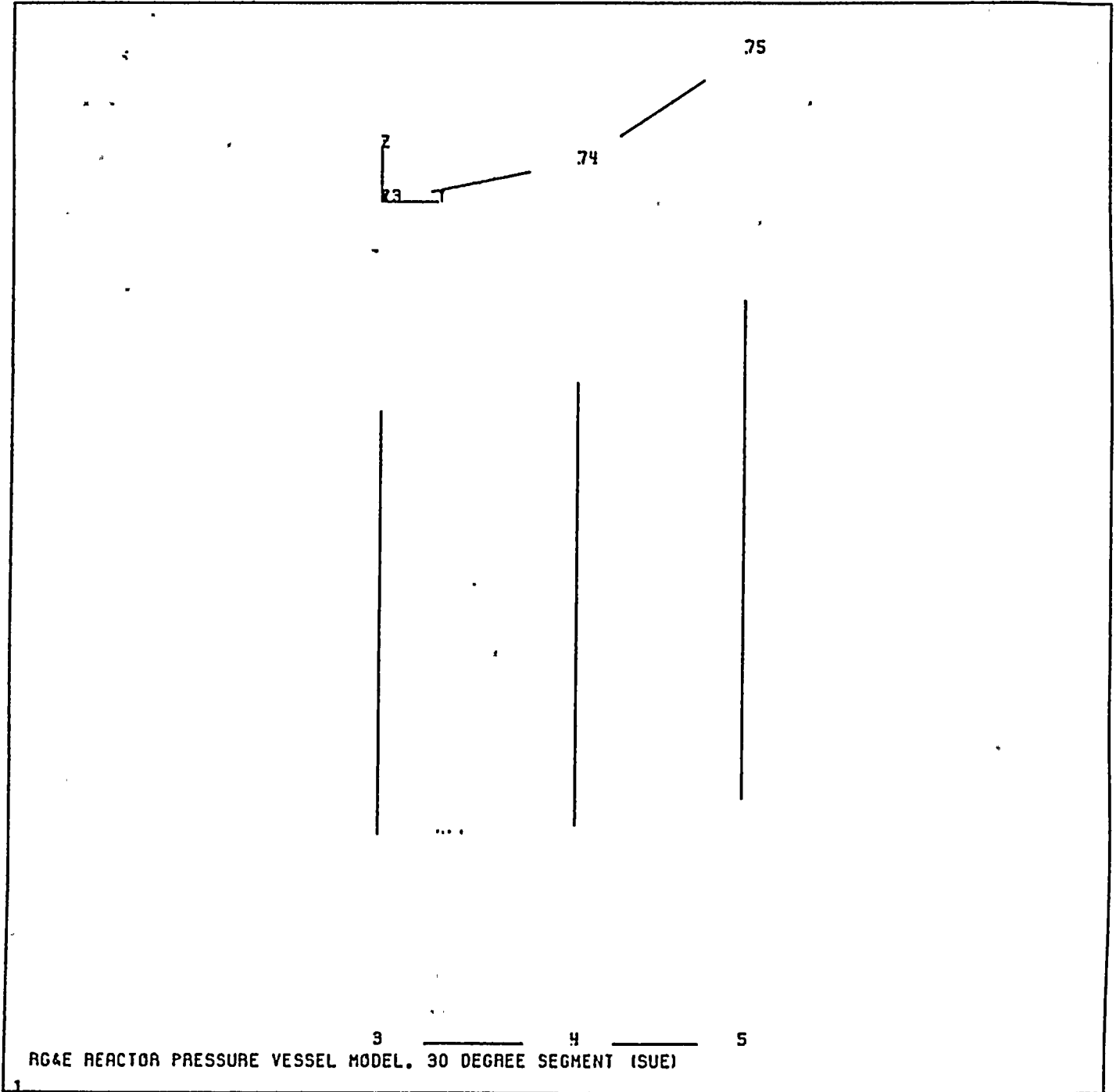
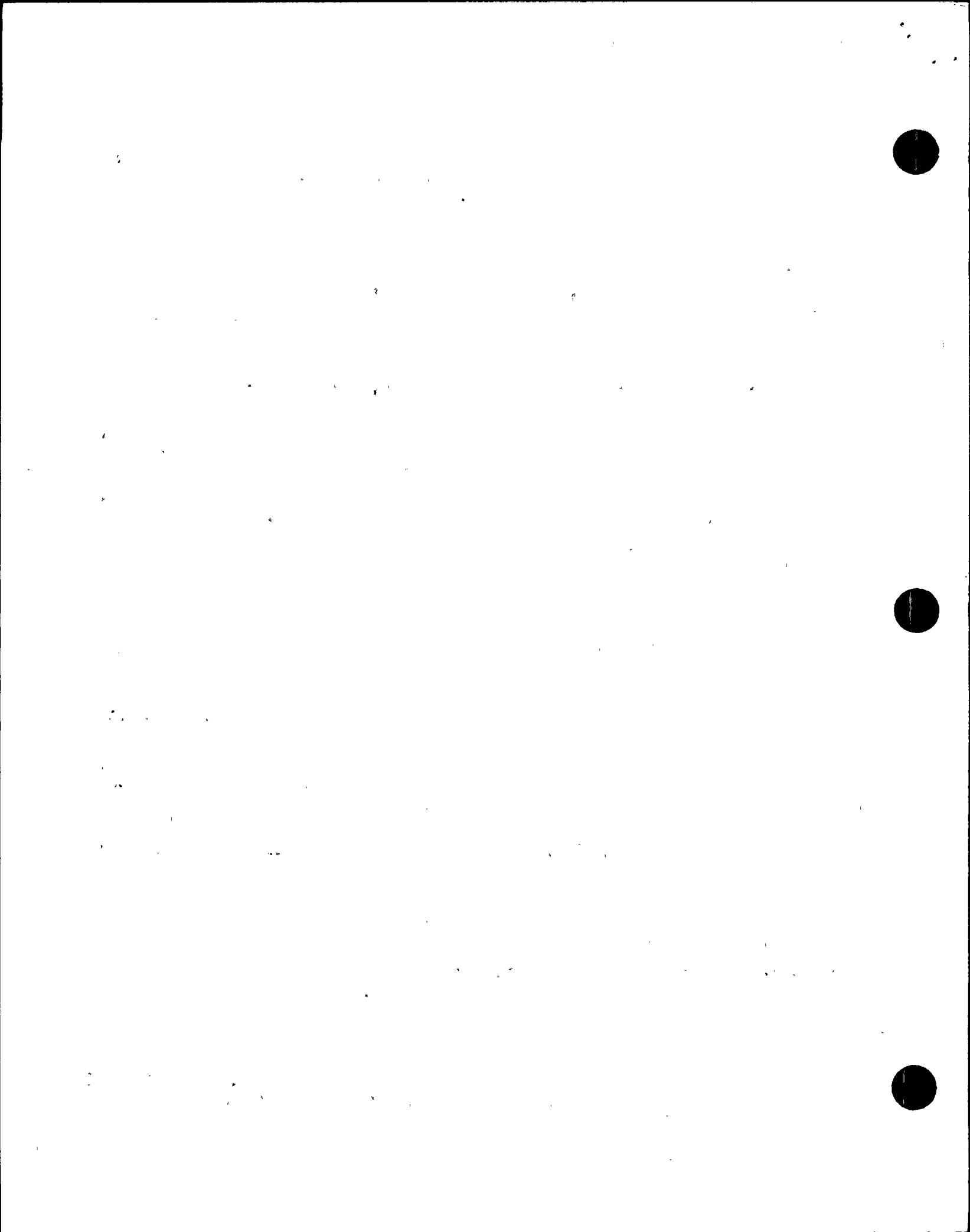


FIGURE 19: Support Saddle Node Numbers for the Uniform Drop Model



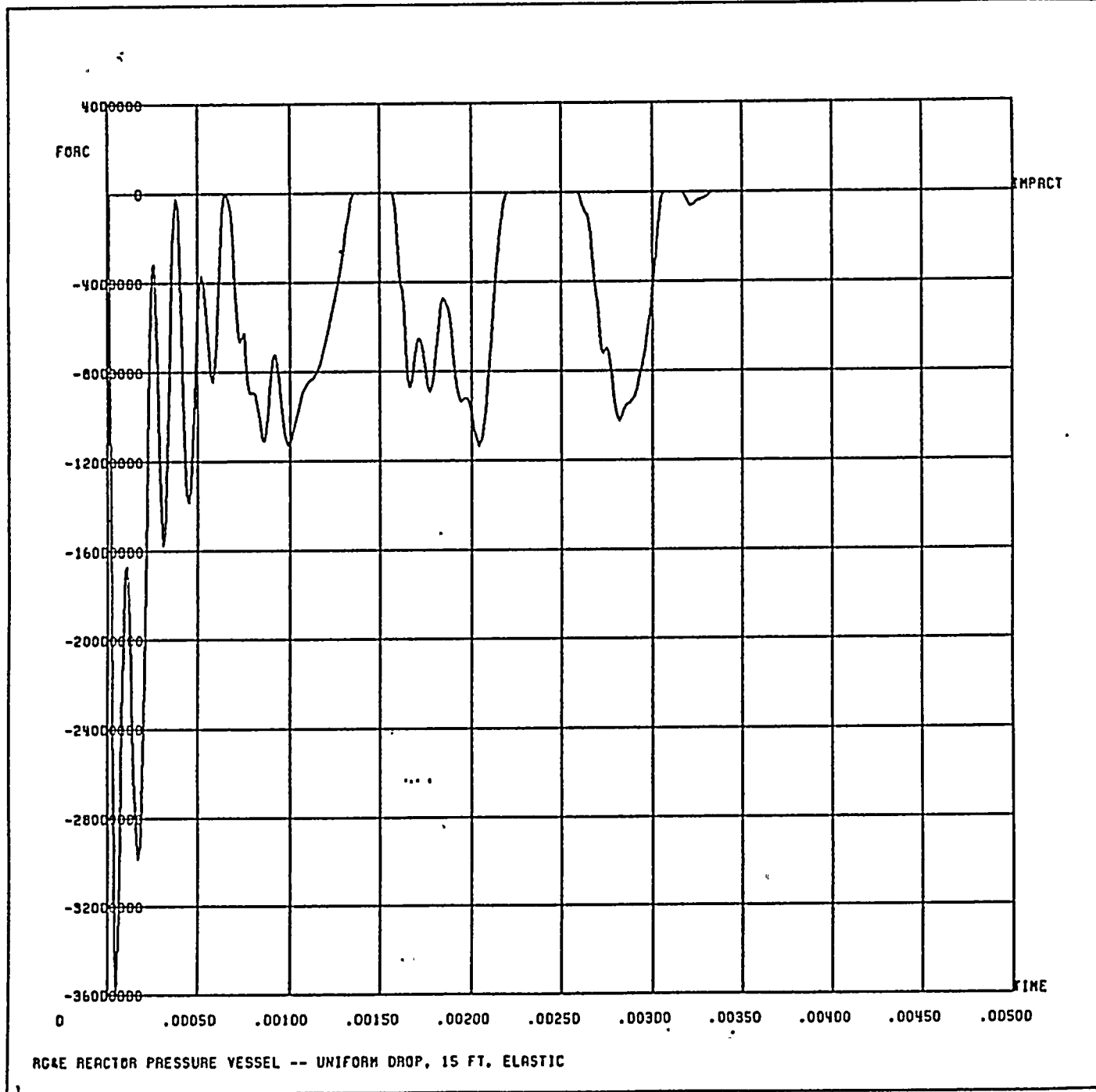


FIGURE 20: Contact Force (lbs) between the Reactor Head and Vessel Flange for a Uniform Drop versus Time (seconds)

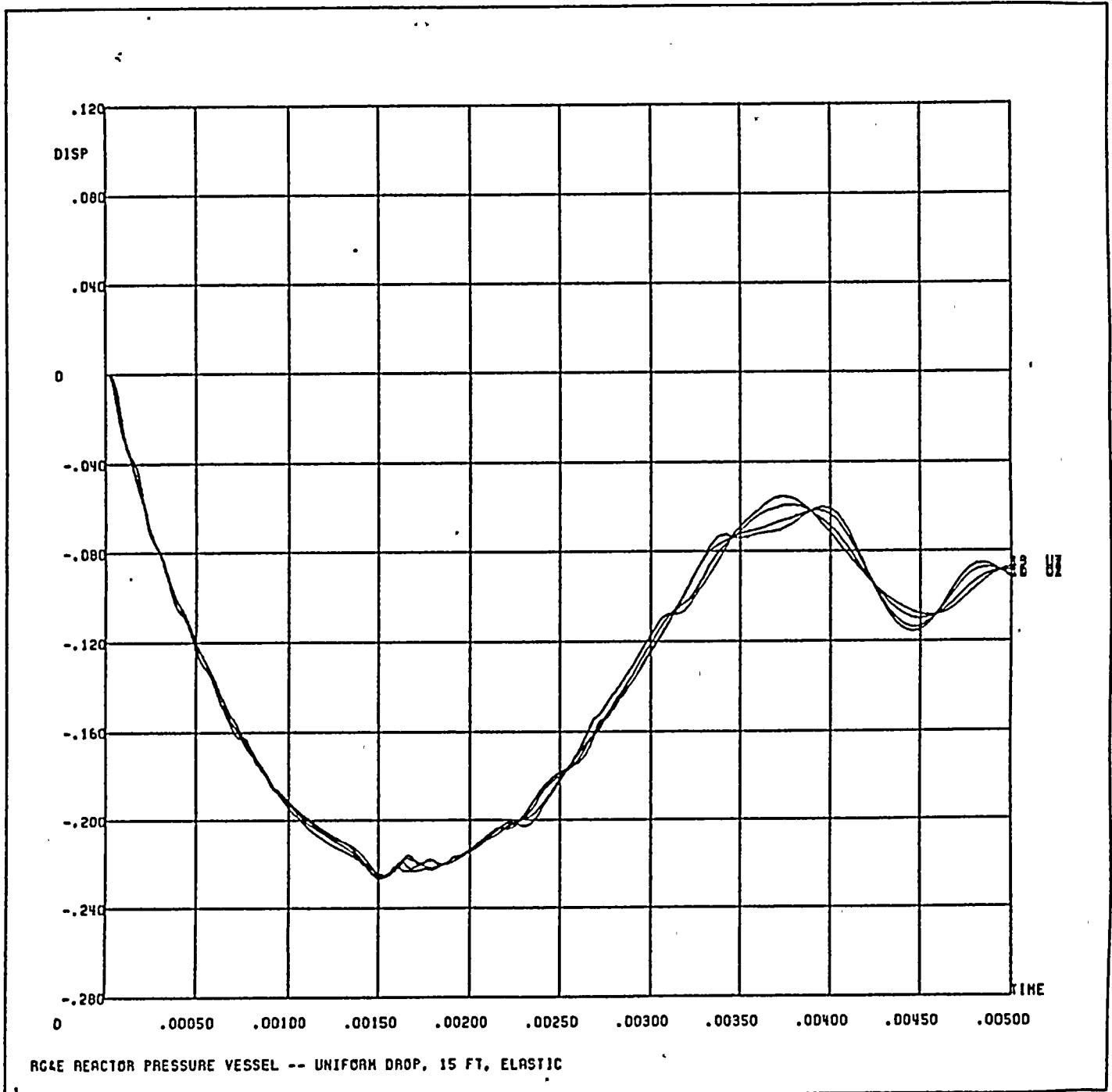
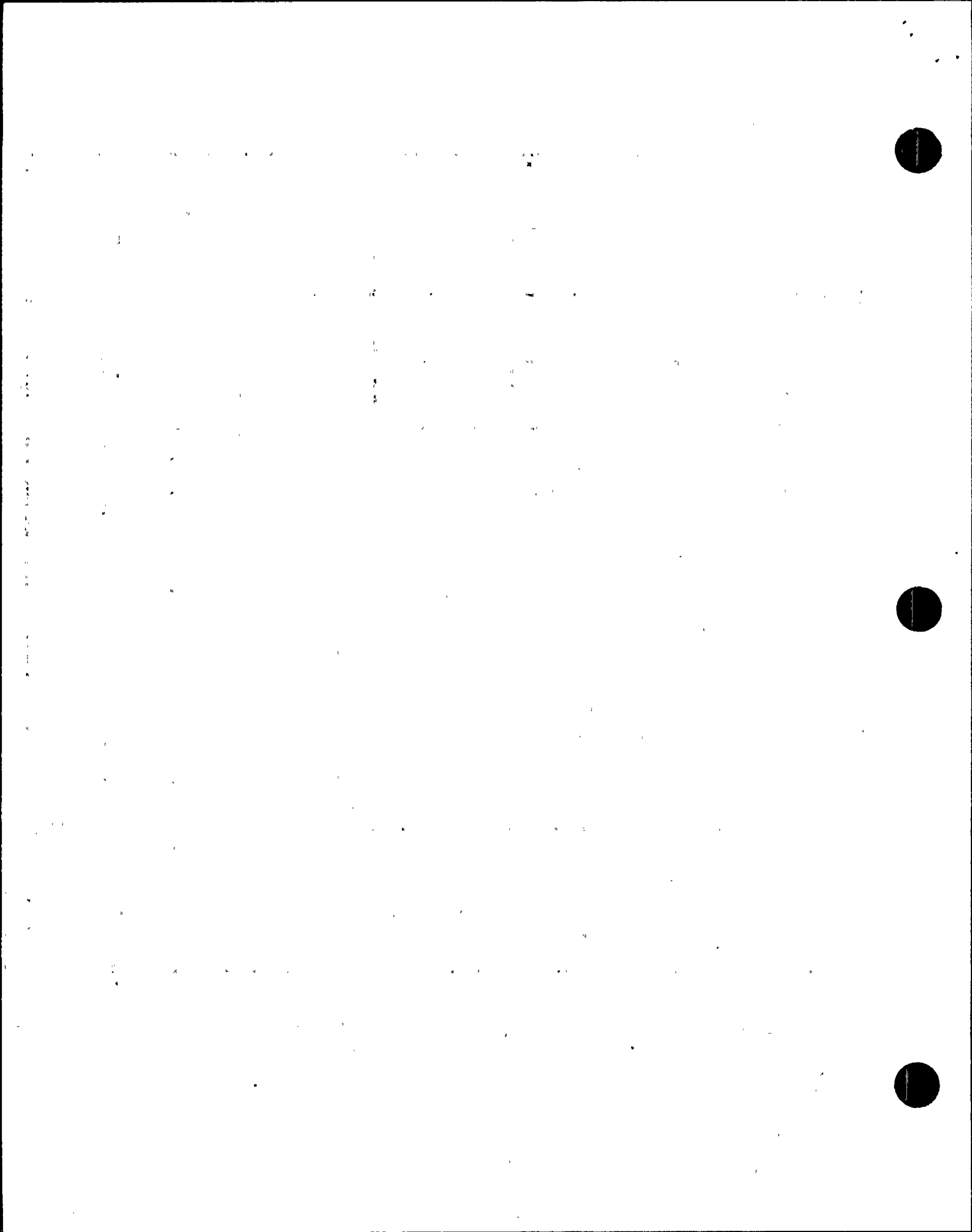


FIGURE 21: Displacement (inches) of Nodes 10, 11, 12 and 13 at the Top of the Reactor Vessel Flange for a Uniform Drop versus Time (seconds)



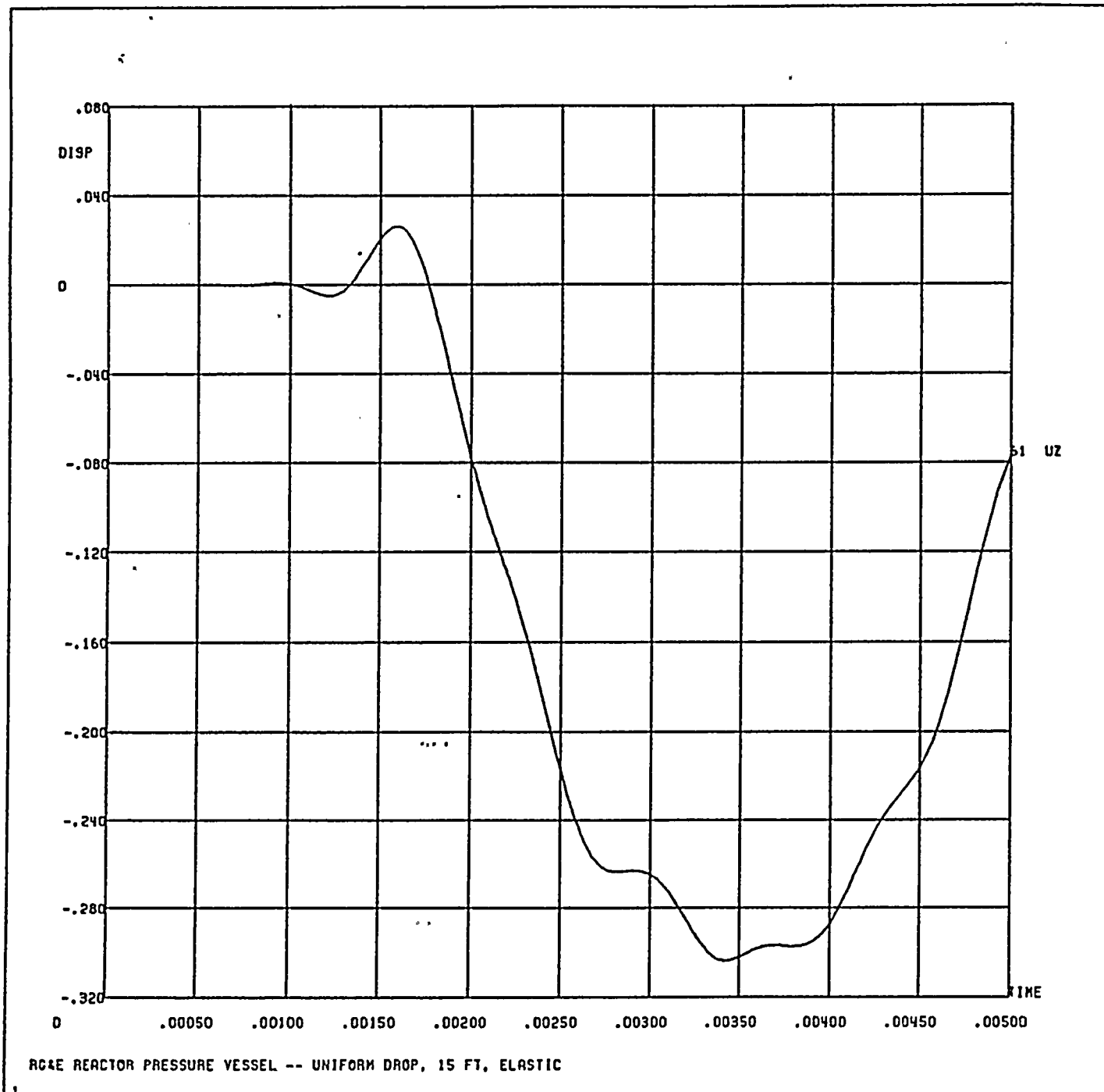


FIGURE 22: Displacement (inches) of Node 61 at the Bottom of the Vessel for a Uniform Drop versus Time (seconds)



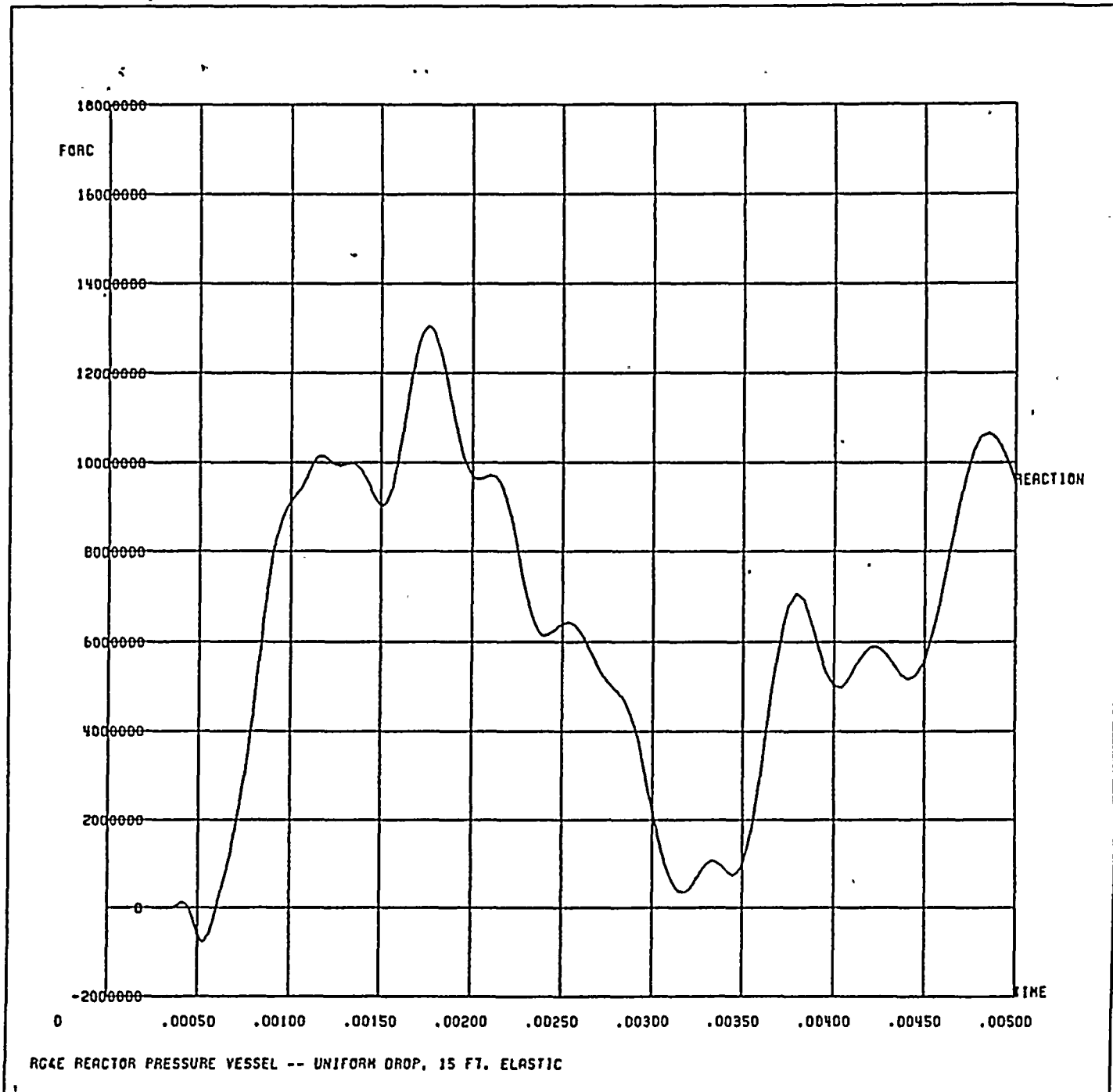


FIGURE 23: Reaction Force (lbs) at the Nozzle Support for a Uniform Drop versus Time (seconds)



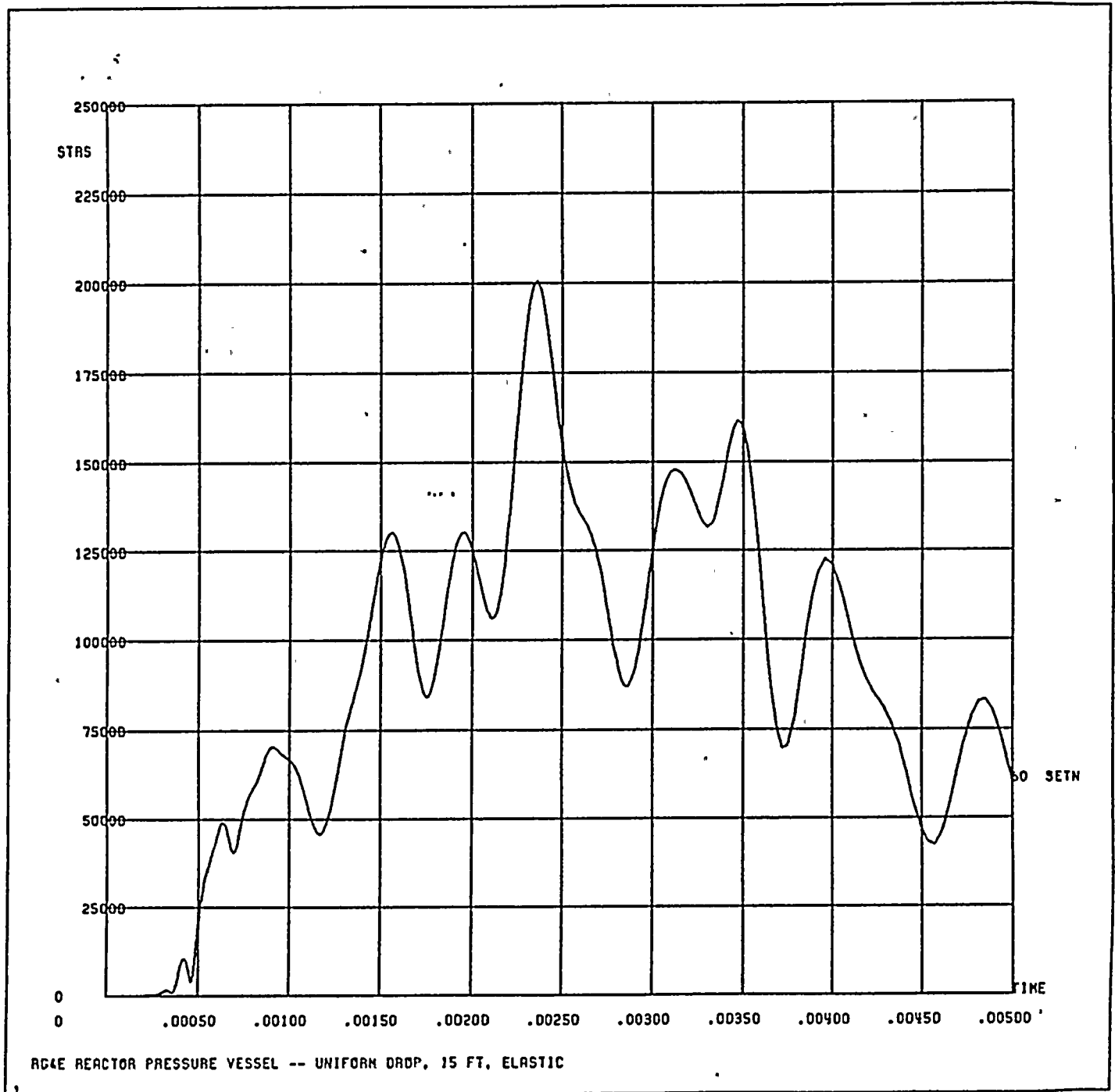


FIGURE 24: Equivalent Stress (psi) in Element 60 at Node 35 versus Time (seconds)

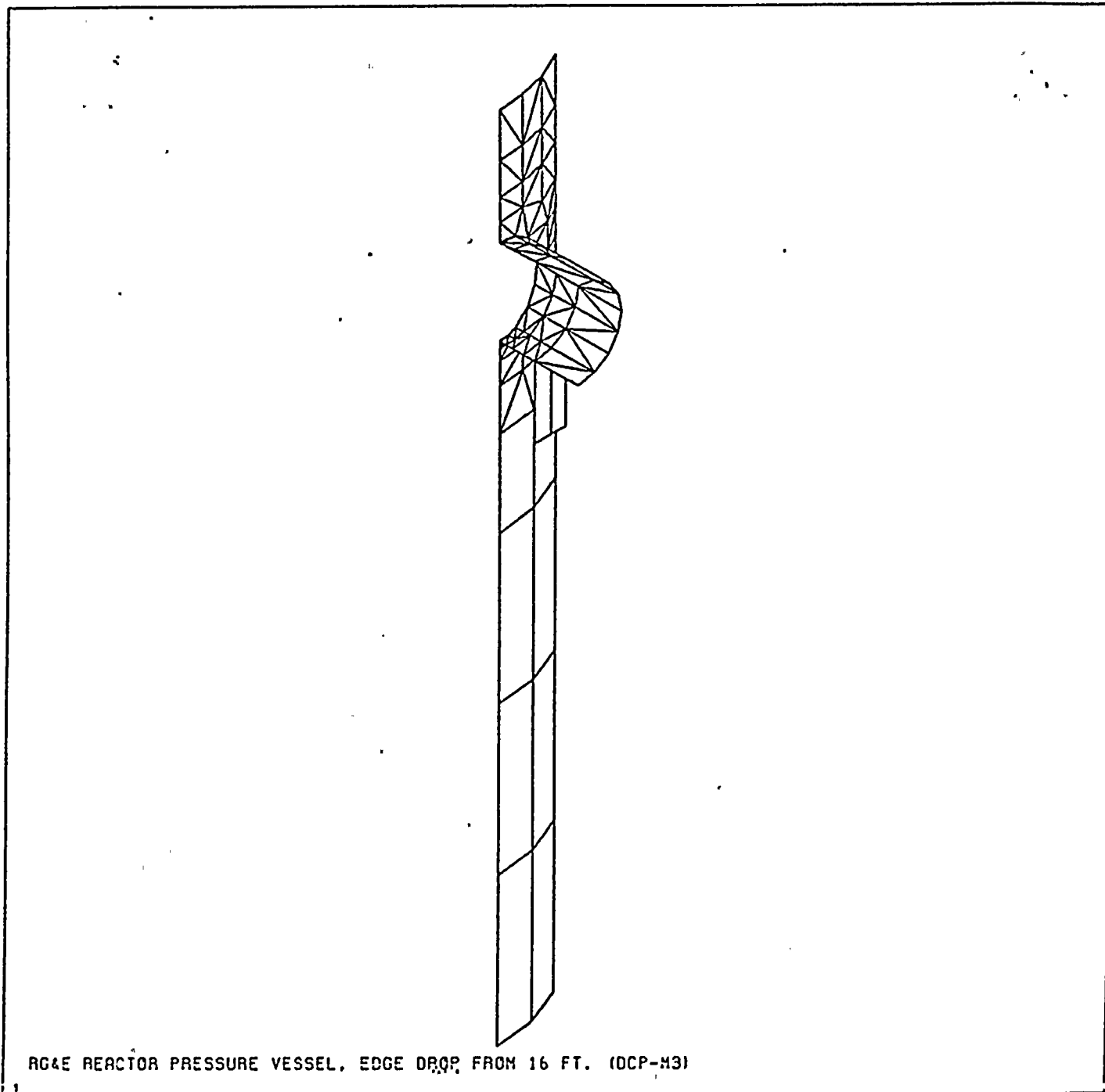


FIGURE 25: ANSYS Finite Element Model for Concentrated Drop Analysis - 3D Hidden Line Plot of Complete Model

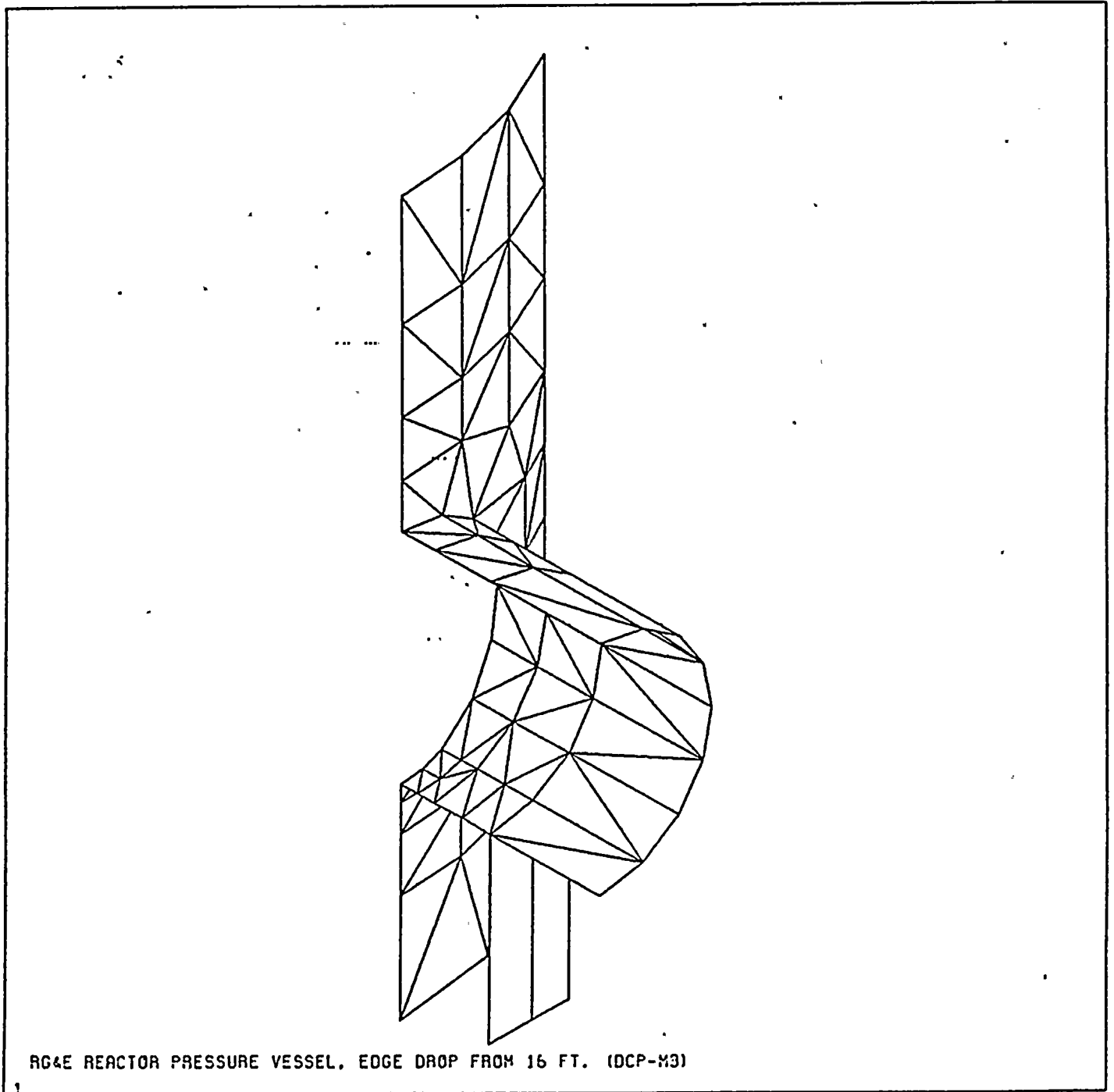


FIGURE 26: ANSYS Finite Element Model for Concentrated Drop Analysis - 3D Hidden Line Plot of the Vessel Flange and Upper Shell

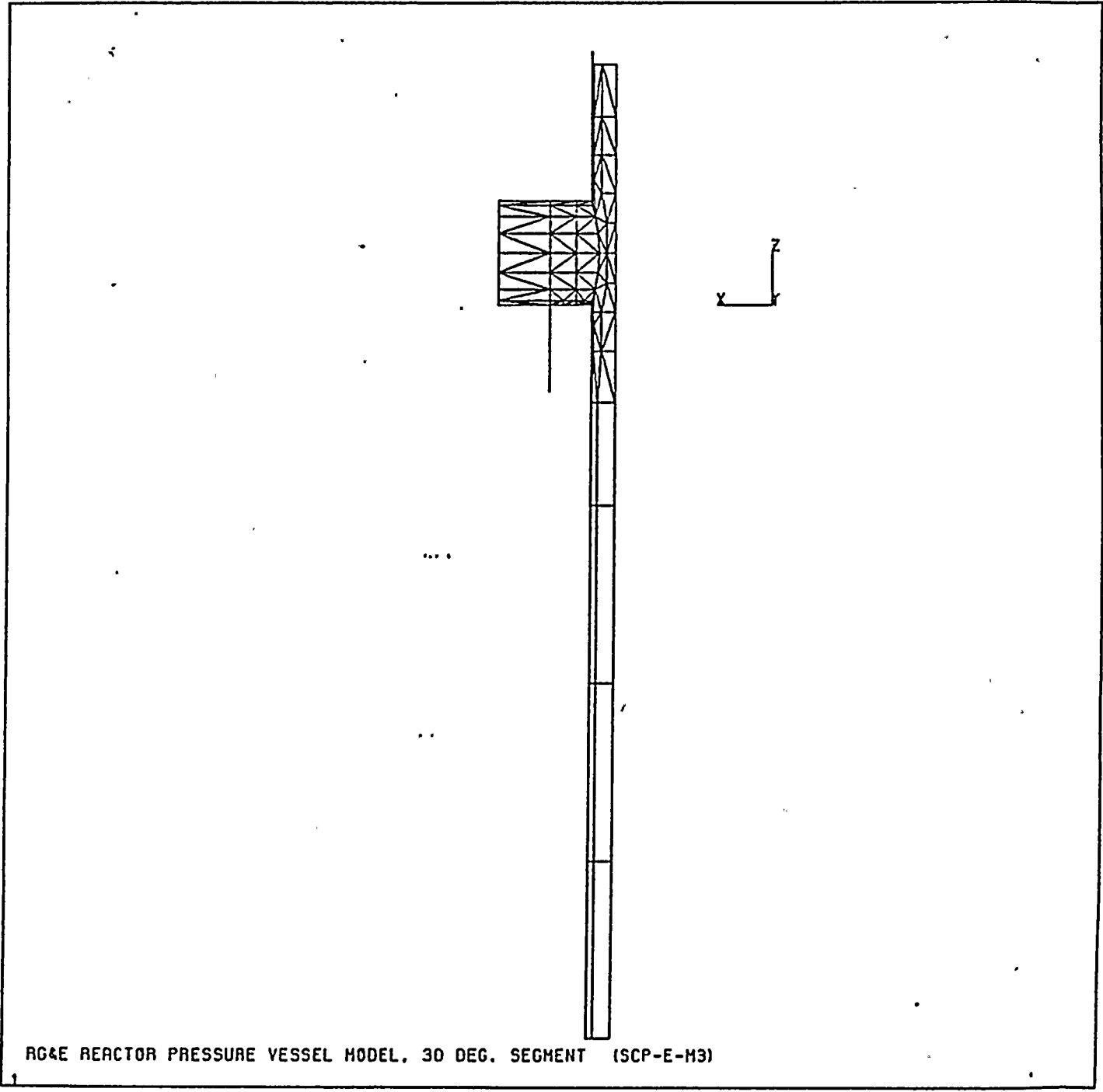


FIGURE 27: ANSYS Finite Element Model for Concentrated Drop Analysis - Side View of Complete Model

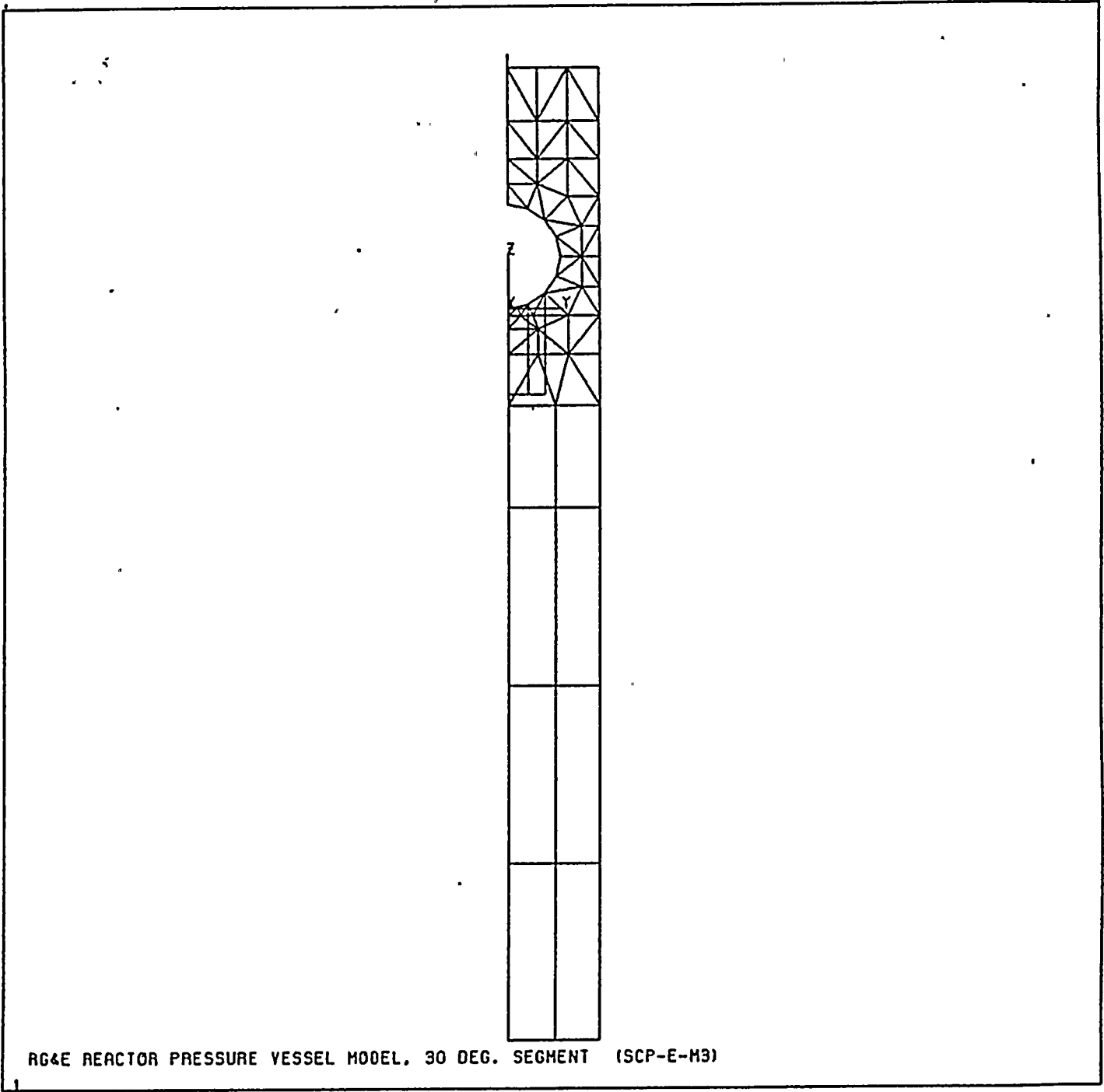


FIGURE 28: ANSYS Finite Element Model for Concentrated Drop Analysis - Front View of Complete Model

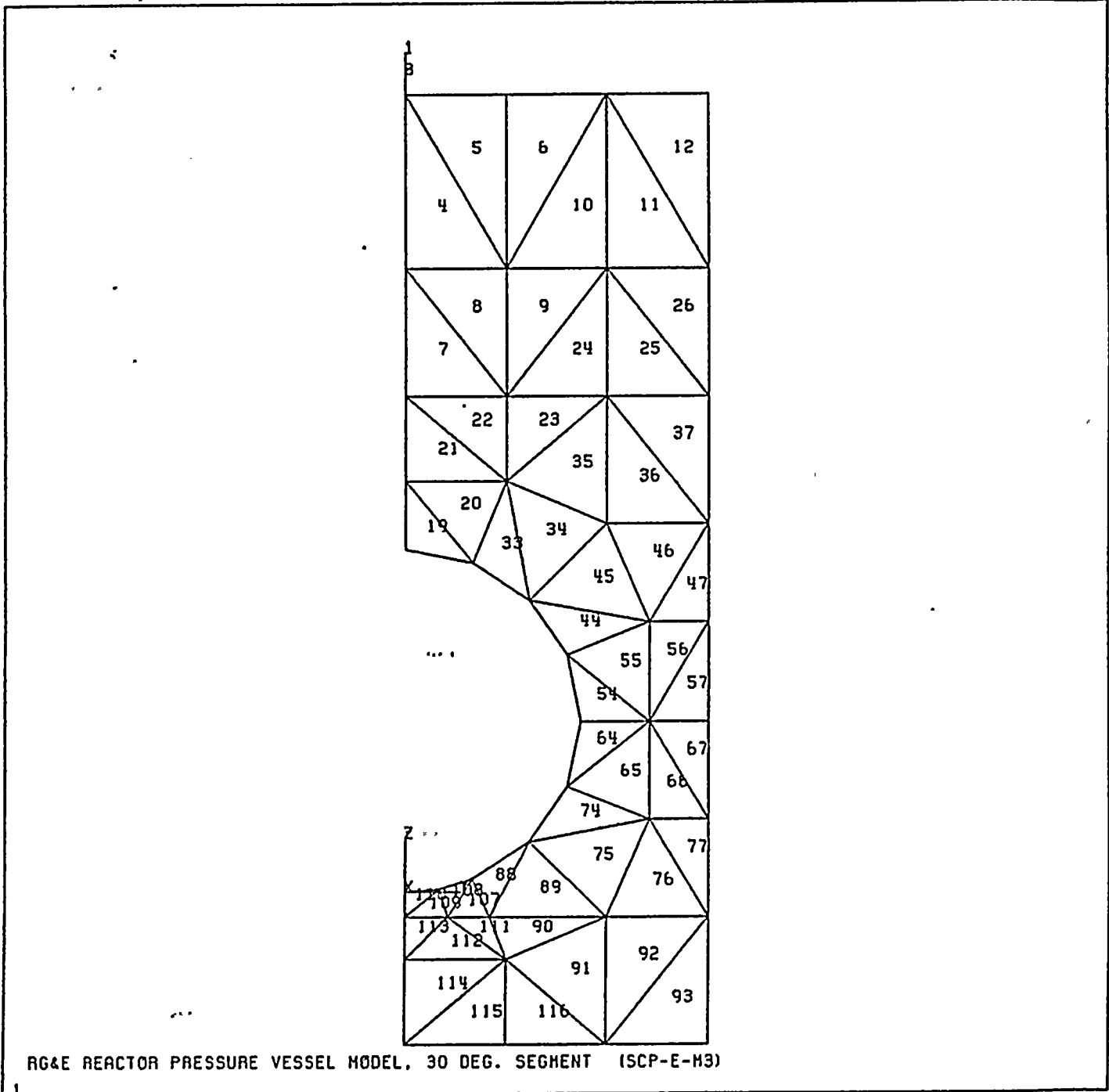


FIGURE 29: Element Numbers for the Flange and Upper Shell Portions of the Concentrated Drop Model

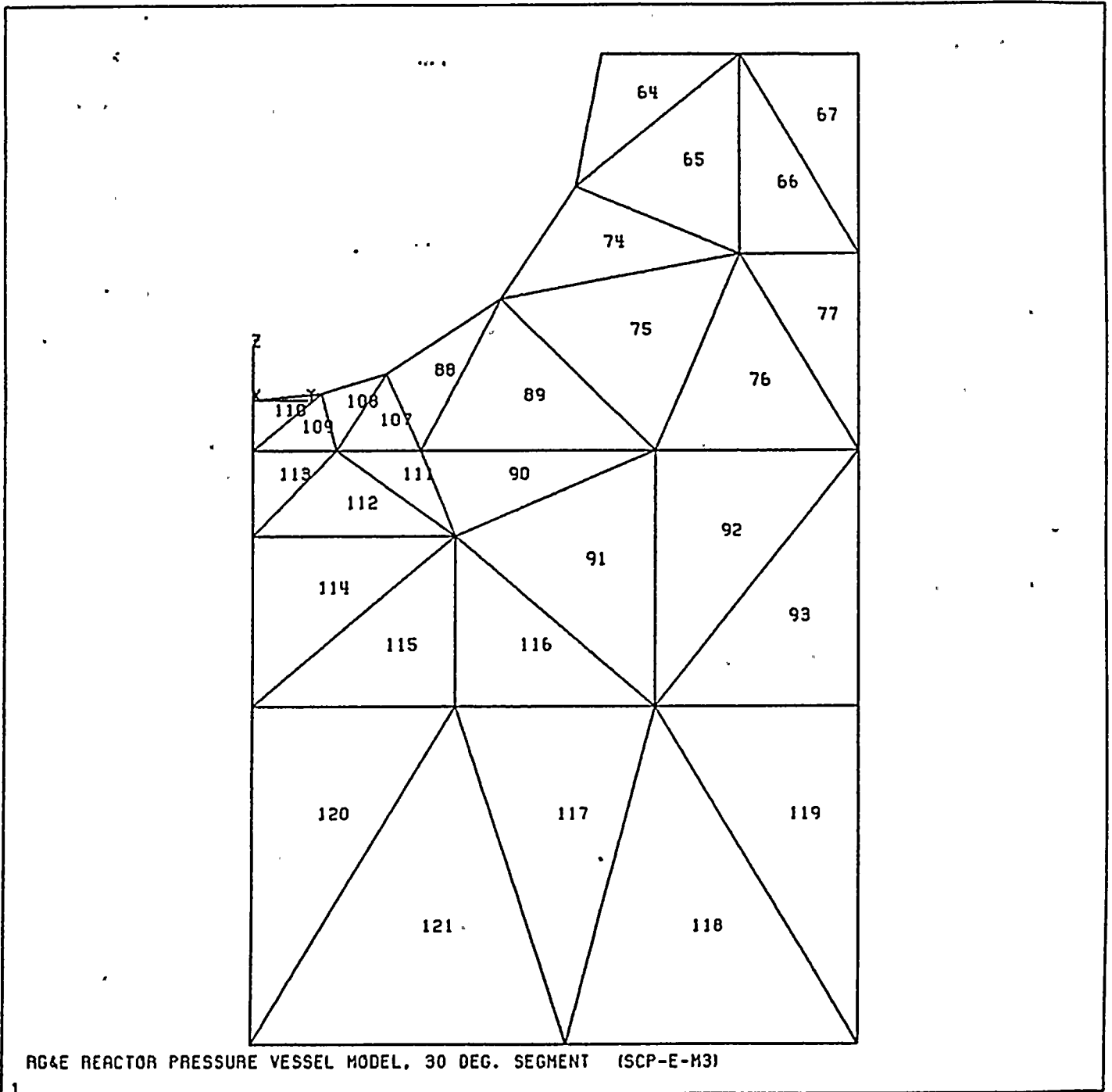


FIGURE 30: Element Numbers for the Lower Half of the Upper Shell Portion of the Concentrated Drop Model

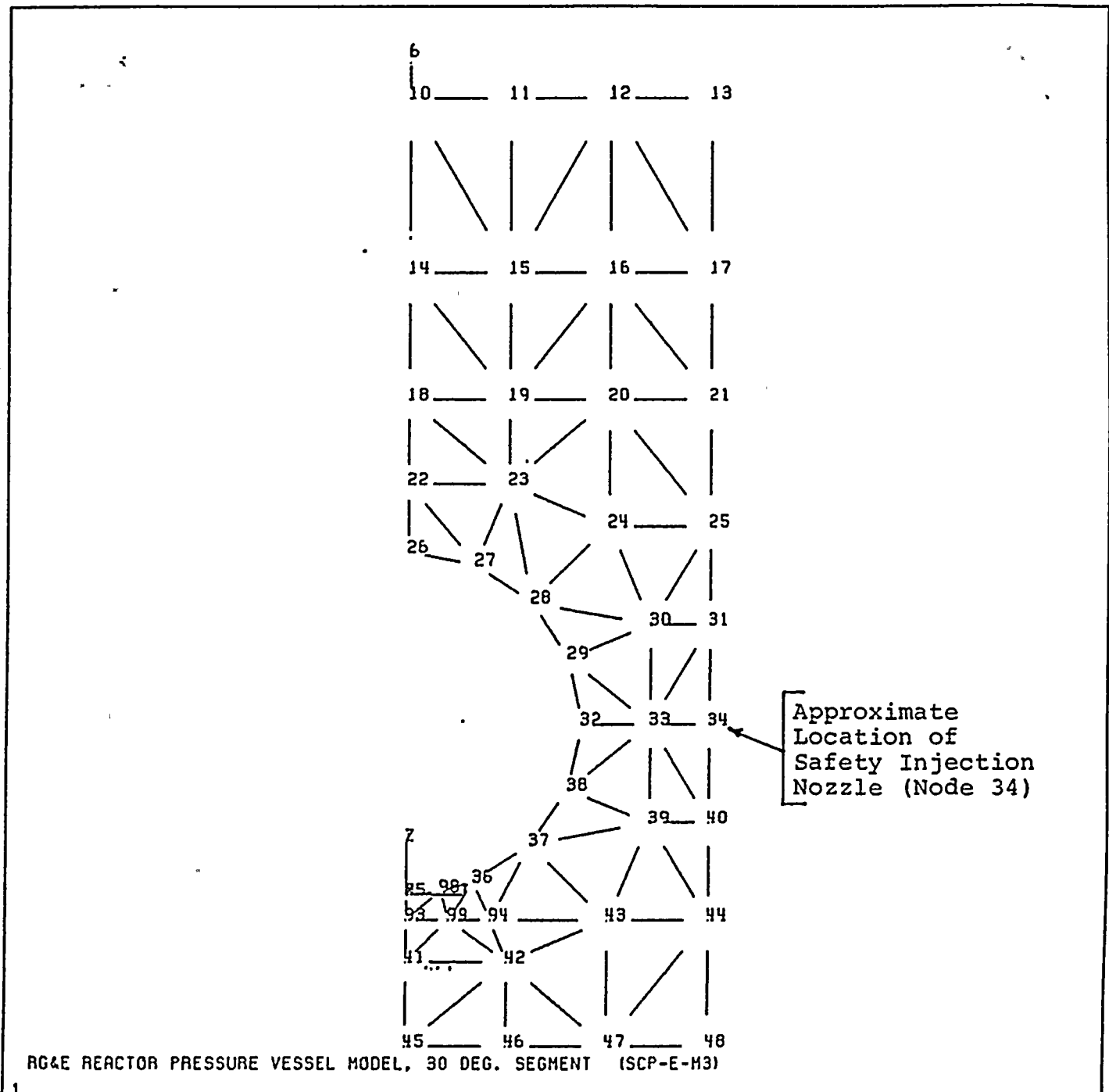
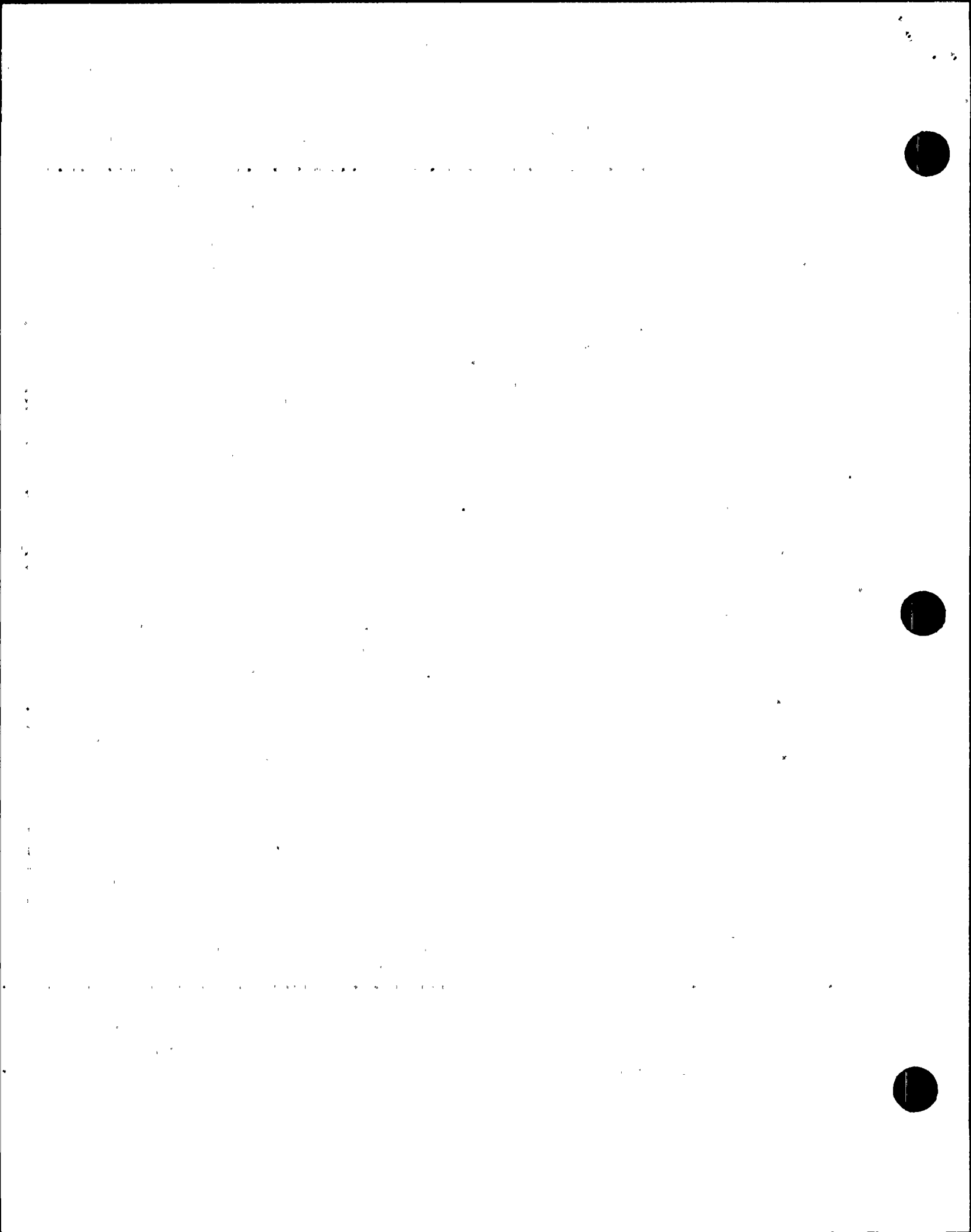


FIGURE 31: Node Numbers for the Flange and Upper Shell Portions of the Concentrated Drop Model



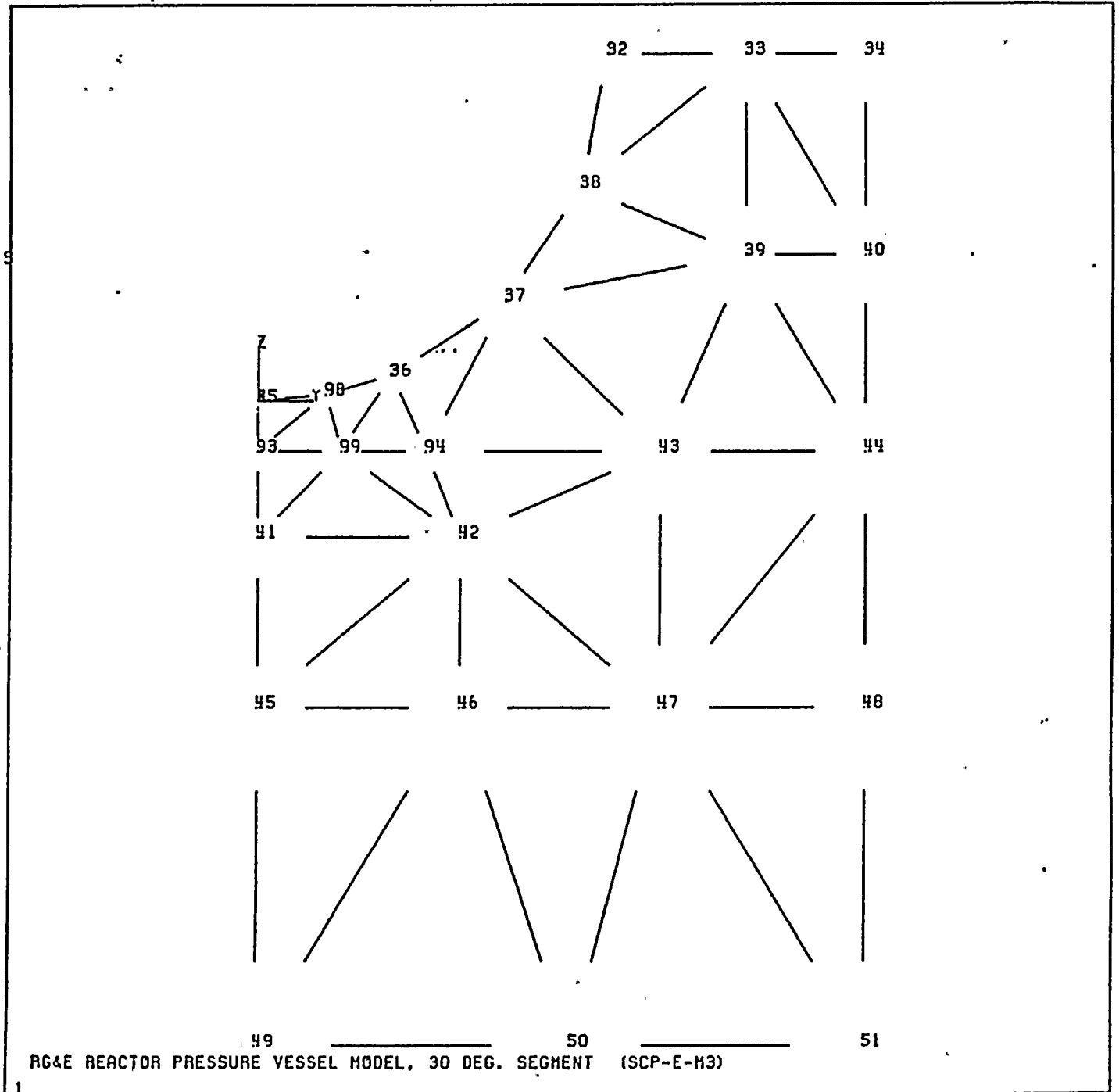


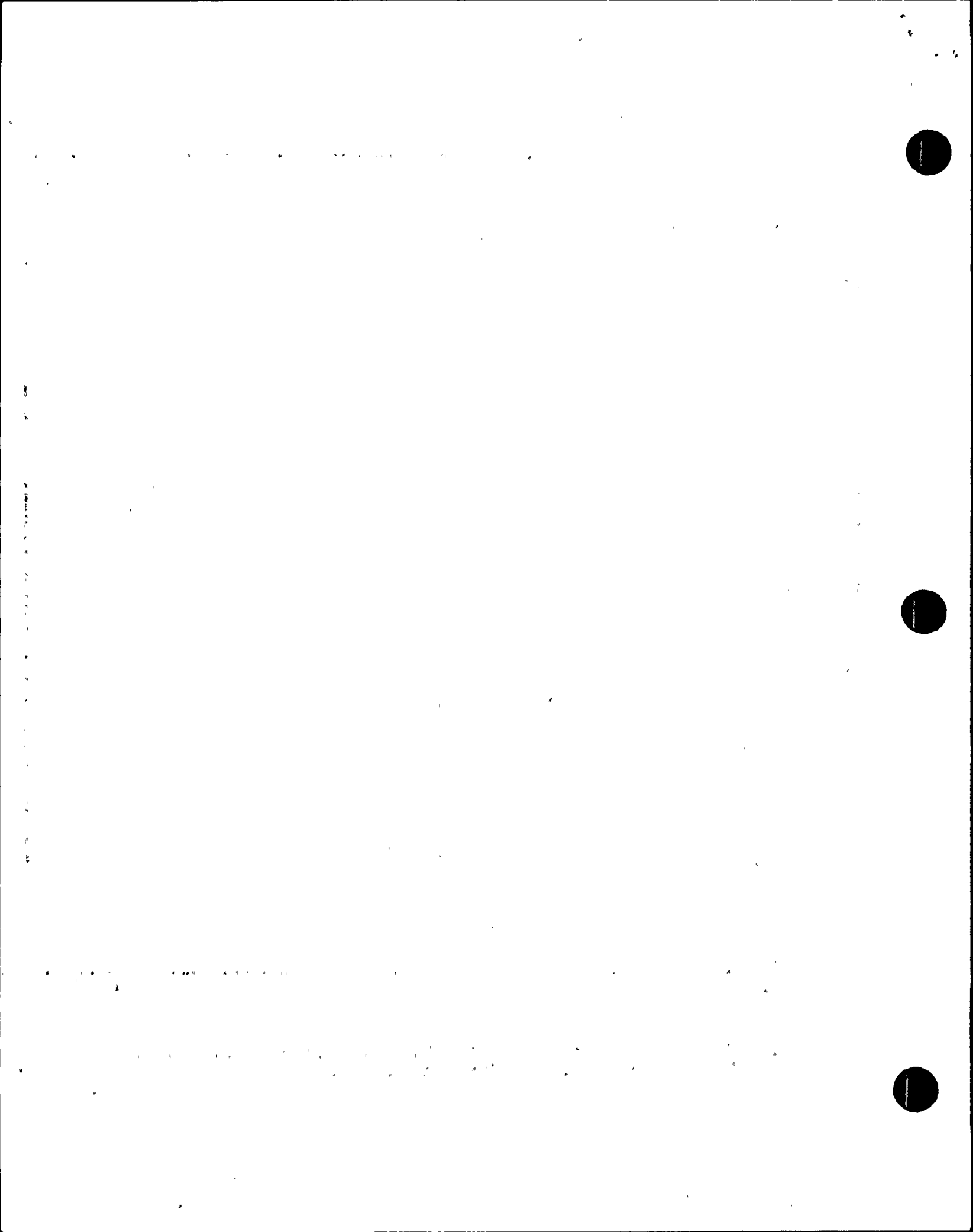
FIGURE 32: Node Numbers for the Lower Half of the Upper Shell Portion of the Concentrated Drop Model



120	117	119
121	118	
122	123	
124	125	
126	127	
128	129	

RG4E REACTOR PRESSURE VESSEL MODEL, 30 DEG. SEGMENT (SCP-E-M3)

FIGURE 33: Element Numbers for the Extended Intermediate Shell Portion of the Concentrated Drop Model



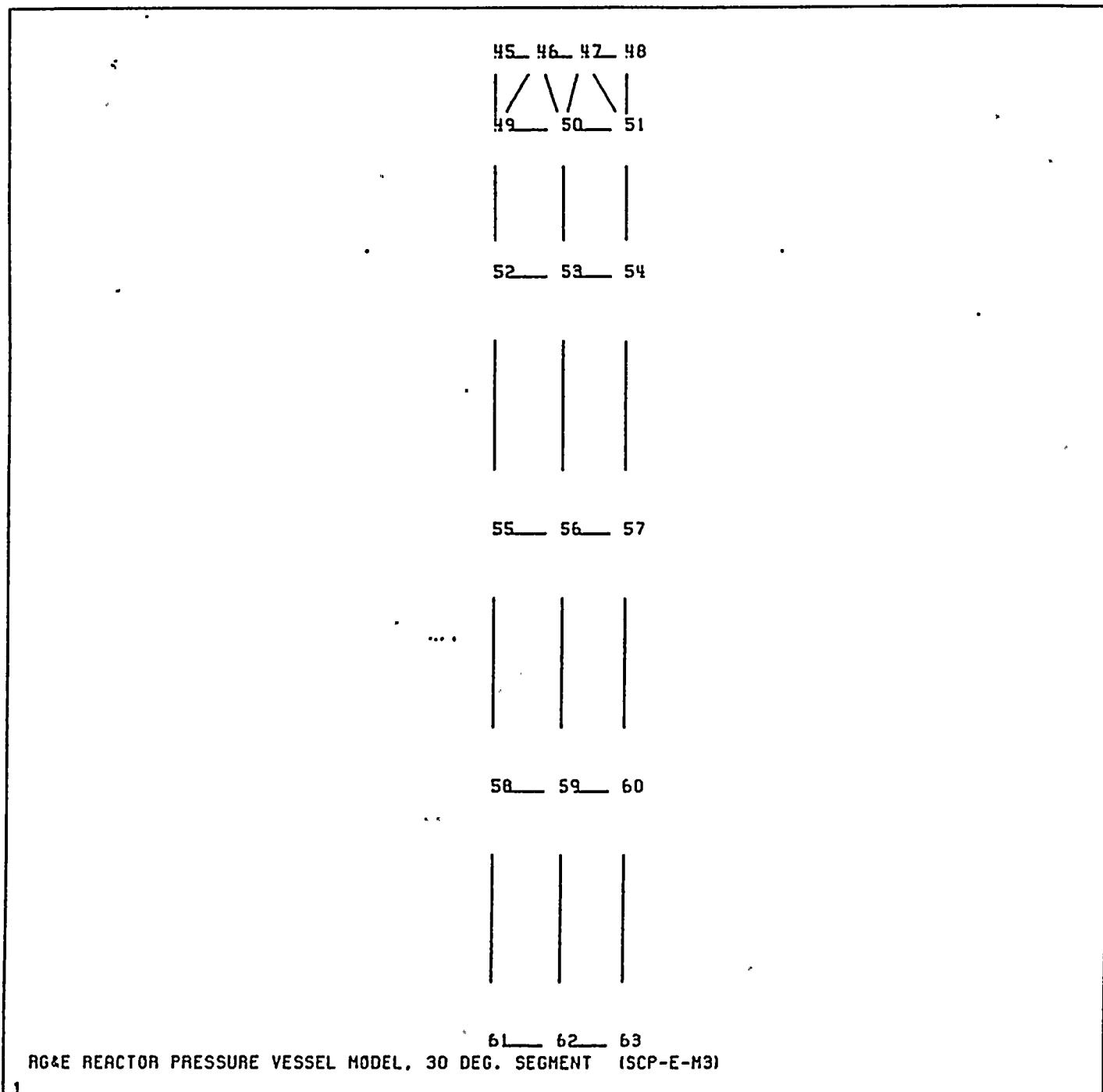


FIGURE 34: Node Numbers for the Extended Intermediate Shell Portion of the Concentrated Drop Model



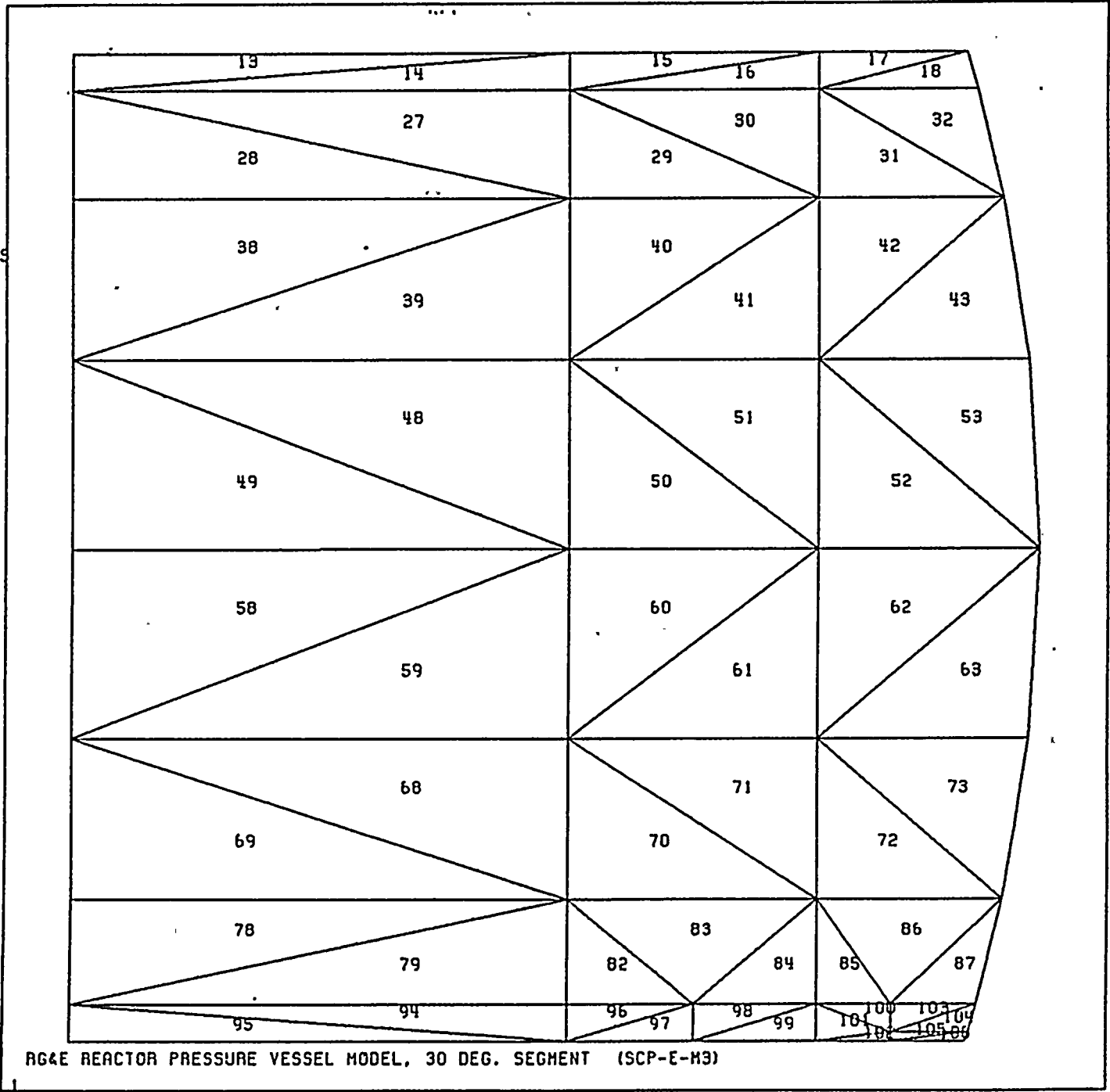
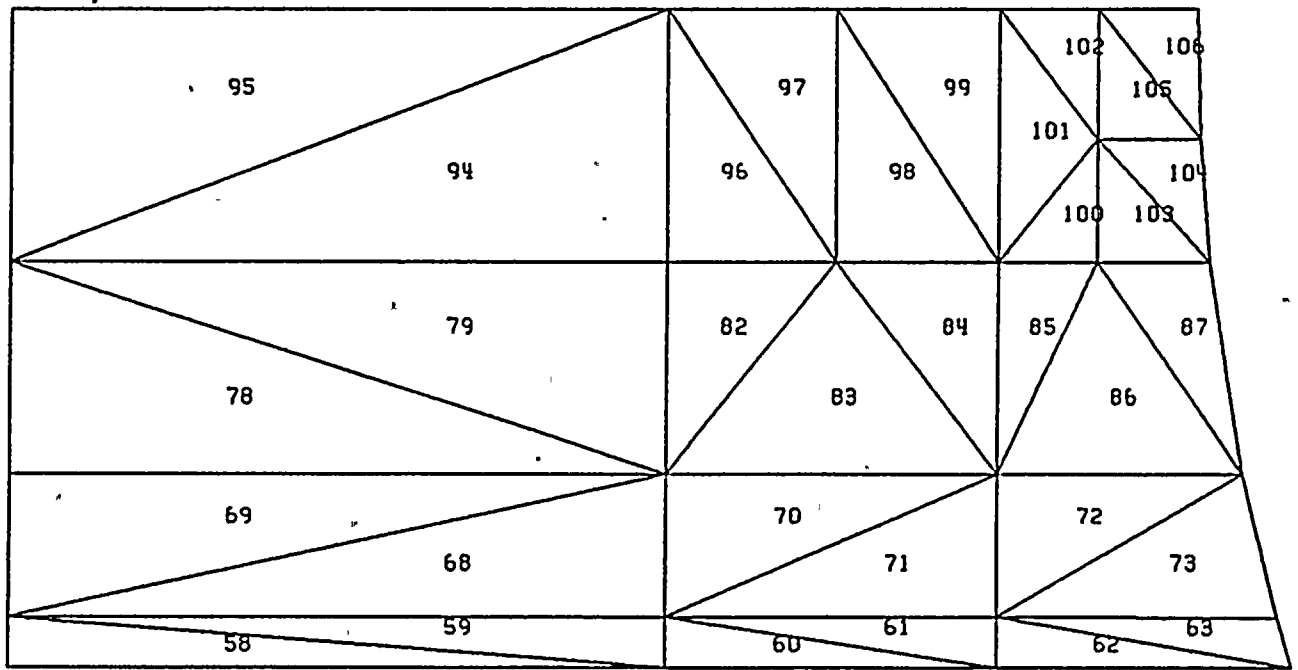


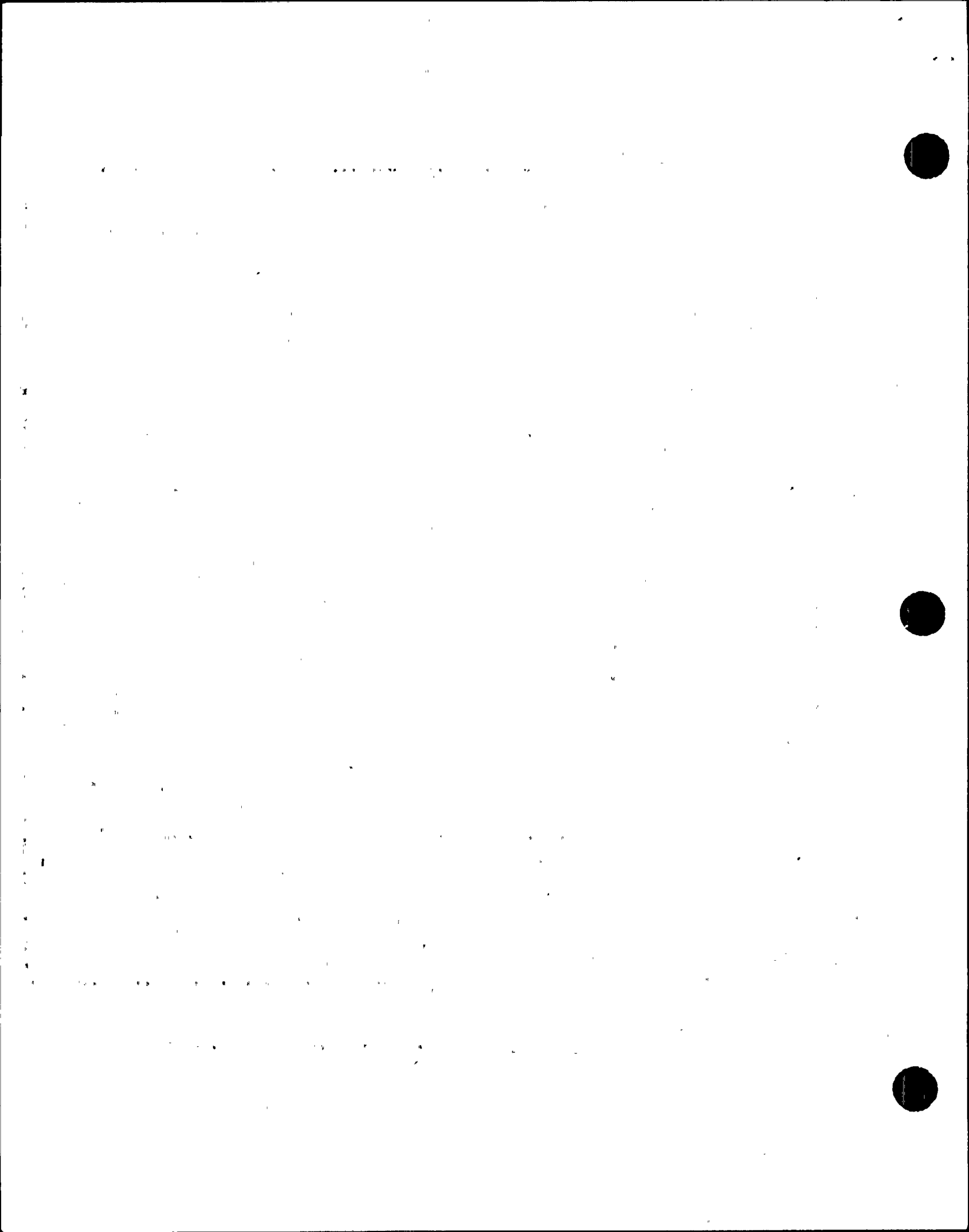
FIGURE 35: Nozzle Element Numbers for the Concentrated Drop Model - Side View





RG&E REACTOR PRESSURE VESSEL MODEL, 30 DEG. SEGMENT (SCP-E-M3)

FIGURE 36: Element Numbers for the Lower Half of the Nozzle - Top View, Concentrated Drop Model



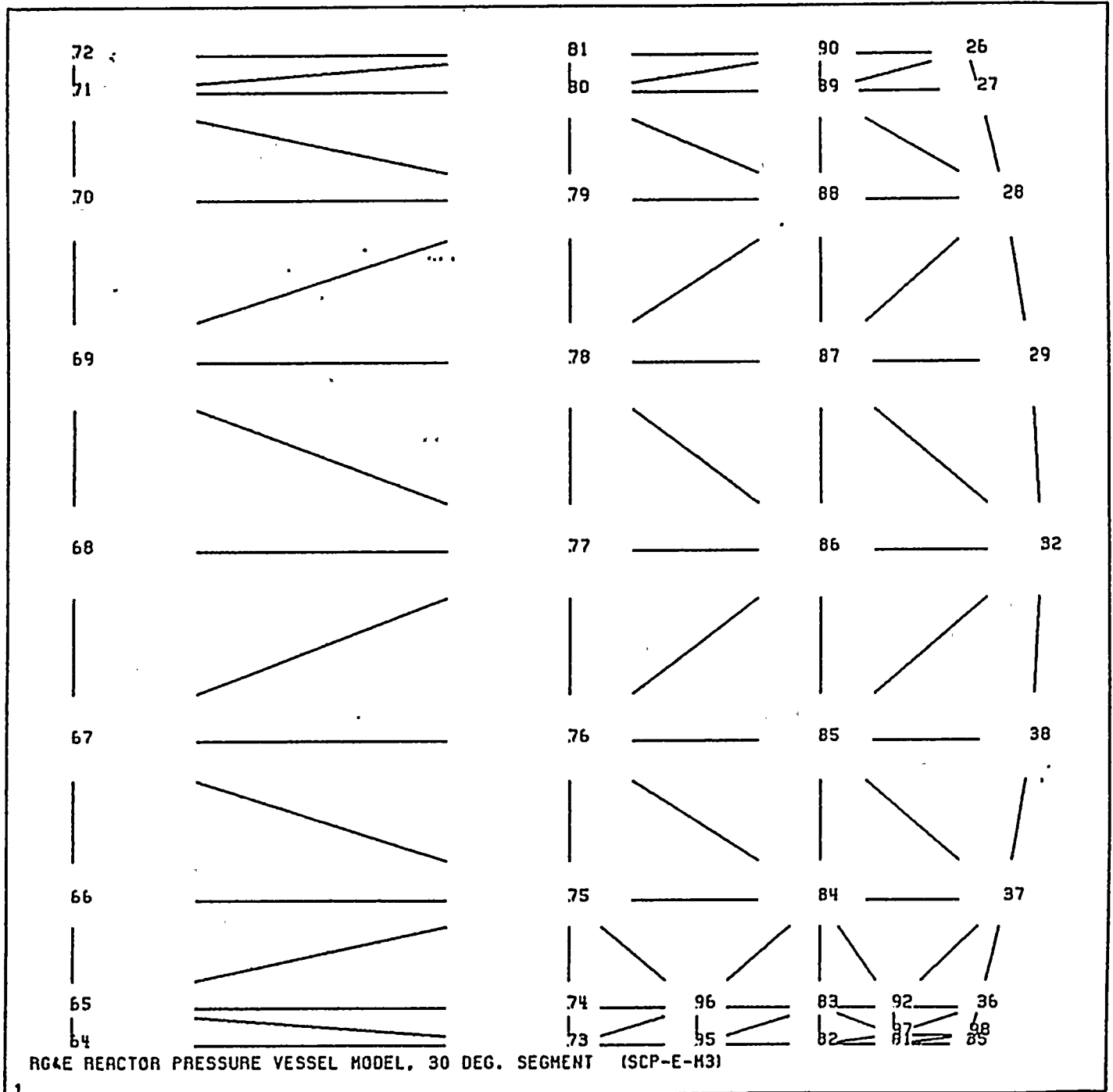
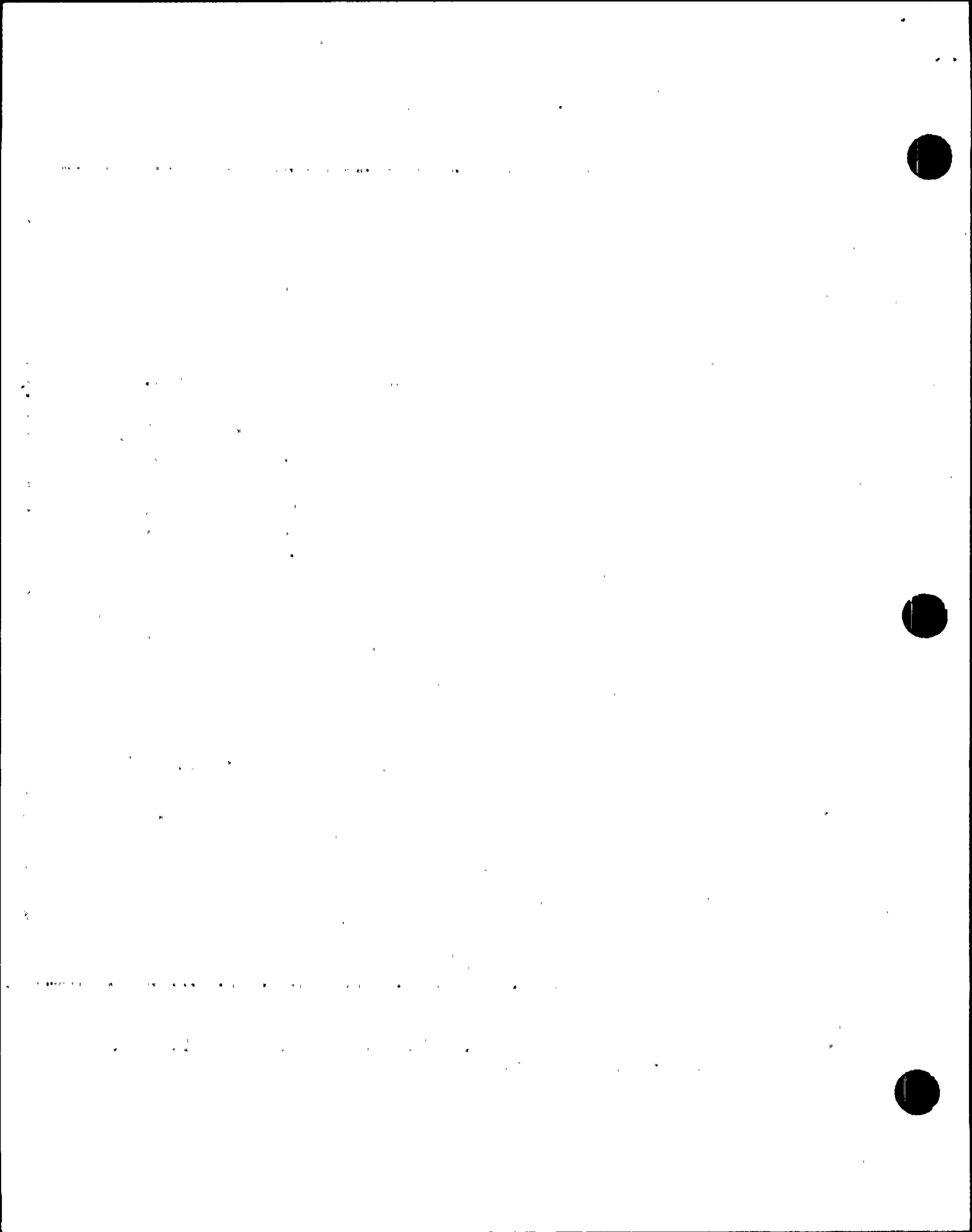


FIGURE 37: Nozzle Node Numbers for the Concentrated Drop Model - Side View



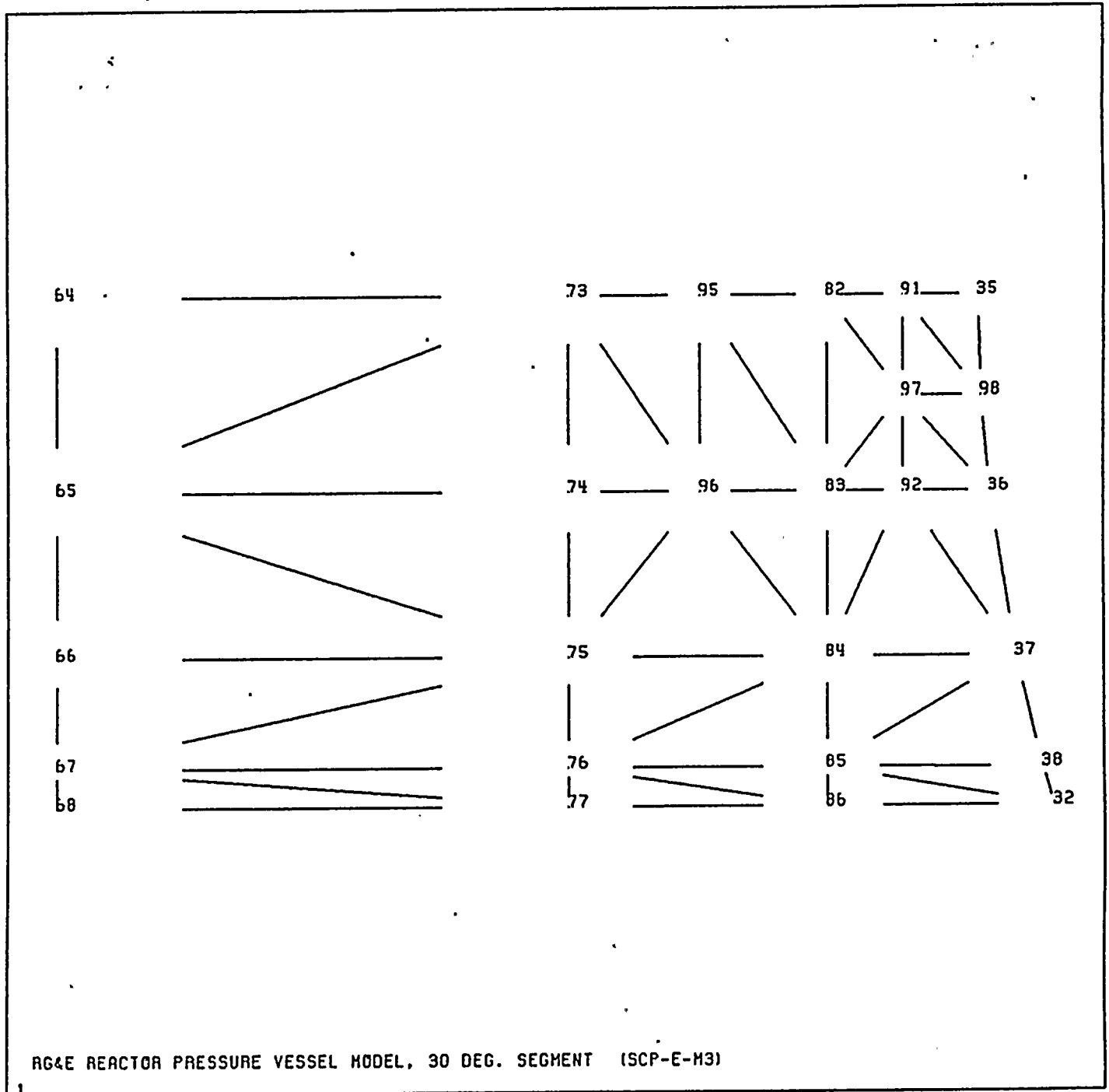


FIGURE 38: Node Numbers for the Lower Half of the Nozzle - Top View, Concentrated Drop Model

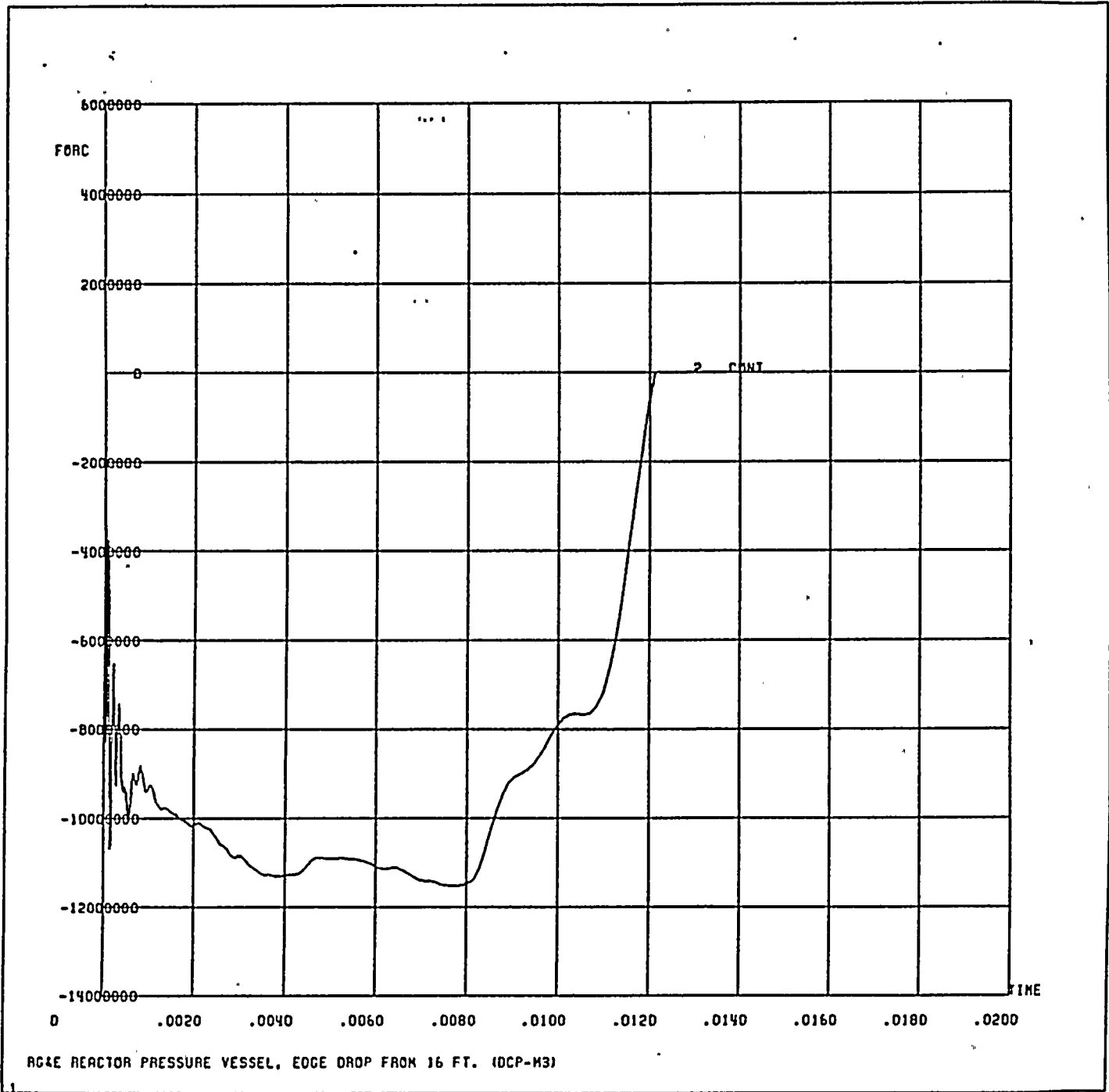
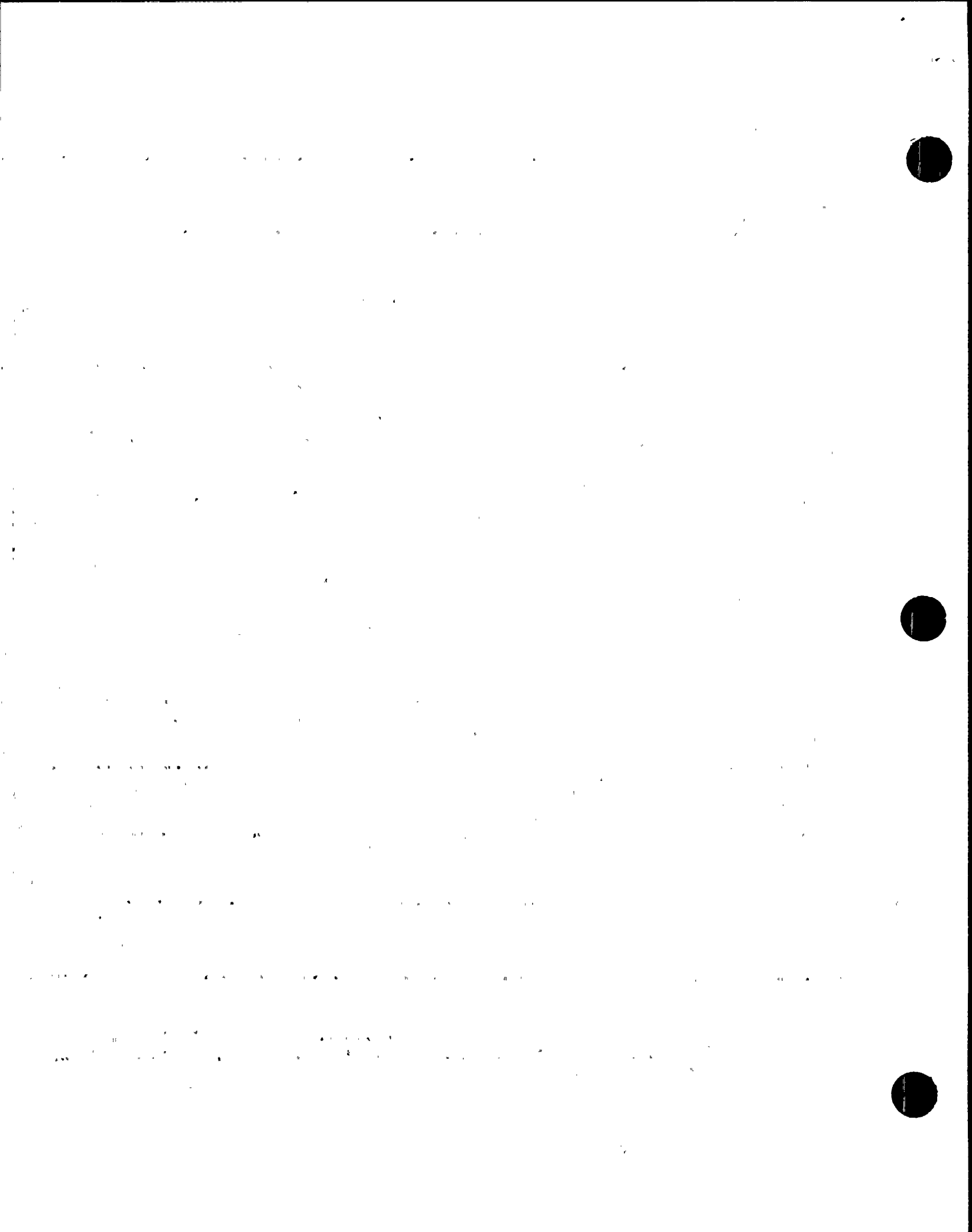


FIGURE 39: Contact Force (lbs) between the Reactor Head and Vessel Flange for a Concentrated Drop versus Time (seconds)



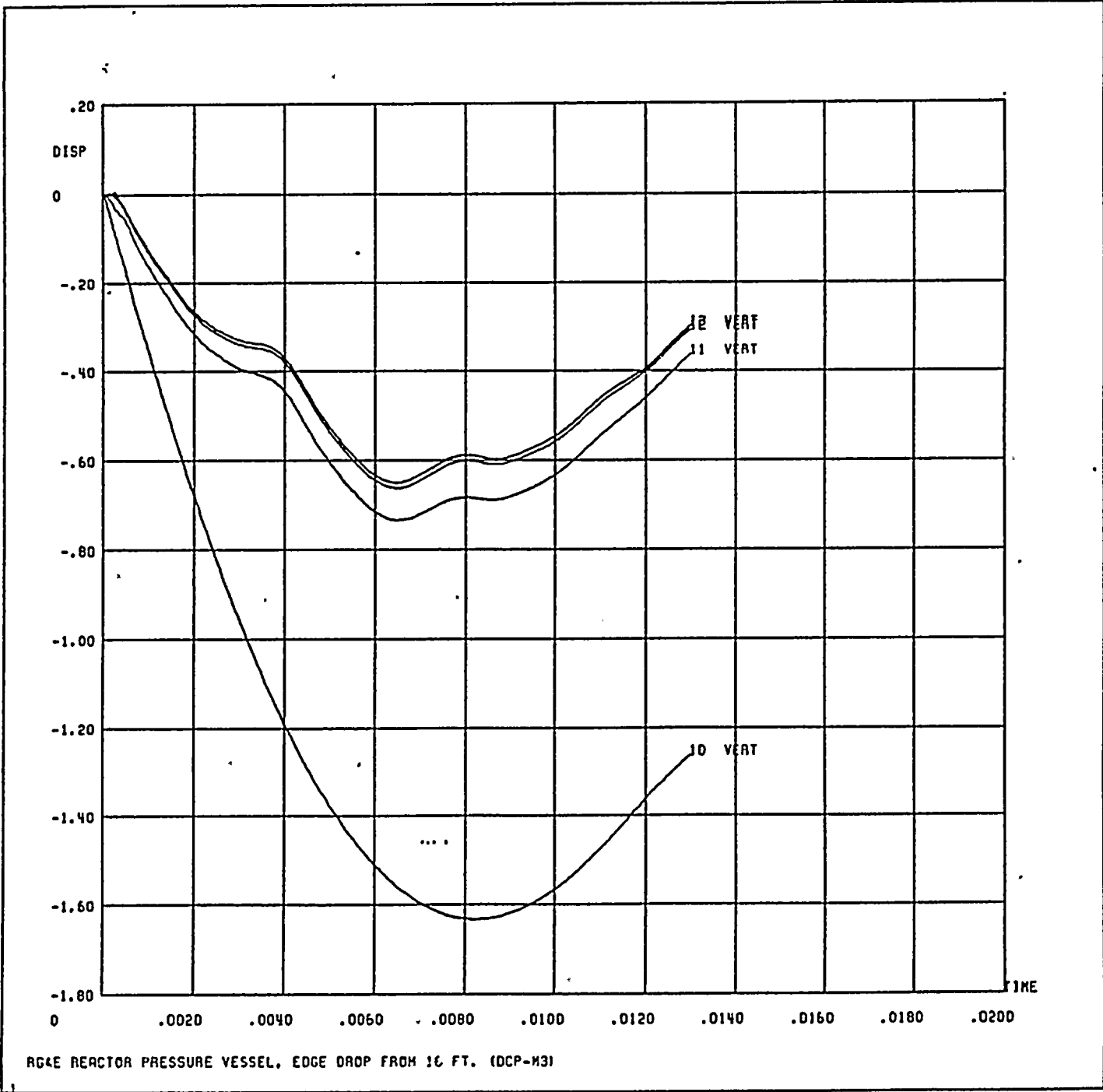


FIGURE 40: Displacement (inches) of Nodes 10,11, 12 and 13 at the Top of the Reactor Vessel Flange for a Concentrated Drop versus Time (seconds)



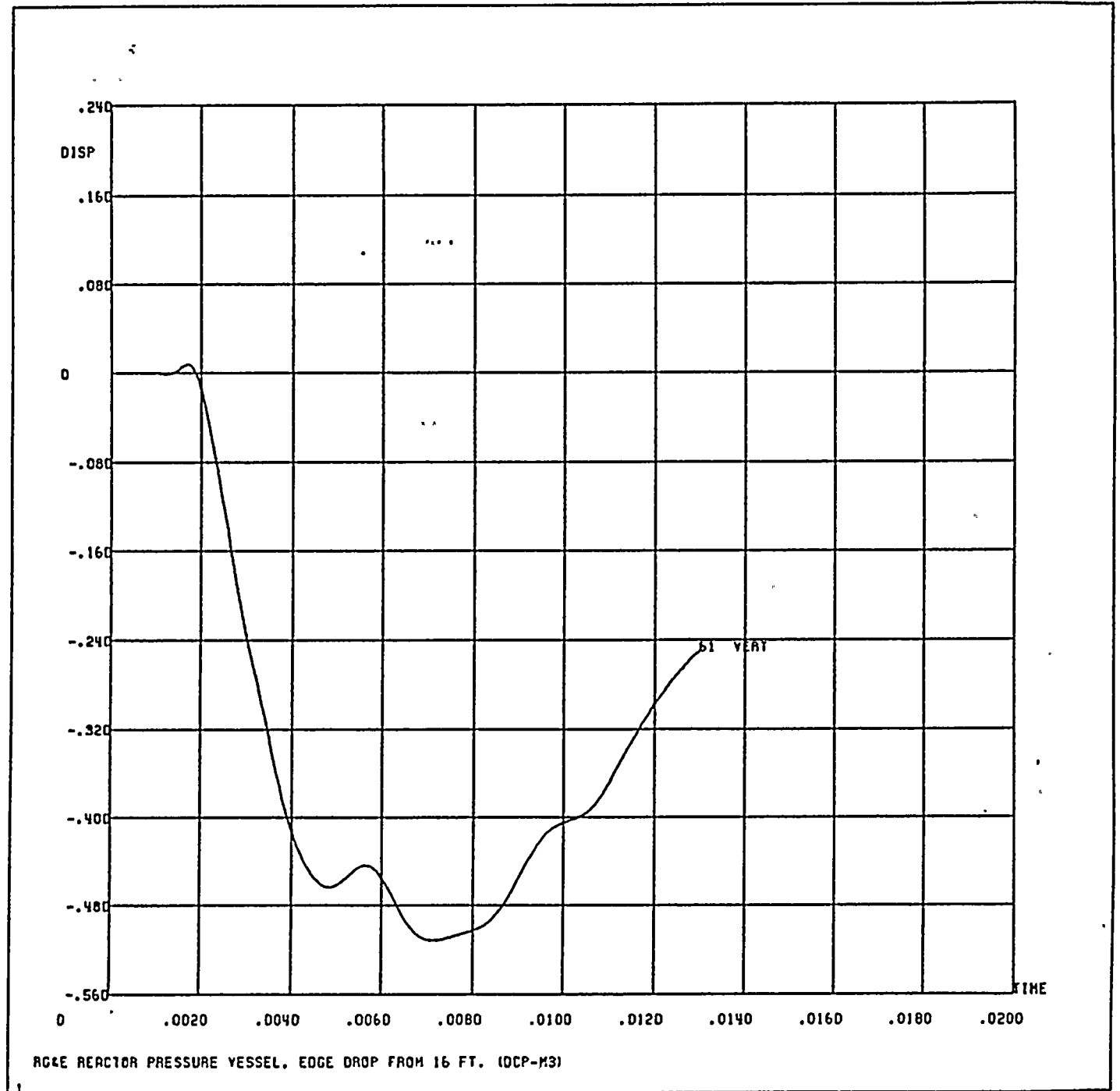


FIGURE 41: Displacement (inches) of Node 61 at the Bottom of the Vessel for a Concentrated Drop versus Time (seconds)



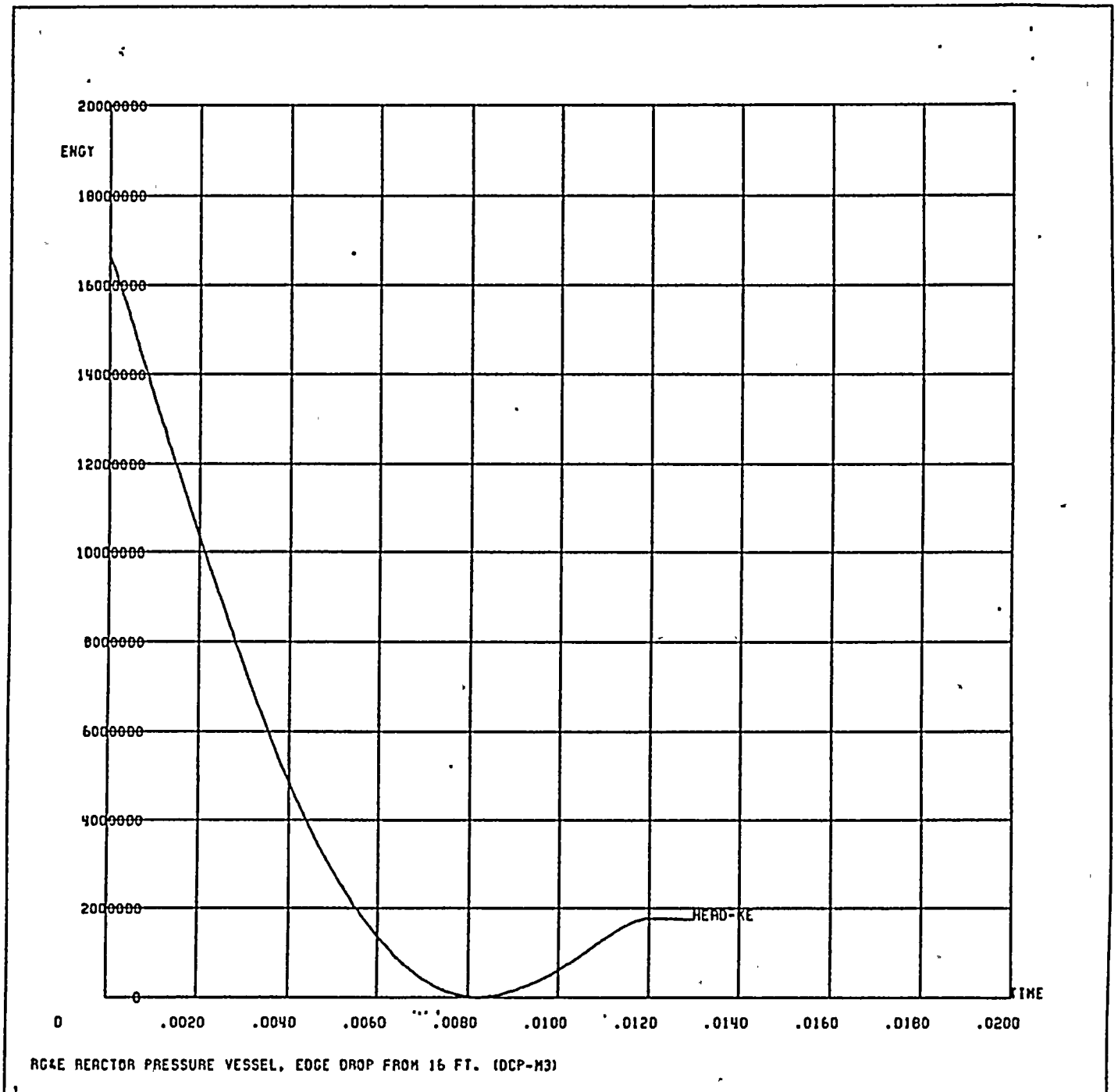
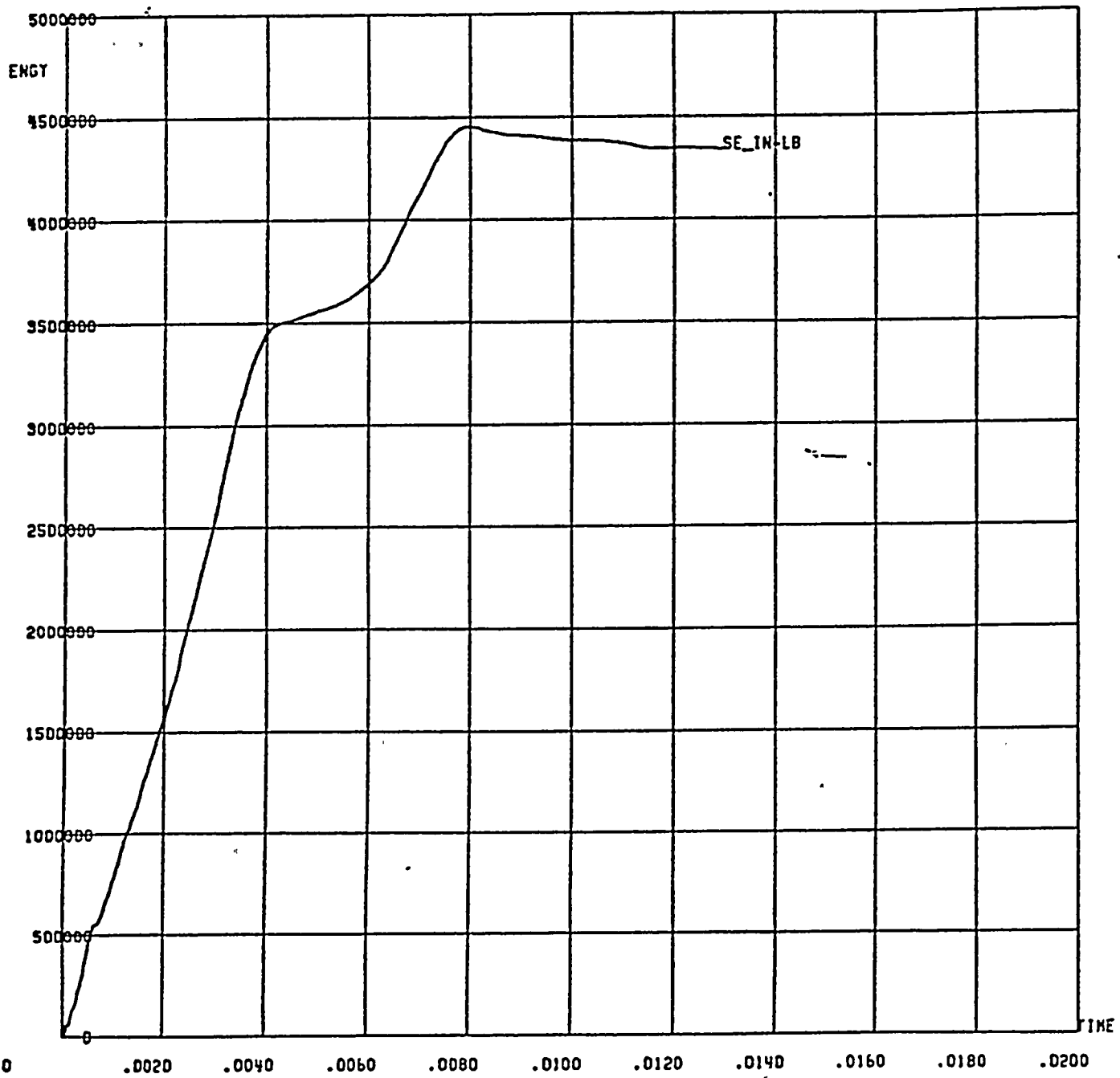


FIGURE 42: Kinetic Energy (inch-pounds) of the Reactor Head versus Time (seconds)



ELEMENT No. 4



RC&E REACTOR PRESSURE VESSEL, EDGE DROP FROM 16 FT. (DCP-N3)

FIGURE 43: Strain Energy (inch-pounds) Absorbed by Element 4 versus Time (seconds)

ELEMENT No. 5

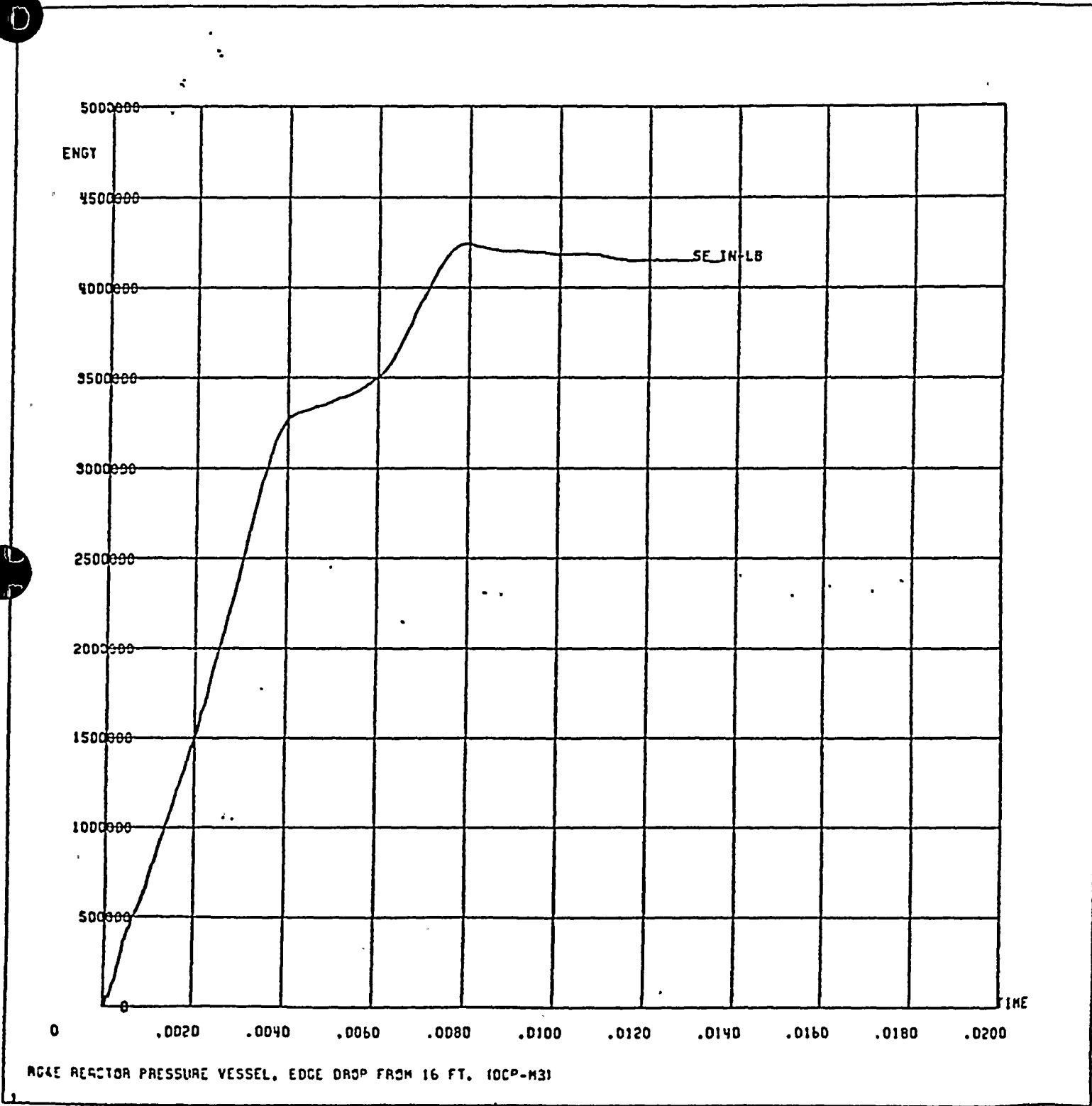


FIGURE 44: Strain Energy (inch-pounds) absorbed by Element 5 versus Time (seconds)

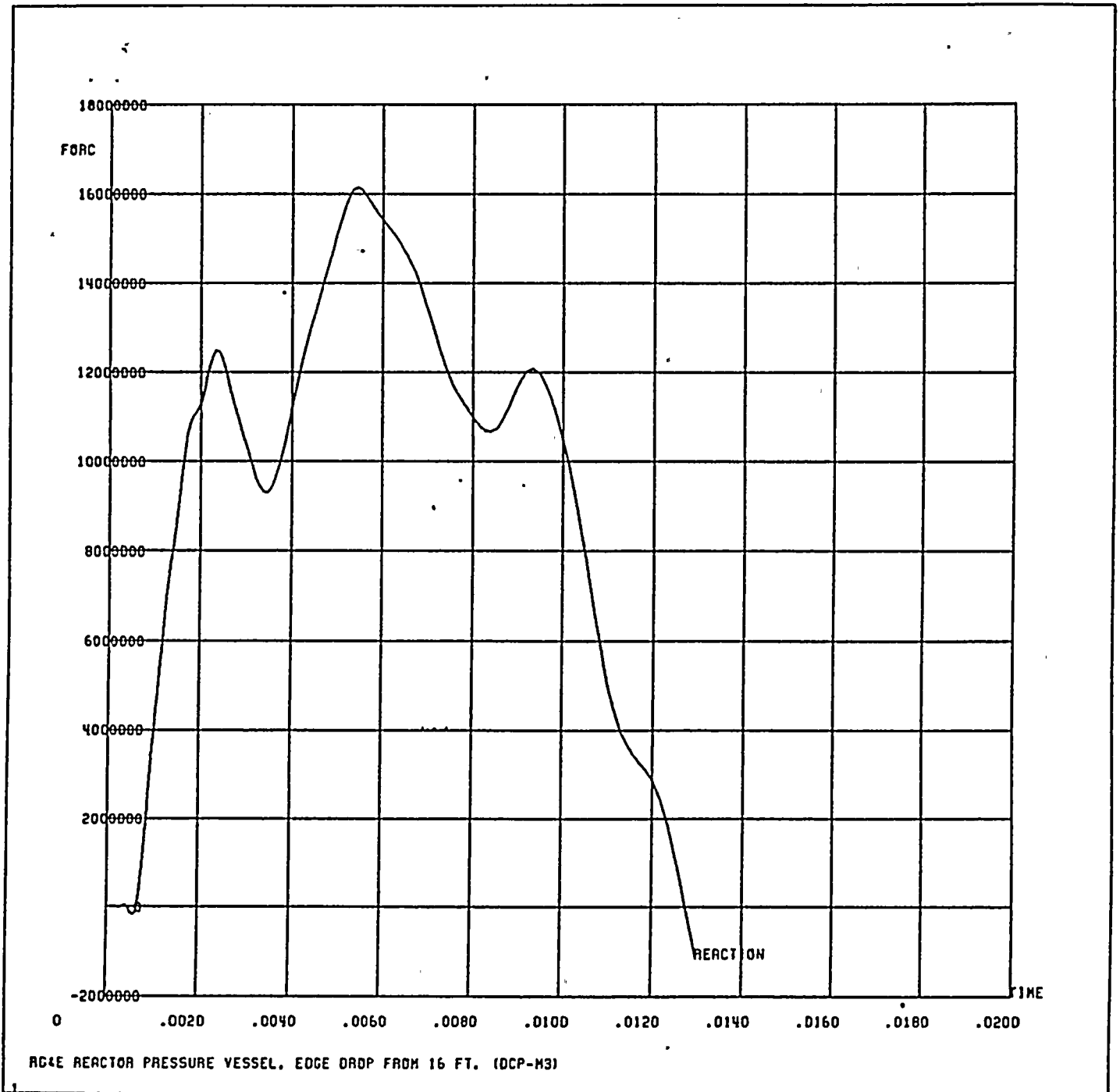


FIGURE 45: Reaction Force (lbs) at the Nozzle Support for a Concentrated Drop versus Time (seconds)

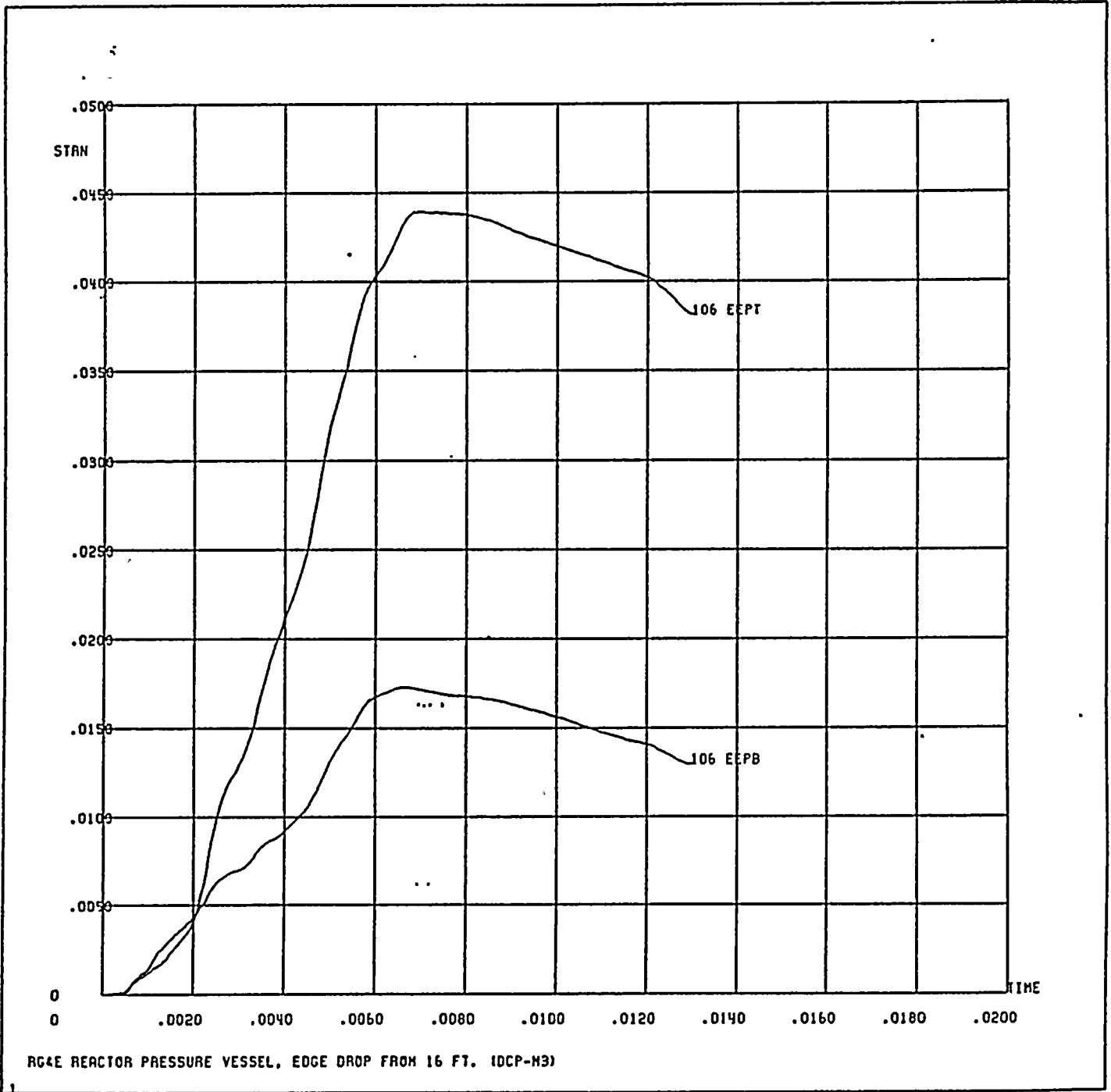


FIGURE 46: Equivalent Strain at the Top (Outside Face) and Bottom (Inside Face) at Element 106 for a Concentrated Drop versus Time (seconds)



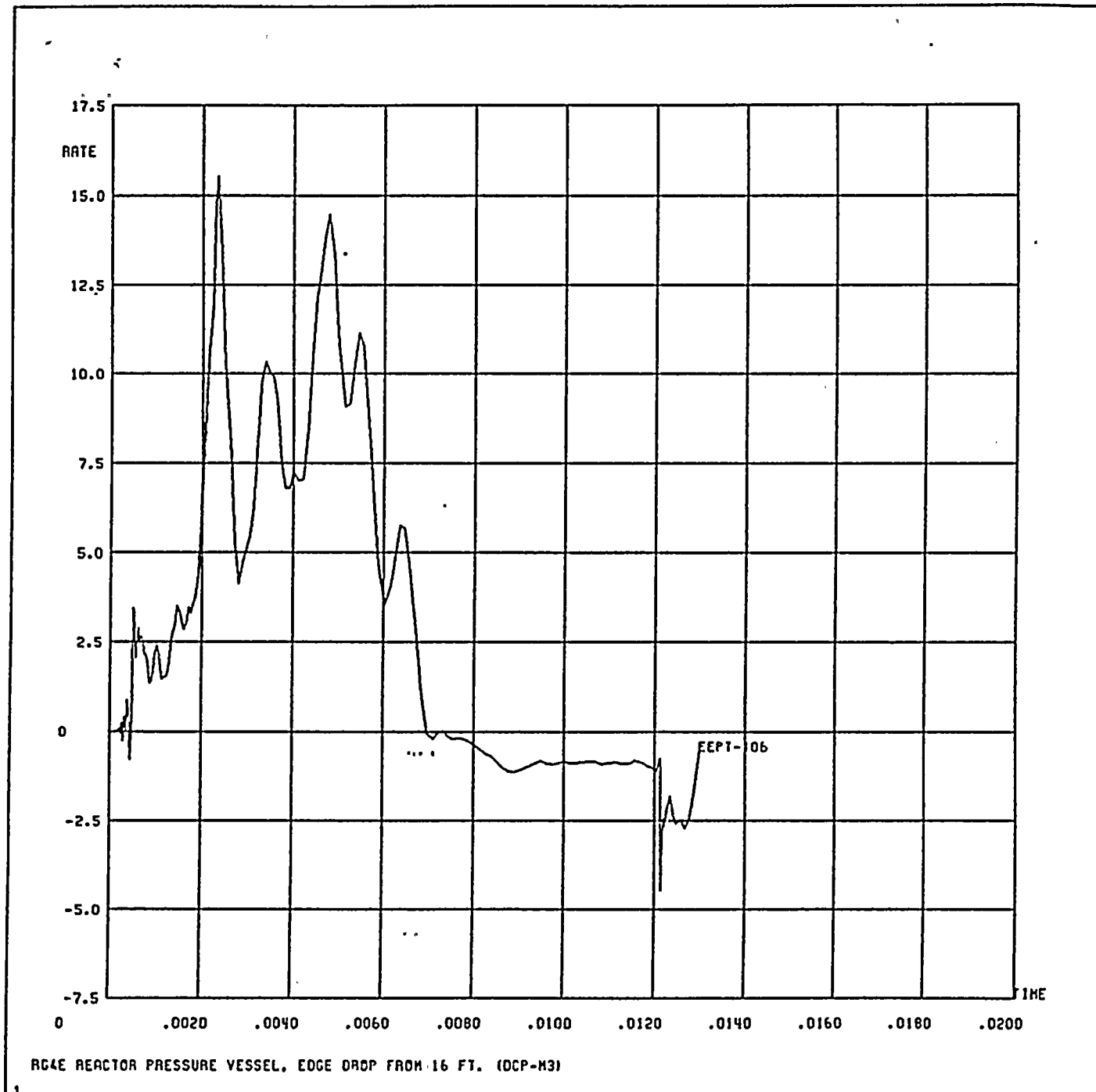


FIGURE 47: Equivalent Strain Rate (in/in/sec) at the Top (Outside Face) of Element 106 for a Concentrated Drop versus Time (seconds)



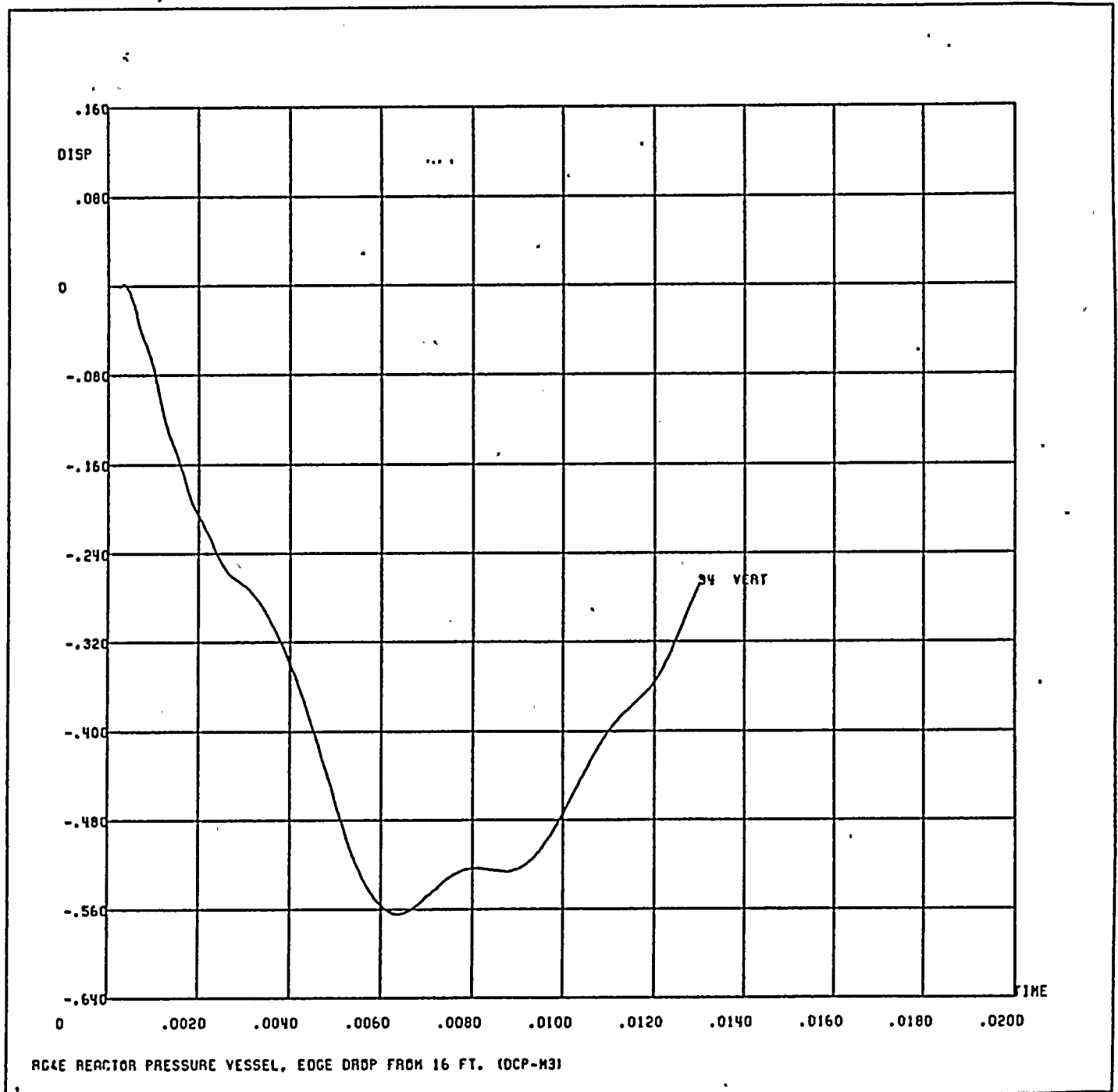


FIGURE 48: Vertical Displacement (inches) of Node 34, which is the approximate location of the Safety Injection Nozzle, versus Time (seconds)

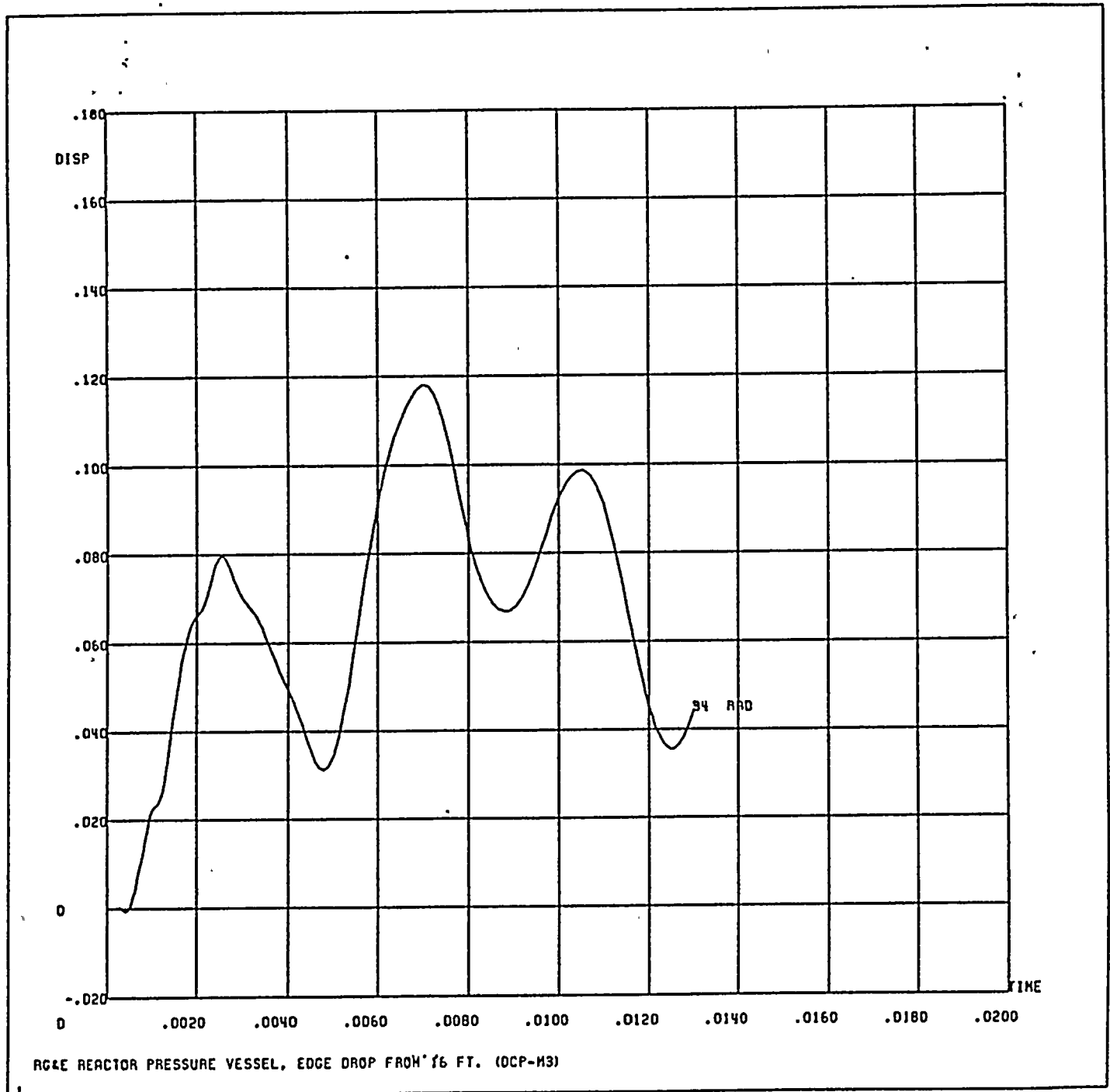


FIGURE 49: Radial Displacement (inches) of Node 34, which is the approximate location of the Safety Injection Nozzle, versus Time (seconds)

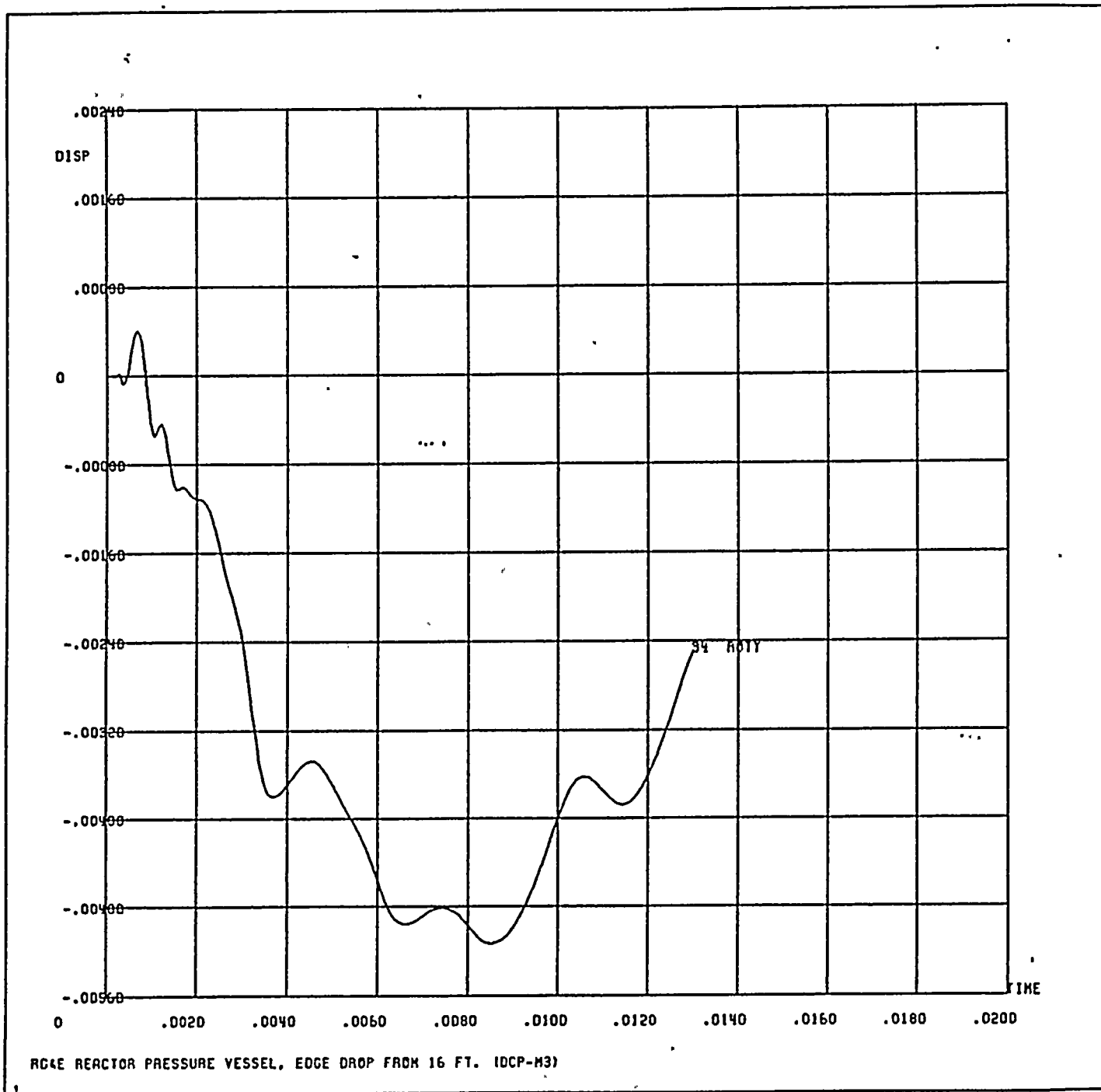


FIGURE 50: Rotation (radians) about the Circumferential Axis of Node 34, which is the approximate location of the Safety Injection Nozzle, versus Time (seconds)

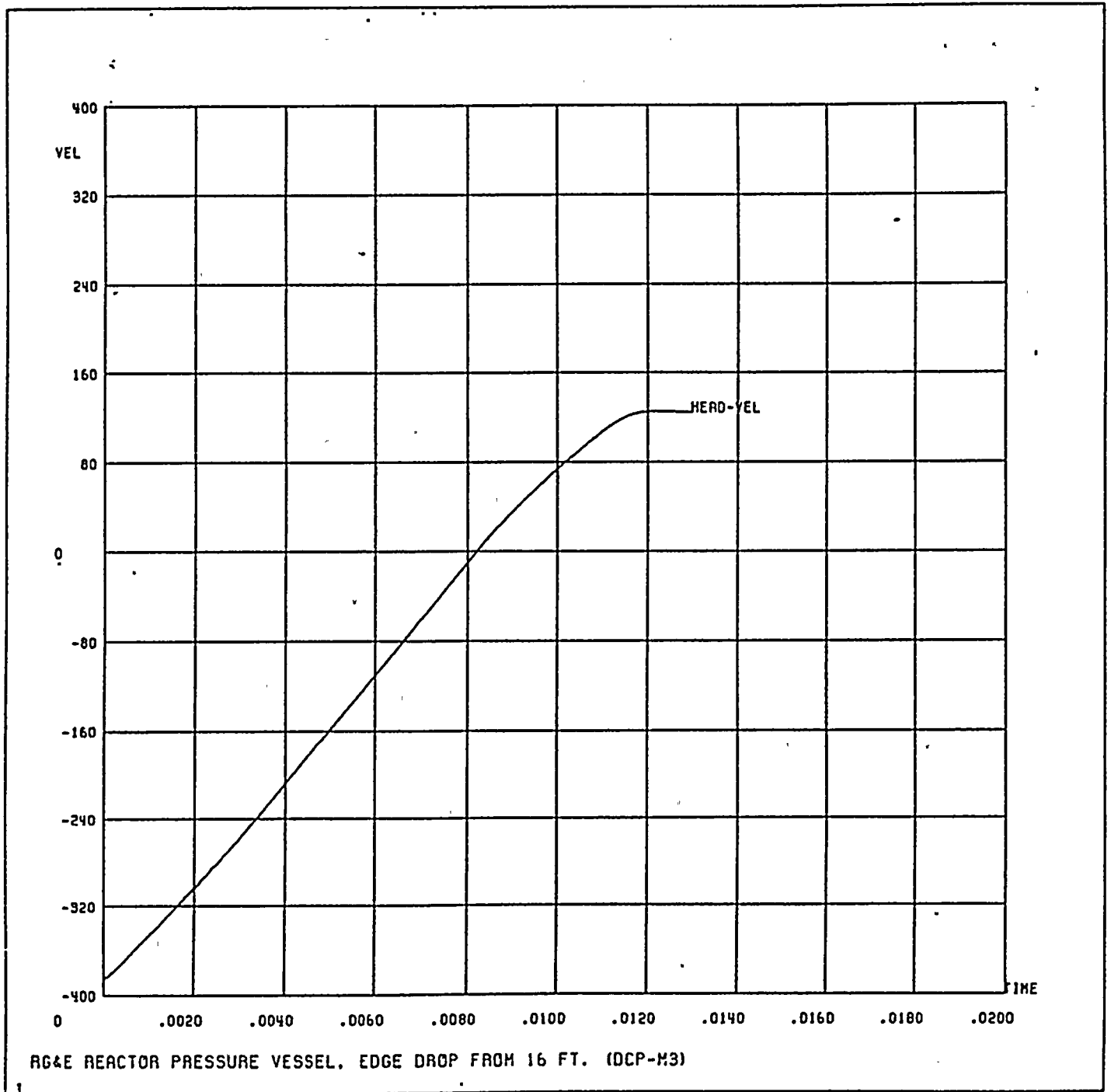


FIGURE 51: Reactor Head Velocity (inches/second, Node 6) versus Time (seconds)

ATTACHMENT 3

Reactor Upper Internals Drop Analysis



FINAL REPORT
FOR THE
UPPER INTERNALS DROP ANALYSIS FOR GINNA STATION
JOB NO. 83084

R. E. GINNA NUCLEAR POWER STATION

ROCHESTER GAS AND ELECTRIC CORPORATION
ROCHESTER, NEW YORK

COPY NO. 2

Prepared Robert B. Bishman 1/30/84
Lead Engineer

Approved John D. McWilliam 1/30/84
Project Manager

Approved Mark B. Fitzsimmons 2/6/84
Rochester Gas & Electric
Mark B. Fitzsimmons 2-6-84

TABLE OF CONTENTS

<u>Section</u>	<u>Page</u>
1.0 Introduction	1
2.0 Upper Internals Description	2
3.0 Problem Description	2
4.0 Acceptance Criteria	3
5.0 Analysis Methodology and Results	4
5.1 Energy at Impact	5
5.2 Fuel Assembly Buckling	8
5.3 Upper Support Plate Deformation	10
5.4 Other Considerations	12
6.0 Conclusions	13

Appendices

A	References
B	Figures 1 through 12

2000



2000



FINAL REPORT

Upper Internals Drop Analysis

1.0 INTRODUCTION

This report documents the results of Cygna's analysis of the upper internals dropping into the core barrel of the reactor at Ginna during refueling operations. The report is intended to form the basis for a response to issues raised in NUREG-0612.

Three basic analyses were conducted. The first was an analysis to determine the total impact kinetic energy developed by the upper internals as it falls freely through water within the reactor cavity pool and reactor core barrel. The second was a non-linear finite element plasticity analysis of the upper support plate of the upper internals performed to determine the strain energy absorbed upon impact. The third was an elastic buckling analysis of the fuel assemblies performed to determine the additional strain energy absorbed when the fuel assemblies are impacted by the upper internals. The total strain energy absorbed through plastic deformation of the upper support plate and elastic buckling of the fuel assemblies was compared to the impact kinetic energy. The report concludes that a postulated drop of the upper internals from a height of fifteen feet above the core is acceptable.

2.0 UPPER INTERNALS DESCRIPTION

The upper internals package at Ginna is a cylindrical structure consisting of top and bottom plates separated by a series of vertical support columns (Figure 1) and the control rod guide tubes. The top plate, called the upper support plate, is four inches thick and approximately 128 inches in diameter. The bottom plate, called the upper core plate, is one and one half inches thick and approximately 108.5 inches in diameter. The plates are structurally separated by 12 vertical support columns approximately 115 inches in length. The entire upper internals package is supported by the outer edge of the upper support plate which sits on an "O" ring at the top of the core barrel flange (i.e., the upper internals "support ledge"), (Figures 2 and 3).

3.0 PROBLEM DESCRIPTION

During refueling operations, the upper internals are removed from the core barrel using a special lifting device attached to the 100 ton containment overhead crane. The lifting device has three support legs which engage three threaded holes evenly spaced along the outer periphery of the upper support plate. To insure vertical alignment during the lift, the special lifting device also has three vertical sleeve attachments that fit over three widely spaced guide studs which are threaded into the reactor vessel flange (Figure 4). The guide studs project approximately 15 feet above the top of the upper support plate.

At any time while the upper internals package is directly over the reactor vessel, there is a possibility that, if dropped, the upper internals could impact the fuel assemblies in the reactor

core. However, once the lifting rig guide sleeves are above the top of the three guide studs, the upper internals can be moved out of concentric alignment with the reactor vessel core barrel (Figure 5). With the upper internals sufficiently out of concentric alignment with the vessel, it is impossible for the upper internals to impact the fuel assemblies. At a height of 15 feet, the guide sleeves are approximately one foot above the top of the guide studs. This is the maximum height for which concentric alignment of the upper internals and vessel must be maintained and is therefore considered the maximum height from which the upper internals could still impact the fuel assemblies in the reactor (Figure 6).

The weight of the upper internals was determined from the maximum load cell readings recorded when lifting the upper internals package during several recent refueling outages. It was conservatively assumed that, in addition to the weight of the upper internals (52,100 pounds), the total load dropped onto the fuel assemblies included the weight of the lifting rig (12,000 pounds) and the crane hook block (8,500 pounds). Thus, the total dry weight used in the drop analysis was conservatively taken as 72,600 pounds.

4.0 ACCEPTANCE CRITERIA

The final basis for the acceptability of the consequences of a postulated upper internals drop is that neither the fuel rods shall rupture nor shall the fuel be crushed. Under these conditions, no radioactive gases can be released. To prohibit fuel rod rupture and fuel crushing, the following conservative criteria were established:

1. The strain in the Zircaloy-4 fuel rod shall remain in the elastic range after axial and lateral deformation. The material maximum strain is limited to the yield strain of 0.0047 inches/inch. This is well below the allowable strain used for design of 0.01 inches/inch.
2. The strain energy absorbed in the Zircaloy-4 guide tube shall be limited to the energy absorbed prior to elastic buckling. Energy absorbed during inelastic deformation shall not be considered.
3. The strain energy absorbed by the upper support plate shall be strain limited such that the equivalent strain in the stainless steel upper support plate of the upper internals shall not exceed one half of the minimum ultimate strain of 0.4 inches/inch. Thus, the actual equivalent strain in the upper support plate shall not exceed 0.2 inches/inch.

If the above criteria are satisfied and the energy absorbed during impact is greater than the kinetic energy of the internals at impact, the consequences of the load drop are acceptable.

5.0 ANALYSIS METHODOLOGY AND RESULTS

Three principal evaluations were performed. First, an analysis was made to determine the total kinetic energy developed by the upper internals falling freely through water (both in and out of the core barrel) and impacting the upper internals support ledge. Next, a non-linear finite element plasticity analysis of the upper support plate was performed to determine the strain energy absorbed upon impact with the upper internals support ledge.

Finally, an elastic buckling analysis of the fuel assemblies was done to determine the additional strain energy absorbed when the fuel assemblies are impacted by the downward displacement of the upper internals. The total strain energy absorbed through plastic deformation of the upper support plate and elastic buckling of the fuel assemblies was then compared to the kinetic energy of the internals at impact.

5.1 Energy at Impact

The upper internals package was assumed to fall through a lifted height of 15 feet, which is approximately one foot above the height at which the lifting rig guide sleeves are decoupled from the three guide studs. At this point, the bottom of the upper internals is approximately five feet above the vessel flange (Figure 5). The analysis assumed the upper internals would initially fall through five feet of water above the vessel, fit perfectly into the vessel core barrel (with only 1/4 inch clear space all around), and fall through ten feet of water in the core barrel before impacting the support ledge. It was conservatively assumed that no binding or wobble would occur along either the guide studs or the core barrel that would tend to reduce the impact kinetic energy (or possibly even prevent impact).

To determine the impact velocity of the upper internals at the instant it strikes the upper internals support ledge, the calculation of the resisting (drag) forces acting on the upper internals as it falls freely in water is required. The basic expression for the resisting forces has the form

$$F = \frac{1}{2} C A \rho V^2$$

where ρ is the mass density of water, V is the velocity of fall, A is a projected area on a plane perpendicular to the direction of travel, and C is the drag coefficient which depends on the shape of the falling object and confining conditions. Drag coefficients were derived for three separate regions: above the vessel, in the core barrel at the reactor coolant loop outlet nozzle openings, and in the core barrel above and below the nozzle openings (Figure 7).

To determine the resisting force acting during the free fall above the vessel, only the gross area of the upper support plate was used in conjunction with a drag coefficient for a solid circular disc of 1.0. The use of this drag coefficient together with the gross area of only the upper support plate is reasonable since the reduction in drag due to the openings in the upper support plate is more than compensated by neglecting the drag on the net area of the upper core plate.

The resisting force for free fall of the upper internals in the core barrel was derived from first principles (i.e., the equations of motion, continuity and momentum). In the derivation, the only portion of the upper internals on which resisting forces were considered to act was the upper core plate. Resisting forces acting on the upper support plate, support columns and control rod guide tubes were neglected. Considering the upper core plate to be a flat circular ring falling freely within a fluid filled cylinder, the expression for the resisting force becomes

$$F = \frac{1}{2} \left[\frac{A}{C_d A_o} - 1 \right]^2 \rho A V^2$$

where V and ρ are defined as before, A is the area of the core barrel opening and

$$\left[\frac{A}{C_d A_o} - 1 \right]^2$$

is the "drag coefficient". Within this expression for the drag coefficient, A_0 is the area of all openings through which fluid can pass from one side of the upper core plate to the other, and C_d is the discharge coefficient which accounts for the effects of the vena contracta. The discharge coefficient generally ranges between 0.5 and 1.0. A value of 0.8 is reasonable for the upper core plate and was used in the analysis.

When the internals enters the core barrel, the net flow area of the upper core plate for the region of the core barrel above the outlet nozzles results in a computed drag coefficient of 5.4. As the upper core plate falls past the openings for the two outlet nozzles, the net flow area is increased and the drag coefficient becomes 2.1. The value 2.1 is conservative since it assumes that for the entire nozzle depth water can flow around the upper core plate through an area equal to one half of the nozzles open area. This is the maximum area and occurs only when the upper core plate is at the midheight of the nozzle opening. Once the upper core plate reaches the bottom of the opening, a drag coefficient of 5.4 is again used until impact.

Equilibrium of the free body diagram of the falling internals results in a second order non-linear differential equation. This equation was solved for velocity as a function of displacement. Assuming the velocity to be zero at the time of the drop, the velocity was calculated at the beginning and end of each of the four regions through which the internals must fall, as well as at several intermediate points. A plot of the internals velocity profile during free fall is shown in Figure 8. The final velocity of the upper internals at the instant of impact with the fuel assemblies is 15.3 feet per second. This velocity results in a total kinetic energy at impact of 263,000 foot-pounds.

5.2 Fuel Assembly Buckling

Due to the small gap which initially exists between the upper internals and the fuel assemblies and the fact that the upper support plate must deform by several inches after impact in order to absorb 263,000 foot-pounds of energy, it was apparent that some of the impact kinetic energy must be absorbed by the fuel assemblies themselves. Thus, the analysis of the fuel assemblies provided two important results: (1) the amount of elastic strain energy that could be absorbed by the fuel assemblies and (2) the amount of vertical displacement the fuel assemblies would experience while absorbing this energy. The magnitude of this displacement, together with the known gaps between the upper internals and fuel assembly nozzles and between the nozzles and fuel rods, determined the permissible vertical displacement of the upper internals. Knowing this permissible vertical displacement, the total strain energy absorbed by the upper support plate of the upper internals could be determined.

The actual analysis of the fuel assemblies conservatively considered only the energy absorbed during elastic buckling. The analysis assumed that the guide tubes buckled at their narrowest section between the two lowest grid spacers and that the fuel rods buckled between all nine grid spacers which tie the guide tubes and the fuel rods together. Since the distance between the grid spacers was somewhat variable, an average length was assumed in the buckling analysis. An end restraint factor of 3.4 (4.0 is fixed and 1.0 pinned) was used for the guide tubes, while a factor of 1.08 was used for the fuel rods. Both the guide tube and fuel rod cladding material is Zircaloy-4.

The energy absorbed by the 16 guide tubes in axial deformation prior to elastic buckling was calculated for each assembly.



(The energy absorbing capability of the instrument tube has been conservatively neglected in this analysis.) Based on the structure of the fuel assemblies (Figure 9), the guide tubes must buckle prior to the fuel rods because they attach directly to the fuel assembly nozzles, whereas a total gap of 1.565 inches exists between the nozzles and the fuel rods. After the guide tube critical buckling load was reached, no further energy was assumed to be absorbed by the guide tubes. Downward displacement still continued until the 179 fuel rods per assembly were loaded. Again, the fuel rods were assumed to deform only to the elastic limit. The lateral deformation due to an applied axial load was determined from an initial fuel rod bow of 0.001 of the span length. The resulting strain energy from axial and bending deformation due to initial curvature was calculated. The combined strain energy from the elastic buckling of the guide tubes and the fuel rods for each assembly was determined.

The elastic buckling of the 16 guide tubes in each fuel assembly results in 163 foot-pounds of absorbed strain energy. As the 179 fuel rods per assembly are loaded, a total of 2,130 foot-pounds of strain energy is absorbed prior to reaching the elastic limit. Therefore, for each fuel assembly a total of 2,293 foot-pounds of strain energy is absorbed during elastic deformation. The total strain energy for all 121 fuel assemblies in the core (Figure 10) was thus determined to be 277,000 foot-pounds.

The analytic determination of the energy absorbed by the fuel assemblies is conservative since no credit has been taken for energy absorbed in the inelastic range. The yield strain value of 0.0047 inches per inch for Zircaloy-4 material is well below the minimum allowable strain of 0.01 inches per inch used in the



design of the fuel assemblies. If the material were allowed to go into the plastic range, a significant amount of additional strain energy would be absorbed. Furthermore, additional deformation in the fuel assemblies due to non-linear effects would result in significant additional energy being absorbed by the upper internals support plate, since the internals could deflect downward through an additional finite distance.

From the displacement of each fuel assembly due to axial shortening, the total downward displacement of the upper internals was computed. This displacement in turn determined the final strain energy absorbed by the upper support plate.

5.3 Upper Support Plate Deformation

The upper support plate was analyzed using the elastic-plastic finite elements available within the ANSYS program, Version 4.1B. Due to symmetry considerations, only a 45° segment of the upper support plate was modeled. The mass of the attached structures below the upper support plate (support columns, upper core plate, etc.) as well as the mass of the load block and lifting rig were conservatively distributed over the inner regions of the plate directly above the open core barrel. The basic geometry of the initial finite element mesh was determined from several test problems for which the results could be compared to known exact solutions. A fine finite element mesh was not required since only displacement and strain energy calculations were required. Thus, an accurate yet cost effective mathematical model was developed. An elastic static analysis was performed to insure proper model behavior.

With the results from the elastic analysis, the model was revised to account for plasticity. Those elements identified as poten-

tially capable of developing plastic strains were modified from elastic quadrilateral plate bending elements to triangular plasticity plate bending elements as required by the ANSYS program (Figure 11). Static plastic analyses were then performed using a series of applied accelerations ranging from 0.1g to 32g's. In this way, the maximum displacement was determined for each value of acceleration. The total strain energy absorbed by the upper support plate when then found by integrating the stresses and strains over the volume of each finite element. This provided a relationship between the maximum displacement of the plate (at any "g" level) and the total strain energy absorbed.

The energy absorbed by the upper internal's package is directly dependent on the deformation through which it moves. This deformation is equal to the distance between the bottom of the upper core plate and the top of the fuel assemblies at the point where the elastic limit of the fuel rods has been reached. Quantitatively, this distance is the sum of a 0.3 inch gap between the upper core plate and the fuel assemblies under normal conditions, a 1.565 inch gap between the top and bottom fuel assembly nozzles and the tips of the fuel rods, and a 0.549 inch axial shortening of the fuel rods during elastic buckling. The total deformation is 2.41 inches. As shown in the graph of Figure 12, this deformation level corresponds to 107,000 foot-pounds of strain energy absorbed by the upper internal's support plate. The corresponding maximum equivalent strain in the upper support plate at this deformation level is approximately 0.014 inches/inch. This is well below the acceptance value of 0.2 inches/inch.

5.4 Other Considerations

In addition to the conservative assumptions already incorporated in the analysis, three other important conservative assumptions have been made in this evaluation. First, the upper internals are free to fall without binding or wobbling. Clearly any small lateral movement or twisting of the upper internals might be sufficient to prohibit the internals from falling entirely back into the core barrel, since only a one quarter inch clearance exists between the core barrel and the upper core plate. As a minimum, some energy will be dissipated each time the lifting rig sleeves slide against the guide studs, or the upper core plate scrapes the core barrel.

Second, the mass of the 12,000 pound lifting rig is assumed to be distributed over and carried by the upper support plate in the area directly over the core, when, in fact, the lifting rig is supported by three relatively stiff leg assemblies and a support ring located directly above the support ledge of the core barrel flange. The kinetic energy due to the lifting rig could actually be applied directly to the core barrel flange, rather than to the upper internals and fuel assemblies as has been assumed in the analysis.

Third, the kinetic energy loss which occurs during the transfer of momentum between the upper internals and the fuel assemblies has been neglected. This energy loss is probably on the order of 60% of the total impact kinetic energy, but since it is generally difficult to quantify, it has conservatively been neglected.

6.0 CONCLUSIONS

The results of the above analyses have conservatively estimated the total energy capable of being absorbed during an impact by the upper internals as 384,000 foot-pounds. This consists of 277,000 foot-pounds absorbed by the fuel assemblies during elastic deformation and 107,000 foot-pounds absorbed by the upper support plate of the upper internals while deforming compatibly with the fuel assemblies. The lower bound estimate of 384,000 foot-pounds for the energy absorbed during impact is well in excess of the 263,000 foot-pounds of kinetic energy possessed by the upper internals at the time of impact. Since all of the absorbed energy has been calculated from deformations which do not exceed the elastic limit of the fuel rods, it is concluded that a postulated drop of the upper internals back into the vessel would neither rupture the fuel cladding nor crush the fuel in the fuel rods.

Thus, a postulated drop of the upper internals from a height of 15 feet will be acceptable. At this height, the bottom of the internals is approximately five feet above the top of the core barrel, and the lifting rig guide sleeves are above the top of the three guide studs by approximately one foot. It is very difficult to conceive of the upper internals falling freely from any higher elevation without any interference, since the smallest lateral movement will preclude a unincumbered fall back into the core barrel.

APPENDIX A

References



REFERENCES

1. Fluid Mechanics, by V. L. Streeter, Third Edition, McGraw-Hill Book Co., 1962.
2. Ordinary Differential Equations, by W. Kaplan, Addison-Wesley Co., 1958.
3. Theory of Elastic Stability, by S. P. Timoshenko and J. M. Gere, Second Edition, McGraw-Hill Book Co., 1961.
4. ANSYS Engineering Analysis Systems User's Manual, Revision 4.1, Swanson Analysis Systems Inc., Houston, PA.
5. ANSYS Engineering Analysis Systems Theoretical Manual, November 1977, Swanson Analysis Systems, Inc., Houston, PA.
6. Kent's Mechanical Engineers Handbook, J. K. Salisbury, Twelfth Edition, John Wiley and Sons Inc., 1950.
7. Letter: M. B. Fitzsimmons (RG&E) to J. D. McWilliam (Cygn), 8/22/83.
8. Letter: M. B. Fitzsimmons (RG&E) to J. D. McWilliam (Cygn), 10/17/83.
9. Letter: M. B. Fitzsimmons (RG&E) to J. D. McWilliam (Cygn), 12/13/83.
10. Letter: M. B. Fitzsimmons (RG&E) to J. D. McWilliam (Cygn), 1/16/84.
11. Gilbert Associates Inc., Drawing D-521-064.
12. Westinghouse Electric Corp. Drawings, 541-F-205, 541-F-321, 541-F-581, 684-J-650, 684-J-652, 684-J-673, 684-J-732, 684-J-783, 684-J-784, 684-J-852, 684-J-988, 685-J-464.

APPENDIX B

Figures 1 through 12

LIST OF FIGURES

1. Upper Internals
2. Upper Internals within the Reactor Vessel
3. Upper Internals Support Ledge
4. Upper Internals Being Raised from the Reactor Vessel
5. Upper Internals Decoupled from Guide Studs
6. Upper Internals Drop into the Reactor Vessel
7. Regions within Upper Internals Drop Path
8. Upper Internals Velocity During Free Fall
9. Fuel Assembly
10. Plan View of Core with 121 Fuel Assemblies
11. ANSYS Finite Element Model of Upper Support Plate
12. Energy Absorbed by Upper Support Plate

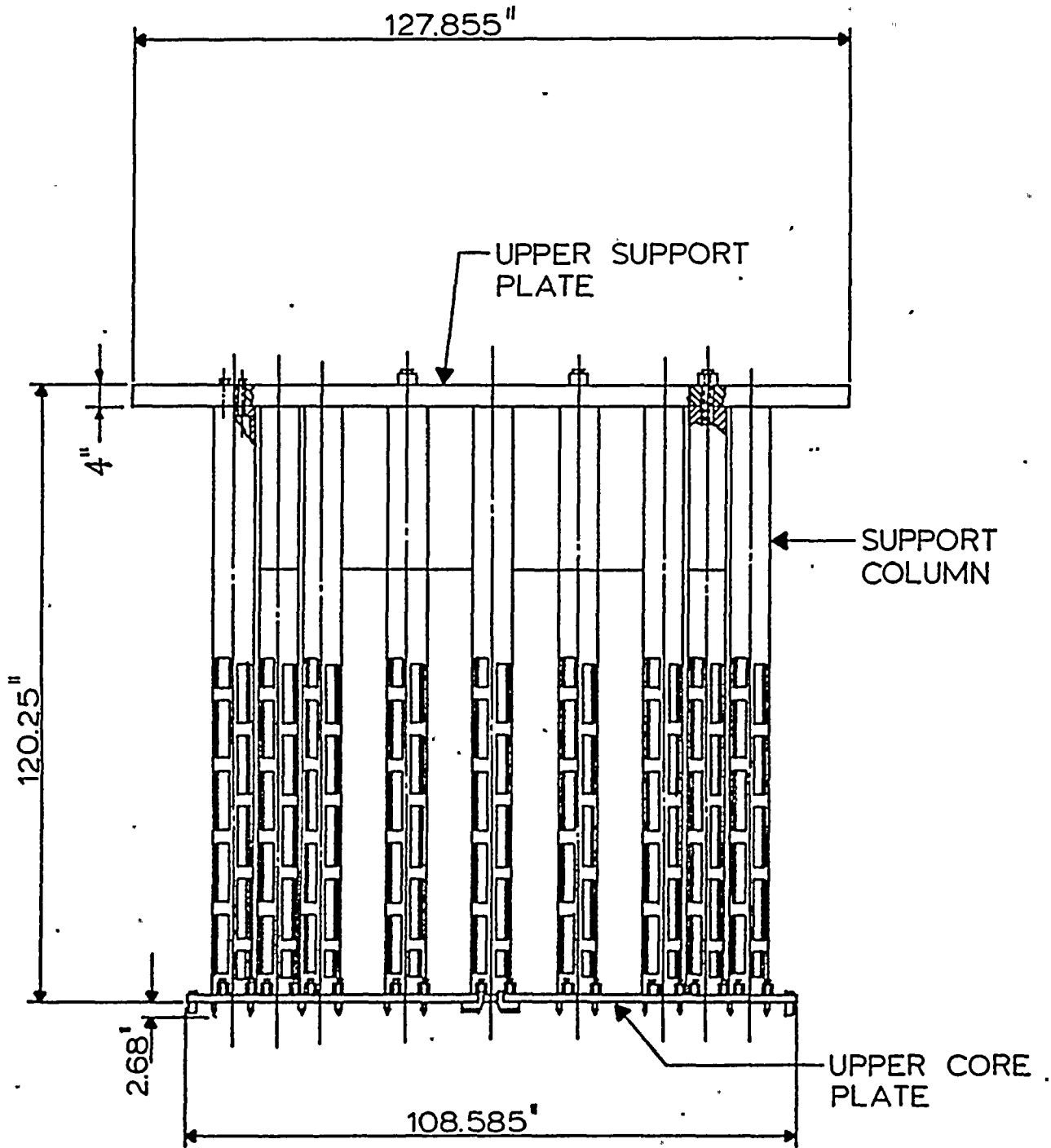
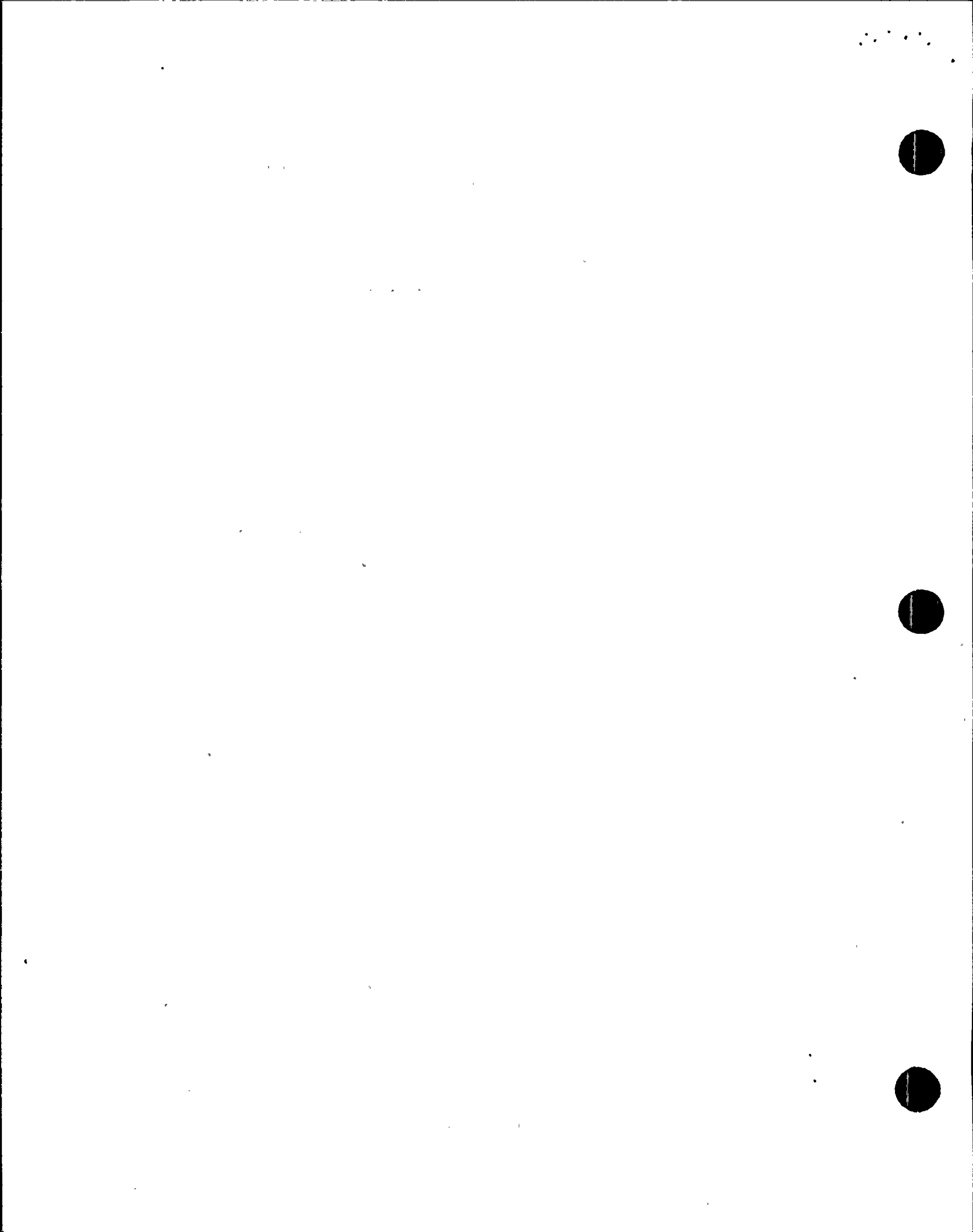


FIGURE 1: UPPER INTERNALS

Note: Control Rod Guide Tubes not Shown for Clarity



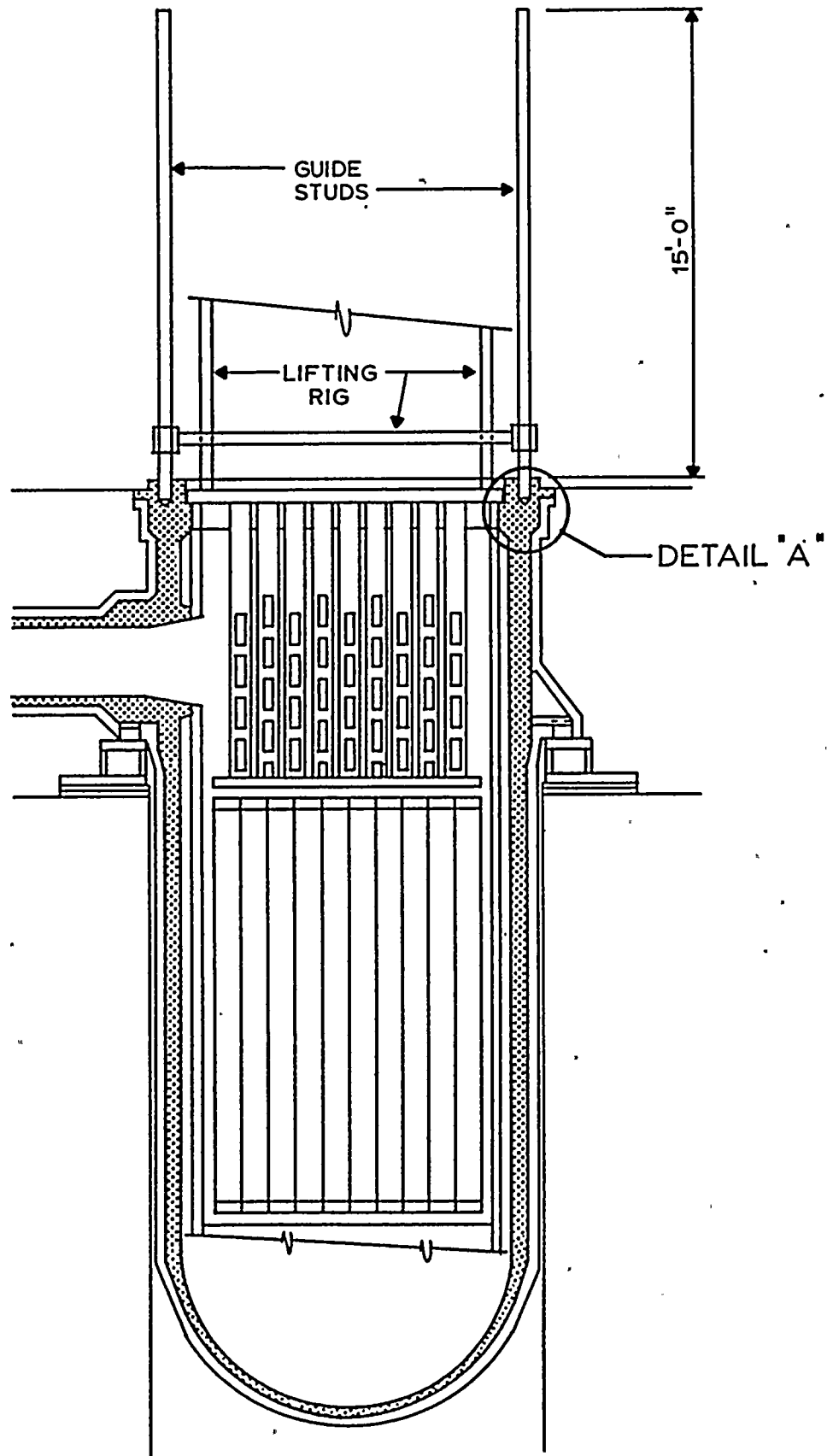
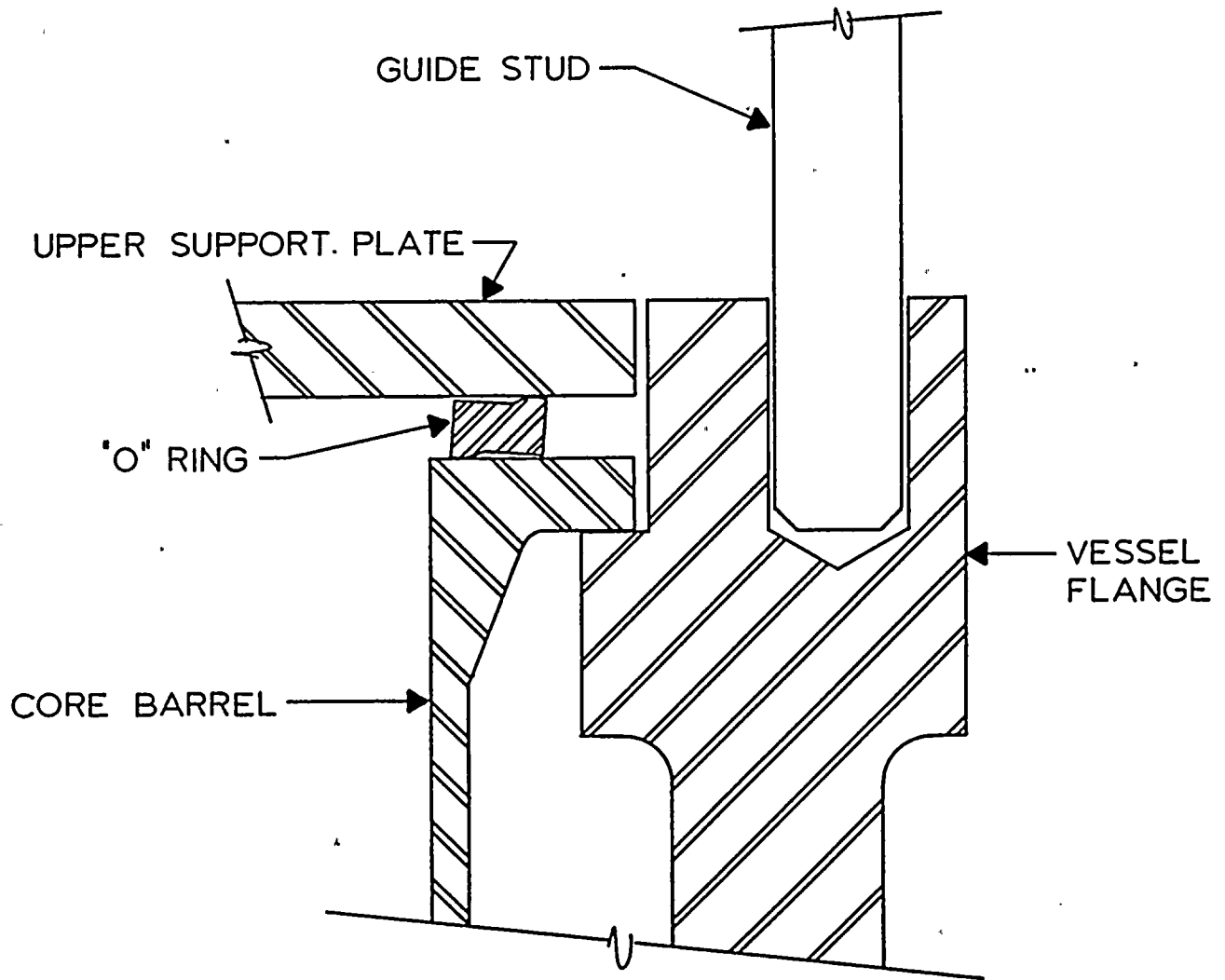


FIGURE 2. UPPER INTERNALS WITHIN THE REACTOR VESSEL





DETAIL "A"

FIGURE 3. UPPER INTERNALS SUPPORT LEDGE



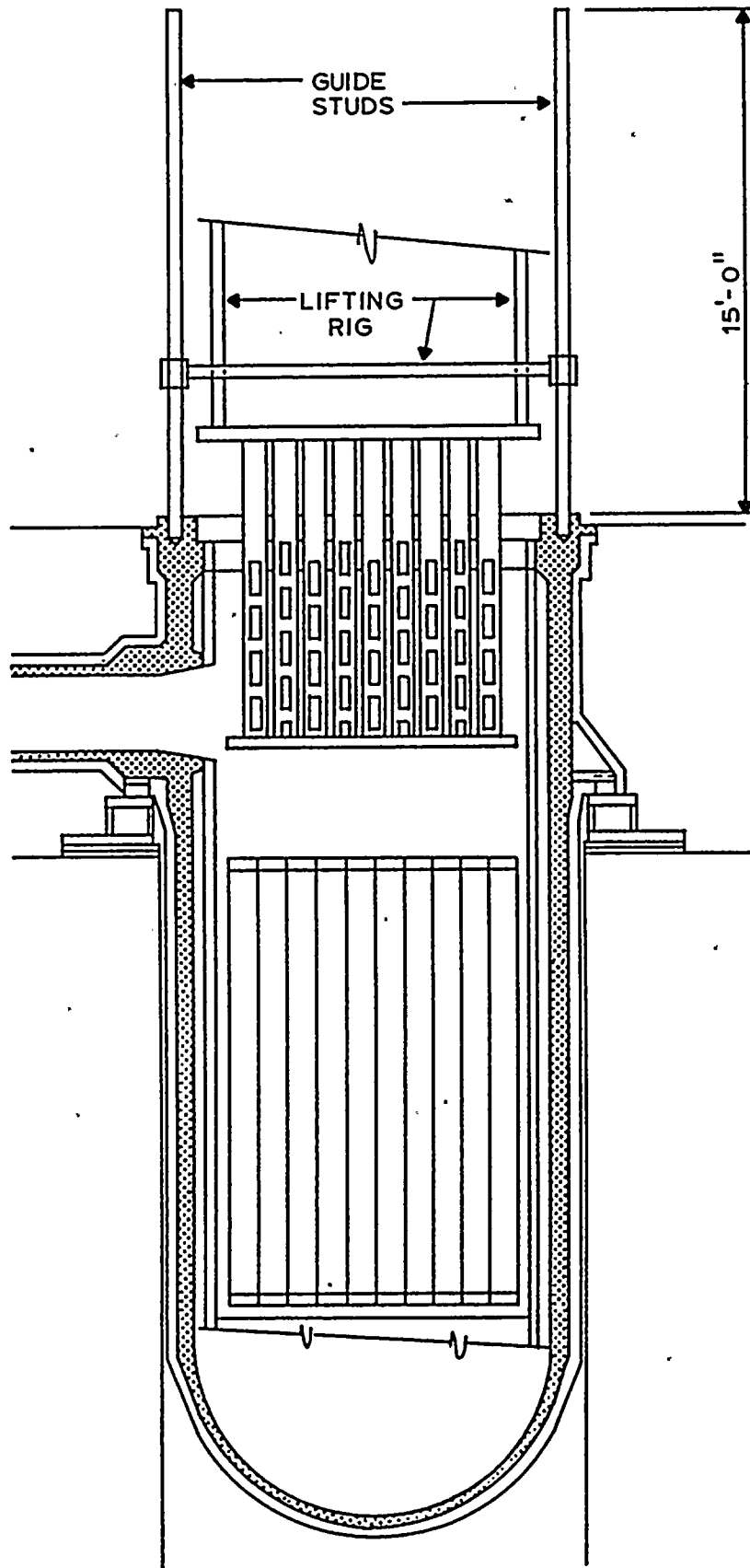
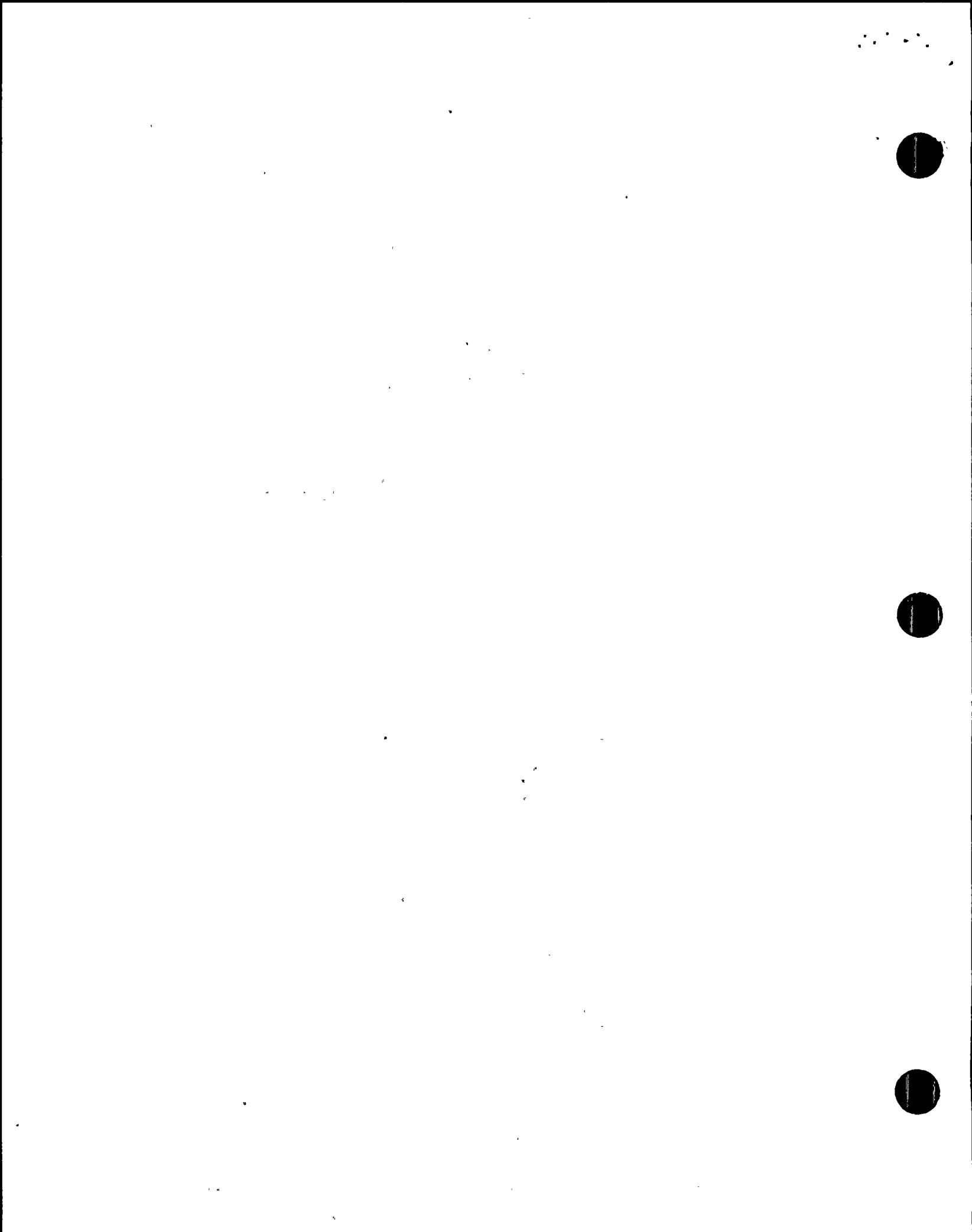


FIGURE 4. UPPER INTERNALS BEING RAISED FROM THE REACTOR VESSEL



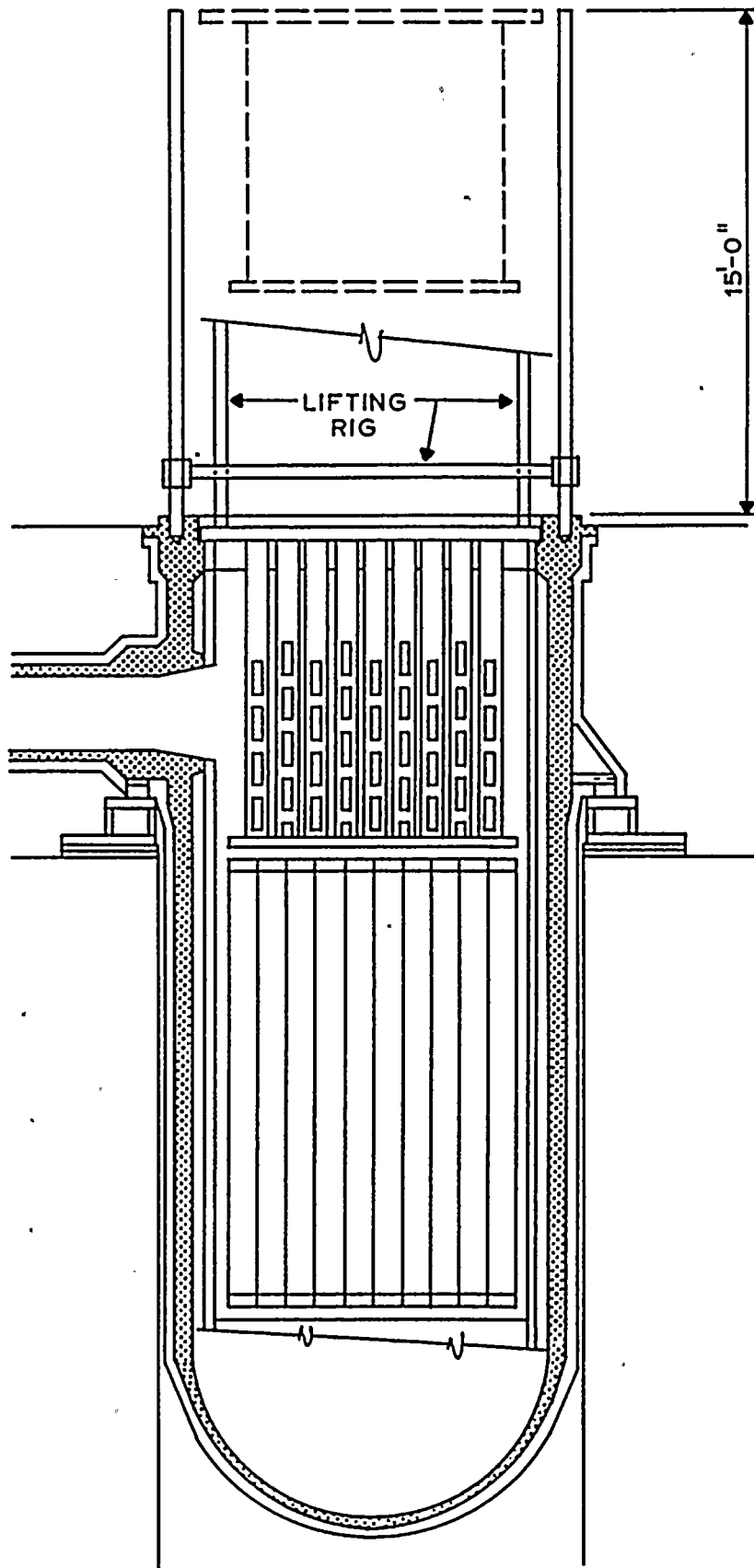


FIGURE 6. UPPER INTERNALS DROP INTO THE REACTOR VESSEL

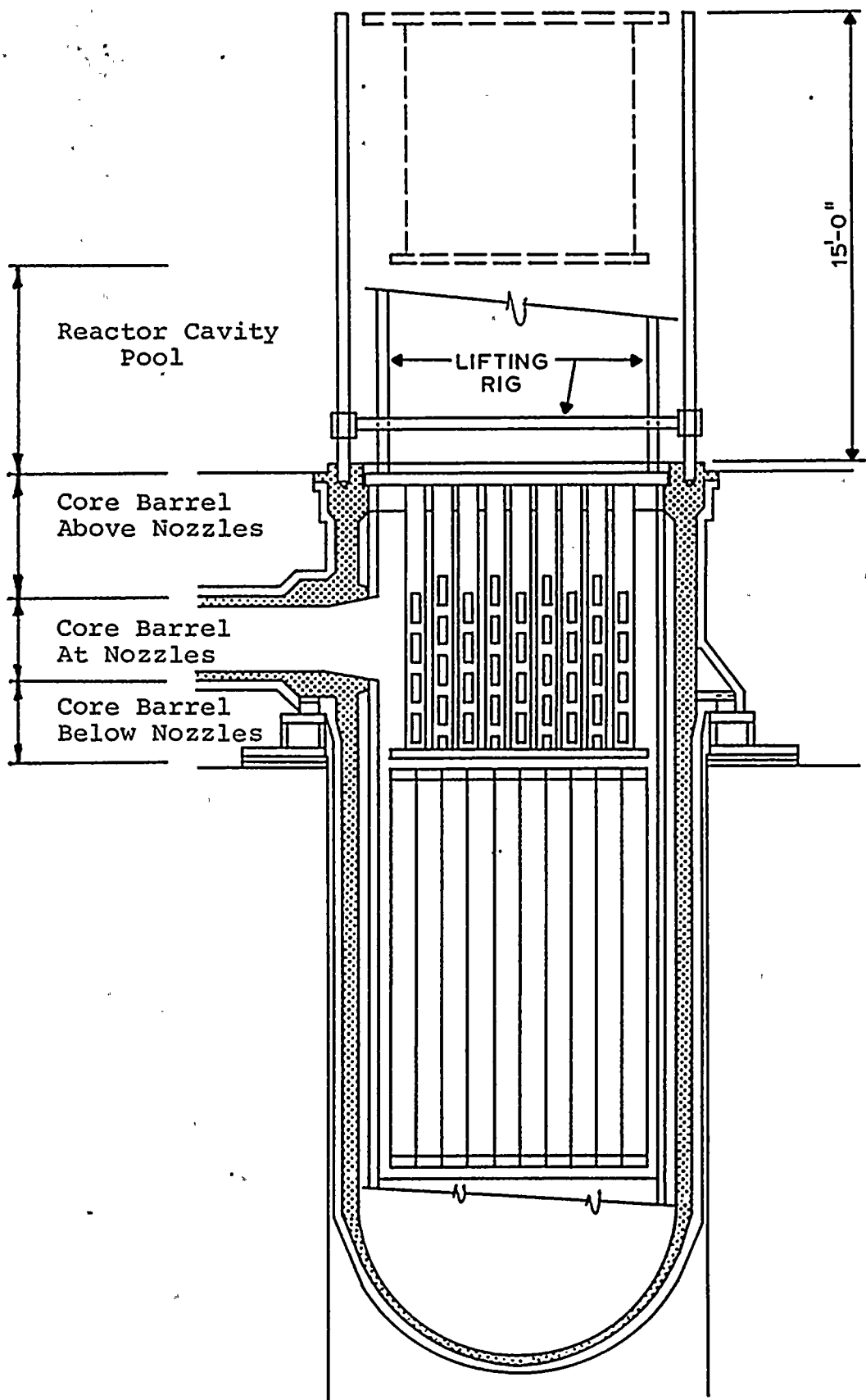


FIGURE 7. REGIONS WITHIN UPPER INTERNALS DROP PATH



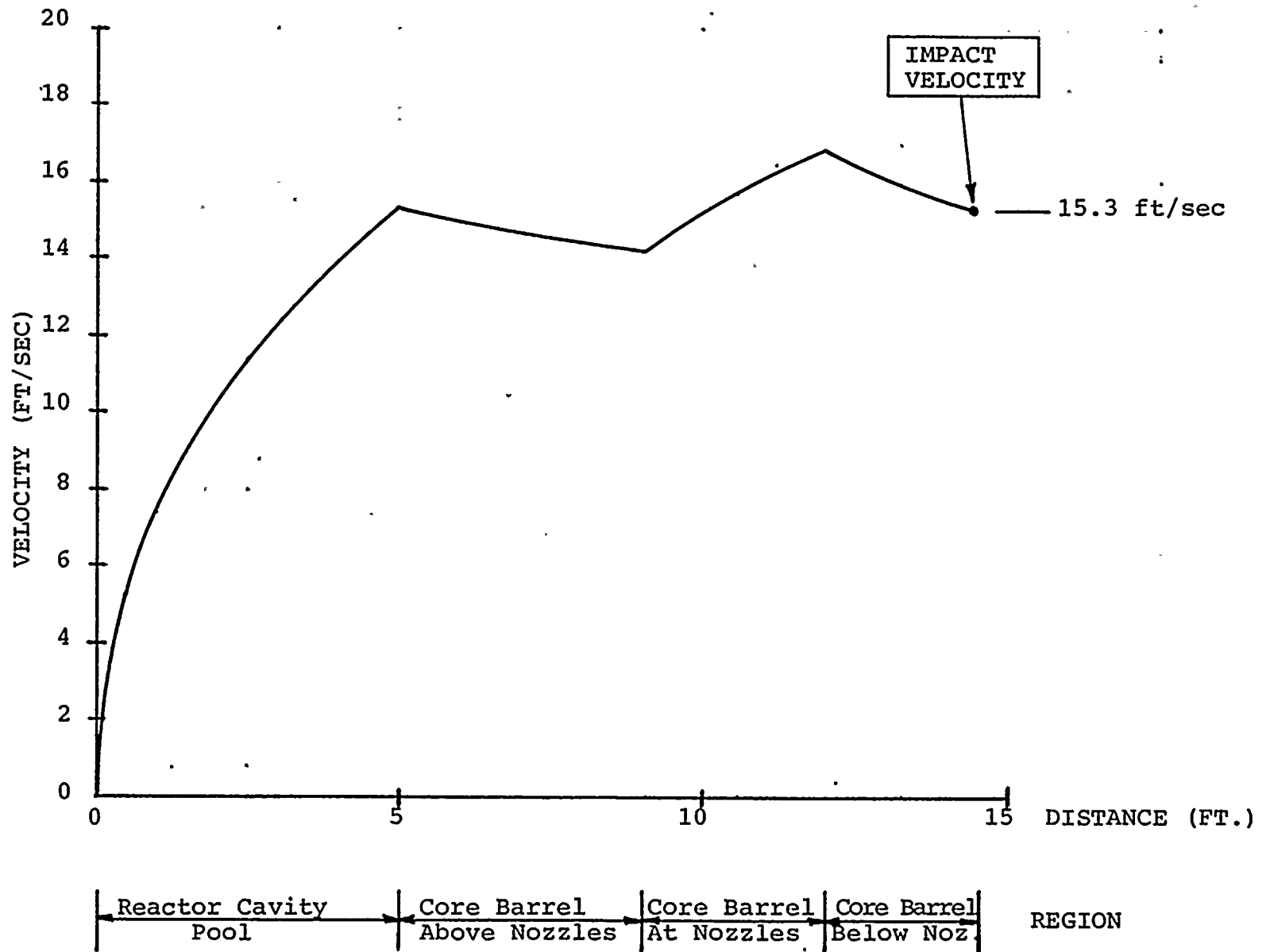


FIGURE 8. UPPER INTERNALS VELOCITY DURING FREE FALL

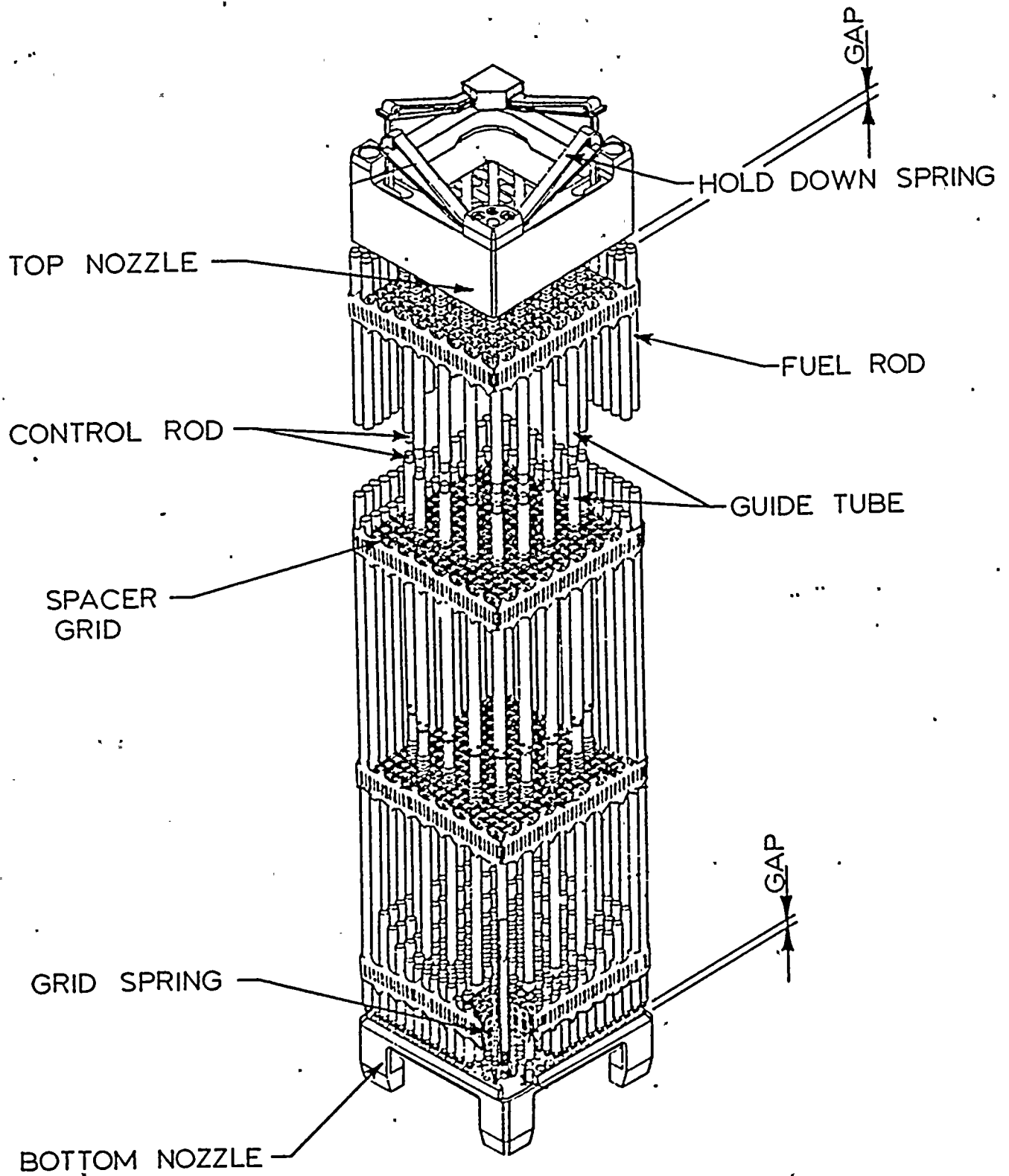


FIGURE 9. FUEL ASSEMBLY

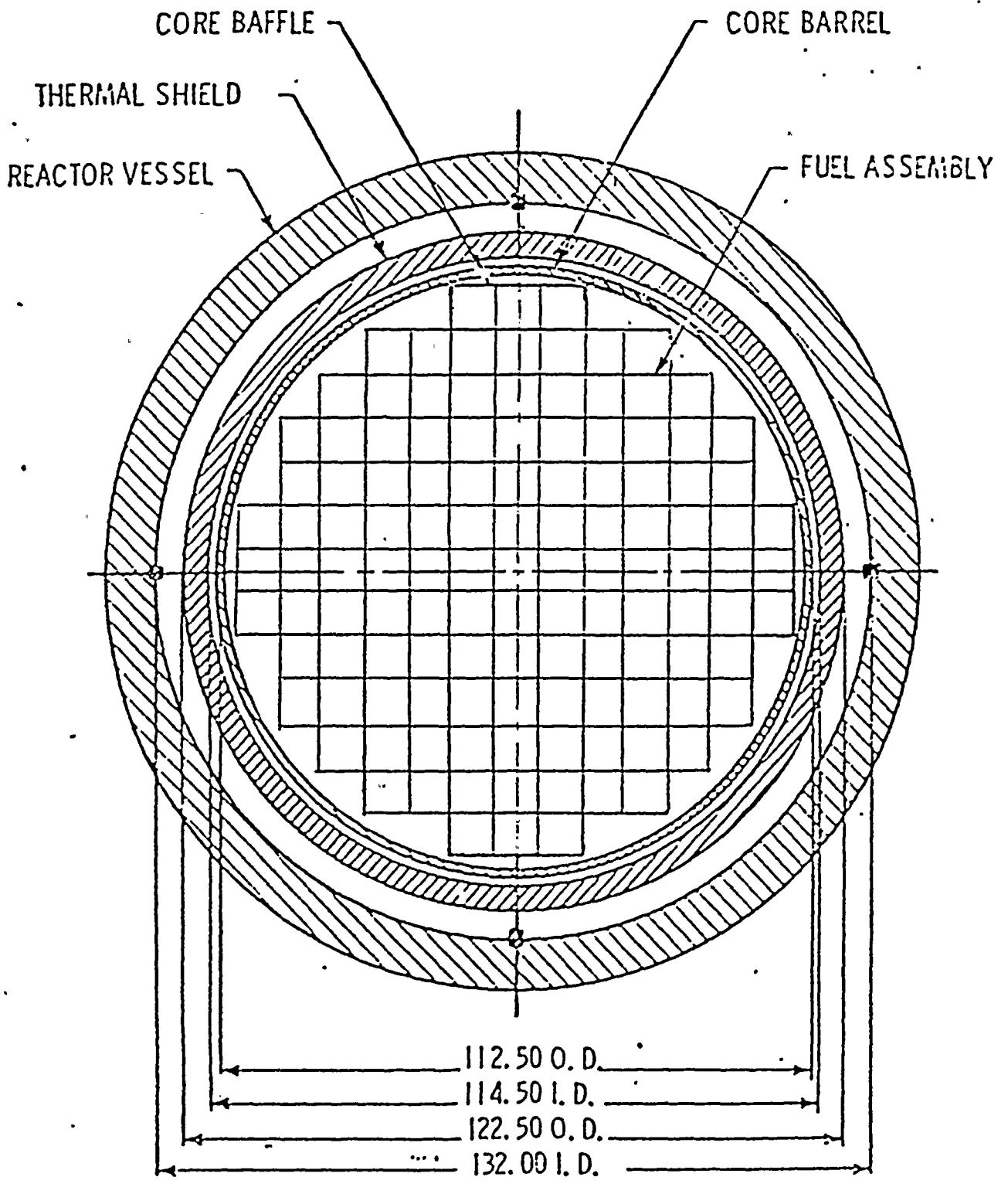
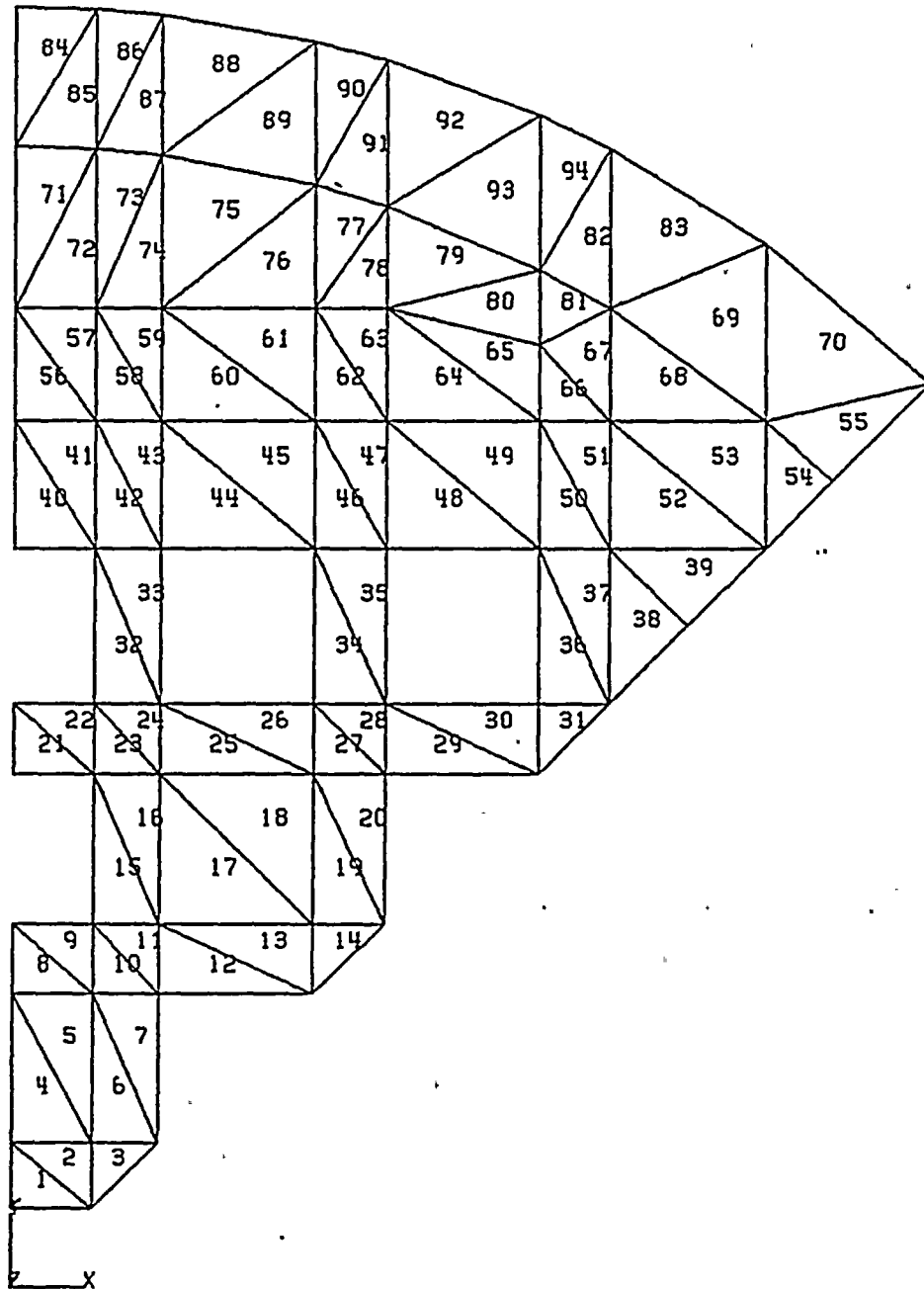


FIGURE 10. PLAN VIEW OF CORE WITH 121 FUEL ASSEMBLIES



RG&E UPPER INTERNALS SUPPORT PLATE MODEL (45 DEG. SEGMENT)

FIGURE 11. ANSYS FINITE ELEMENT MODEL OF UPPER SUPPORT PLATE

100-100000-100000



STRAIN ENERGY (FT-LBS)

1,000,000

100,000

10,000

1,000

100

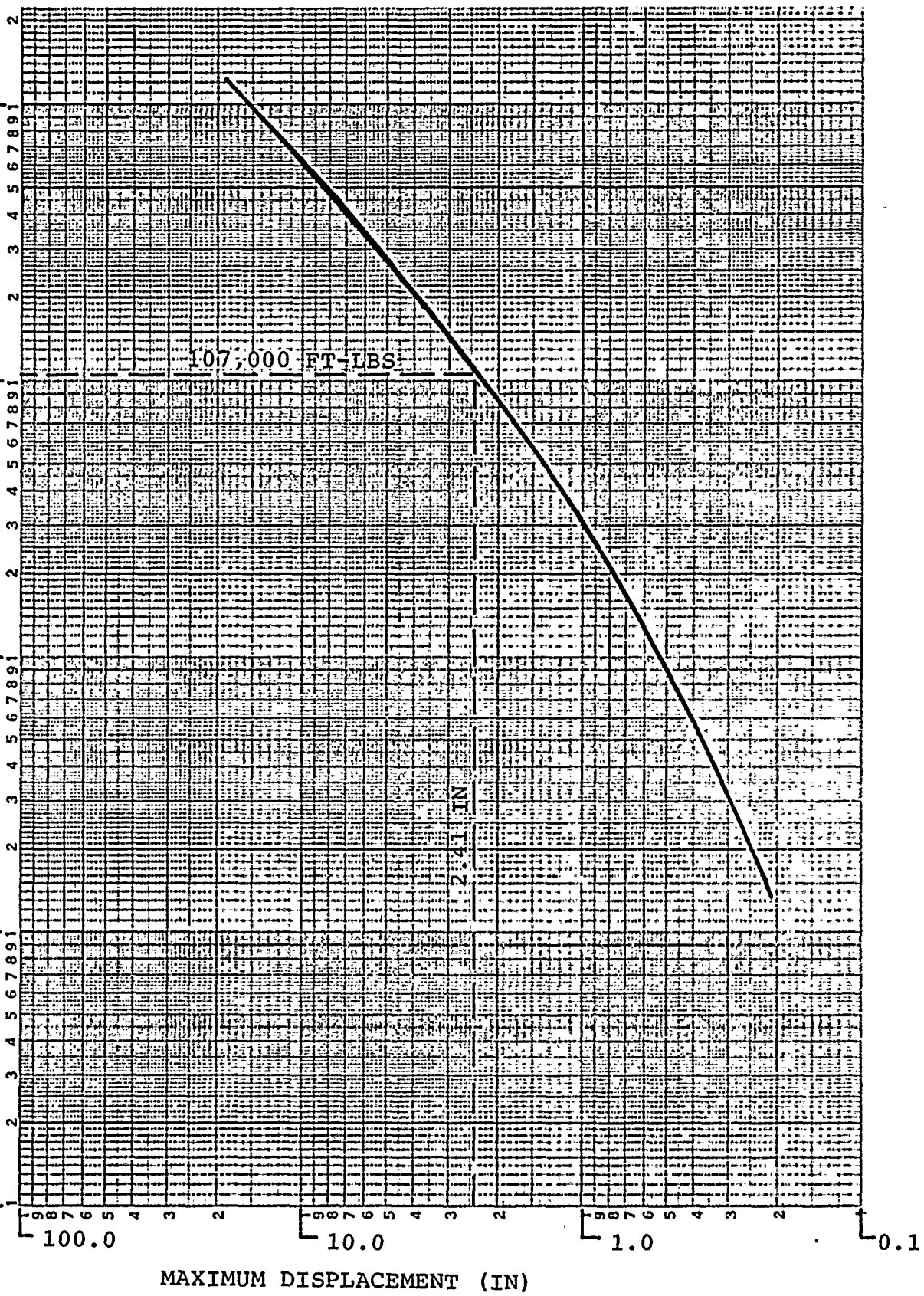


FIGURE 12. ENERGY ABSORBED BY UPPER SUPPORT PLATE

ATTACHMENT 4

Load/Impact Matrix Sheets

CRANE; 7½ Ton Screenhouse (t)

LOCATION	Screenhouse East of Column #5		
IMPACT AREA	Service Water Pump Motors and Associated Electrical Bus		
	LOADS	ELEVATION	EQUIPMENT EVALUATED
S. W. Pumps	Floor Elev. 253'-6"	S. W. System	See Discussion 2.4-2(b)
S. W. Pump Motors	Floor Elev. 253'-6"	S. W. System	See Discussion 2.4-2(b)
Fire Pump Motors	Floor Elev. 253'-6"	S. W. System	See Discussion 2.4-2(b)
Fire Pump	Floor Elev. 253'-6"	S. W. System	See Discussion 2.4-2(b)
Fire Pump Engine	Floor Elev. 253'-6"	S. W. System	See Discussion 2.4-2(b)
S. W. Check Valves	Floor Elev. 253'-6"	S. W. System	See Discussion 2.4-2(b)
S. W. Isolation Valves	Floor Elev. 253'-6"	S. W. System	See Discussion 2.4-2(b)



CRANE: 10 Ton Jib in Containment

LOCATION	Over Pressurizer Cavity		
IMPACT AREA	Pressurizer and Associated Piping/Instrumentation		
	LOADS	ELEVATION	EQUIPMENT EVALUATED
Hatch Covers	Floor Elevation 288'-4"	Pressurizer Piping/Instrumentation	See Response to NRC Section 2.4-2 in report Section 3.0



CRANE; 2-Ton Jib in Containment

LOCATION	At Personnel Hatch in Containment		
IMPACT AREA	Operating Floor of Concrete and Grating		
	LOADS	ELEVATION	EQUIPMENT EVALUATED
Miscellaneous Equipment	Floor Elevation 278'-4" (Maximum Load Height 11'-0")	B Accumulator* Line to Loop A Fan Cooler D and its service water lines*	See Discussion 2.4-2(b) See Discussion 2.4-2(b)
<p>*NOTE: The Safety-Related equipment listed is located 2 floor levels below the crane and assumed to be damaged.</p>			

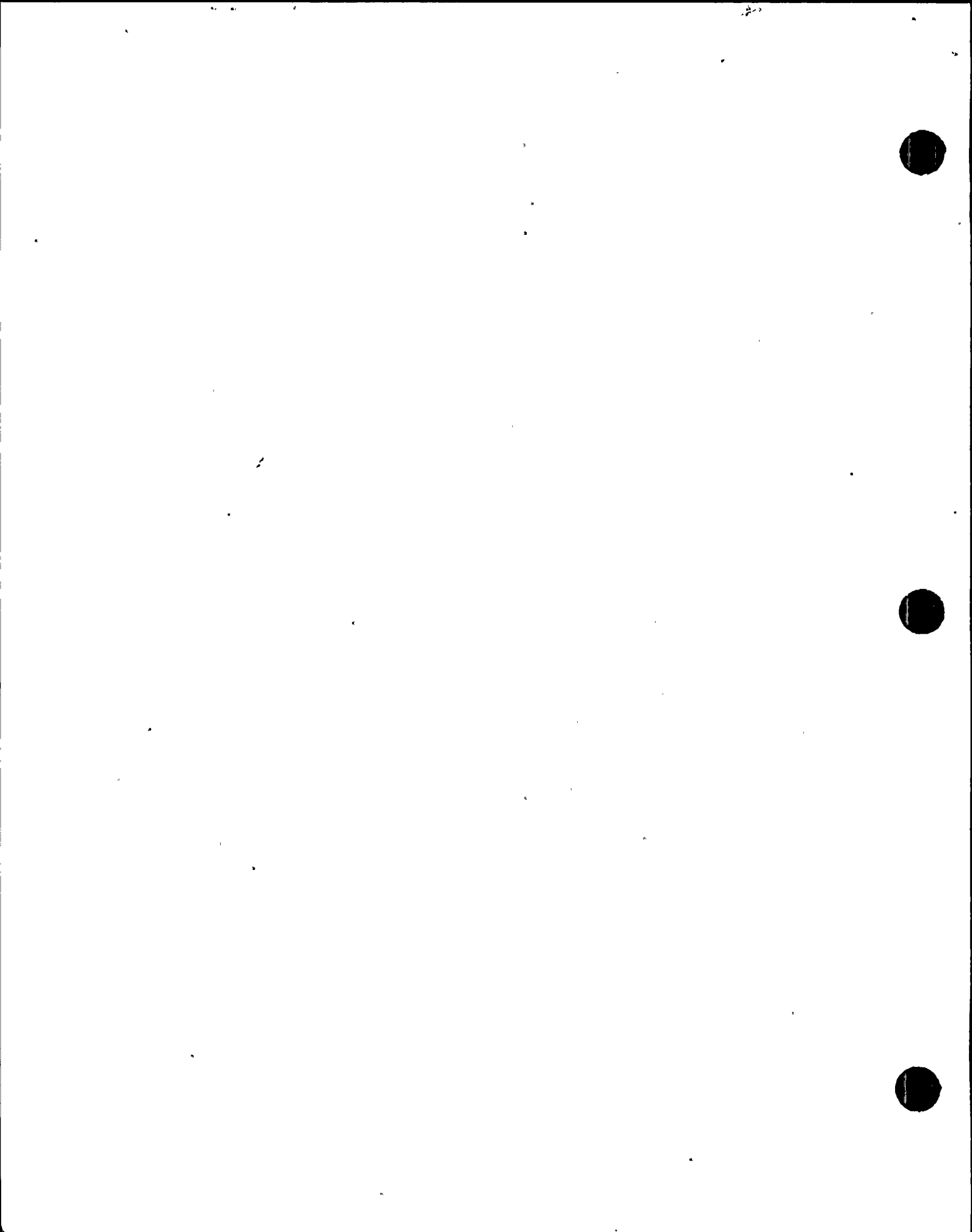
CRANE: Auxiliary Building Basement Monorail

LOCATION	Basement Auxiliary Building, Elev: 235'-8"		
IMPACT AREA	Basement Floor/Equipment in Sub. Basement		
LOADS	ELEVATION	EQUIPMENT EVALUATED	HAZARD ELIMINATION CATEGORY
RHR Pumps RCDT Pumps Removable Floor Sections	Floor Elev. 235'-8"	RHR Pumps RHR Piping	See Discussion 2.4-2(b)



CRANE: 3 Ton Jib

LOCATION	Equipment Hatch/Crane Bay		
IMPACT AREA	Operating Floor of Concrete and Crane Bay Opening/Basement Floor (Piping Around Crane Bay)		
	LOADS	ELEVATION	EQUIPMENT EVALUATED HAZARD ELIMINATION CATEGORY
Misc. Equipment	Floor Elev. 274'-6"	<p>Mechanical Equipment</p> <p>A accumulator line to B loop RHR letdown from A loop LPSI to 852A SI to B cold leg charging line valve 296 and associated piping fan coolers B and C and associated service water B RCP seal water injection</p> <p>Electrical Circuits</p> <p>SG A narrow range level 461, 463 SG A wide range level 460 SG B narrow range level 471, 473 LPSI valve 852A, circuits C729, C731 LPSI valve 852B, circuits C1095, C731 fan cooler B circuit L219 fan cooler C circuit L228 pressurizer pressure PT 430, PT431 pressurizer level LT427, LT428 CVCS valves 294 circuit R536 charging 392A circuit R550 charging 200A circuit R515 letdown 200B circuit R508 letdown 202 circuit R501 letdown 296 circuit R543 pressurizer spray</p> <p><u>NOTE:</u> Some safety-related equipment listed is located 2 floor levels below the crane and assumed to be damaged.</p>	See Discussion 2.4-2 (b)

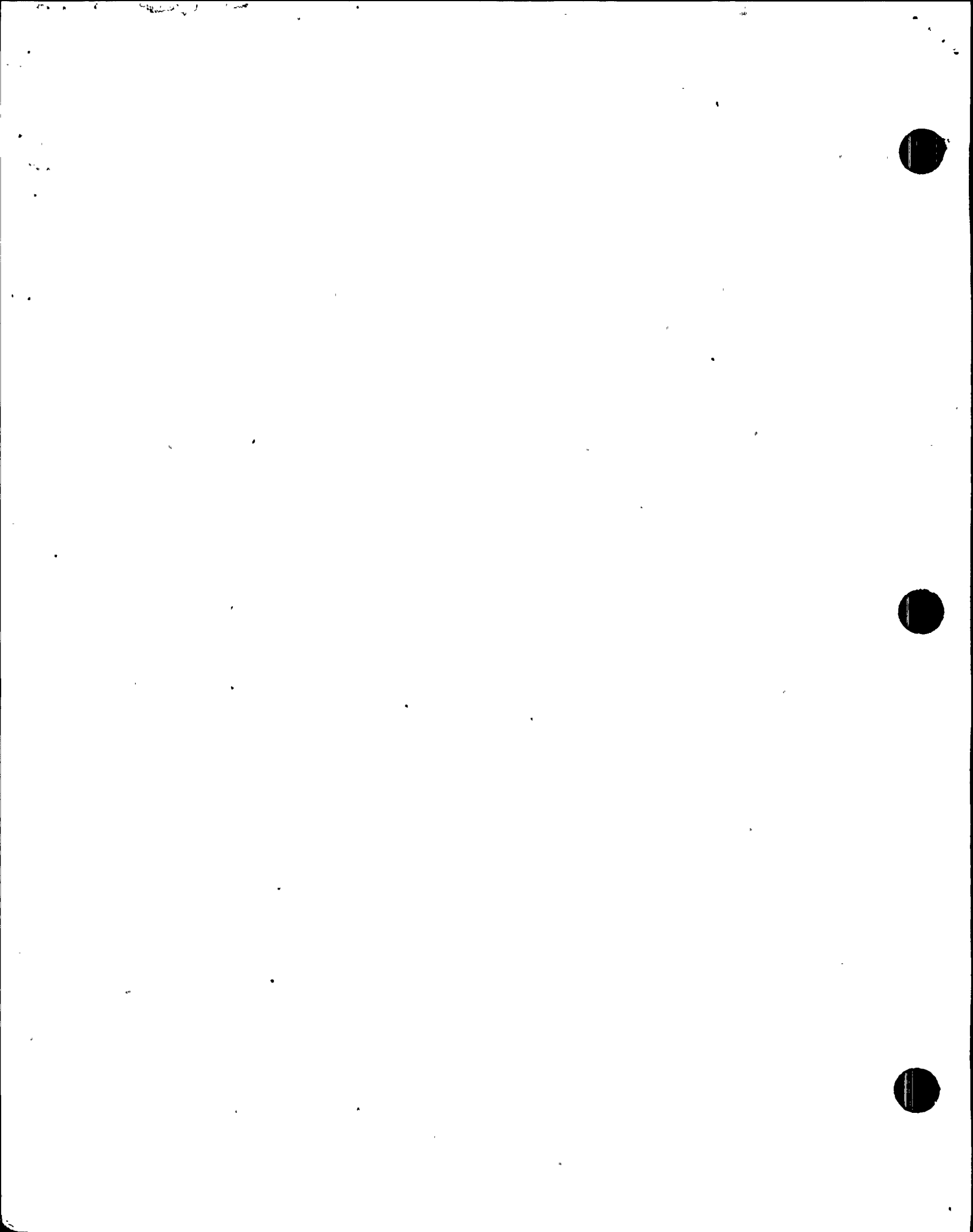


CRANE: 40/5 Ton Auxiliary Building Overhead

LOCATION	Auxiliary Building		
IMPACT AREA	Operating Floor/Crane Bay		
LOADS	ELEVATION	EQUIPMENT EVALUATED	HAZARD ELIMINATION CATEGORY
RHR Pumps	Floor Elevations	RHR	See Discussion in response to NRC 2.2-4 located in report section 3. Also see discussion 2.4-2(b).
Component Cooling Pumps	271'-0" and 278'-4"	Component Cooling	
RCDT Pumps			
Removable Floor Sections			
Vibration Cleaner			
New Fuel Assemblies			
New Fuel Casks			
Steam Generator Tools			
Transfer Canal Gate			
Lead Basket			
Spent Fuel Shipping Cask			

CRANE: 100/20 Ton Containment Overhead

LOCATION	Containment		
IMPACT AREA	Vessel/Cavity Floor/Operating Deck		
LOADS	ELEVATION	EQUIPMENT EVALUATED	HAZARD ELIMINATION CATEGORY
RPV Head on Vessel	16' Lifted above vessel flange	Reactor Vessel	See Response to NRC Section 2.3-4 located in Report Section 3.0.
RPV Head on Cavity Floor and Head Stand	Lifted 42' Max. above cavity 8' above head stand	Mechanical Equipment Reactor coolant system Accumulators RHR LPSI SI Containment fan coolers CVCS - charging letdown SG blowdown Feedwater Mainsteam RCP seal injection Pressurizer spray and auxiliary spray Electrical Circuits SG level wide & narrow range Pressurizer pressure & level LPSI 852 valves Fan coolers Charging valves 294 & 392A Letdown valves 200A, 200B, 202, 427 Pressurizer PORVs 430, 431C Pressurizer spray valves 296, 431A, 431B	See Response to NRC Section 2.4-4 located in Report Section 3.0.



CRANE: 100/20 Ton Containment Overhead

LOCATION	Containment		
IMPACT AREA	Vessel/Cavity Floor/Operating Deck		
LOADS	ELEVATION	EQUIPMENT EVALUATED	HAZARD ELIMINATION CATEGORY
Reactor Upper Internals on Vessel	Lifted 15' above the core	Vessel Core	See Response to NRC Section 2.3-4 located in Report Section 3.0.
Reactor Upper Internals on North Cavity Floor and Storage Stand	Lifted 15' above cavity floor	RHR Outlet from "A" Hot Let LPSI 852A Pipe to Vessel Upper Plenum.	

